International Ocean Discovery Program

Expedition 390/393 Scientific Prospectus

The South Atlantic Transect: a multidisciplinary IODP investigation along a crustal flow line across the western flank of the southern Mid-Atlantic Ridge

Rosalind M. Coggon
Co-Chief Scientist Expedition 390
School of Ocean and Earth Science
University of Southampton
United Kingdom

Jason B. Sylvan
Co-Chief Scientist Expedition 390
Department of Oceanography
Texas A&M University
USA

Emily Estes
Expedition Project Manager/Staff Scientist
Expedition 390
International Ocean Discovery Program
Texas A&M University
USA

Gail L. Christeson
Co-Chief Scientist Expedition 393
Institute for Geophysics
University of Texas at Austin
USA

Damon A.H. Teagle
Co-Chief Scientist Expedition 393
School of Ocean and Earth Science
University of Southampton
United Kingdom

Trevor Williams
Expedition Project Manager/Staff Scientist
Expedition 393
International Ocean Discovery Program
Texas A&M University
USA

IODP
INTERNATIONAL OCEAN DISCOVERY PROGRAM

Publisher's notes

This publication was prepared by the *JOIDES Resolution* Science Operator (JRSO) at Texas A&M University (TAMU). This material is based upon work supported by the JRSO, which is a major facility funded by the National Science Foundation Cooperative Agreement number OCE1326927. Funding for IODP is provided by the following international partners:

National Science Foundation (NSF), United States
Ministry of Education, Culture, Sports, Science and Technology (MEXT), Japan
European Consortium for Ocean Research Drilling (ECORD)
Ministry of Science and Technology (MOST), People's Republic of China
Korea Institute of Geoscience and Mineral Resources (KIGAM)
Australia-New Zealand IODP Consortium (ANZIC)
Ministry of Earth Sciences (MoES), India
Coordination for Improvement of Higher Education Personnel (CAPES), Brazil

Portions of this work may have been published in whole or in part in other IODP documents or publications.

This IODP *Scientific Prospectus* is based on precruise *JOIDES Resolution* Facility advisory panel discussions and scientific input from the designated Co-Chief Scientists on behalf of the drilling proponents. During the course of the cruise, actual site operations may indicate to the Co-Chief Scientists, the Expedition Project Manager/Staff Scientist, and the Operations Superintendent that it would be scientifically or operationally advantageous to amend the plan detailed in this prospectus. It should be understood that any substantial changes to the science deliverables outlined in the plan presented here are contingent upon the approval of the IODP JRSO Director and/or *JOIDES Resolution* Facility Board.

Disclaimer

Copyright

Citation

Coggon, R.M., Christeson, G.L., Sylvan, J.B., Teagle, D.A.H., Estes, E., Williams, T., and Alvarez Zarikian, C.A., 2020. *Expedition 390/393 Scientific Prospectus: The South Atlantic Transect*. International Ocean Discovery Program. https://doi.org/10.14379/iodp.sp.390393.2020

ISSN

World Wide Web: 2332-1385

February 2020

Abstract

The South Atlantic Transect (SAT) is a multidisciplinary scientific ocean drilling project that comprises two International Ocean Discovery Program (IODP) expeditions (390, October–December 2020, and 393, April–June 2021). These expeditions will recover complete sedimentary sections and the upper ~250 m of the underlying oceanic crust along a slow/intermediate spreading rate Mid-Atlantic Ridge crustal flow line at ~31°S. The sediments along this transect were originally spot cored more than 50 y ago during Deep Sea Drilling Project Leg 3 to help verify the theories of seafloor spreading and plate tectonics. Given dramatic advances in drilling technology and analytical capabilities since Leg 3, many high-priority scientific objectives can be addressed by revisiting the transect. The SAT expeditions will target six primary sites on 7, 15, 31, 49, and 61 Ma ocean crust, which will fill critical gaps in our sampling of intact in situ ocean crust with regards to crustal age, spreading rate, and sediment thickness. These sections are required to investigate the history of the low-temperature hydrothermal interactions between the aging ocean crust and the evolving South Atlantic Ocean and quantify past hydrothermal contributions to global geochemical cycles. The transect traverses the previously unexplored sediment- and basalt-hosted deep biosphere beneath the South Atlantic Gyre from which samples are essential to refine global biomass estimates and investigate microbial ecosystems' responses to variable conditions in a low-energy gyre and aging ocean crust. The drilling operations will include installation of reentry cones and casing to establish legacy boreholes for future basement hydrothermal and microbiological experiments. The transect is also located near World Ocean Circulation Experiment Line A10, providing access to records of carbonate chemistry and deepwater mass properties across the western South Atlantic through key Cenozoic intervals of elevated atmospheric CO_2 and rapid climate change. Reconstruction of the history of the deep western boundary current and deepwater formation in the Atlantic basins will yield crucial data to test hypotheses regarding the role of evolving thermohaline circulation patterns in climate change and the effects of tectonic gateways and climate on ocean acidification.

Schedule for IODP Expeditions 390 and 393

International Ocean Discovery Program (IODP) Expeditions 390 and 393 are based on IODP drilling Proposal 853-Full2 and 853-Add (available at **http://iodp.tamu.edu/scienceops/expeditions/south_atlantic_transect.html**). Following evaluation by the IODP Scientific Advisory Structure, the expeditions were scheduled for the R/V *JOIDES Resolution*, operating under contract with the JOIDES Resolution Science Operator (JRSO). At the time of publication of this *Scientific Prospectus*, Expedition 390 is scheduled to start in Rio de Janeiro, Brazil, on 5 October 2020 and end in Cape Town, South Africa, on 5 December. Expedition 393 is scheduled to start in Cape Town on 6 April 2021 and to end in Rio de Janeiro on 6 June. A total of 61 days will be available for each expedition for the transit, drilling, coring, and downhole measurements described in this report (for the current detailed schedule, see **http://iodp.tamu.edu/scienceops**). Further details about the facilities aboard *JOIDES Resolution* can be found at **http://iodp.tamu.edu/labs/index.html**.

Introduction

Despite more than 50 y of scientific ocean drilling, major gaps remain in our observations of the evolving Earth system, such as drill cores of ocean crust of different ages and formed at contrasting spreading rates, virtually unexplored biogeographic microbial provinces, and continuous high–sedimentation rate samples of key times in Earth's climate, changing ocean chemistry, or magnetic field history. Transects of drill holes that sample both the sediment cover and the uppermost oceanic crust in a particular ocean basin can provide essential knowledge of how interconnected processes have evolved over Earth's history and responded to changes in external drivers such as atmospheric CO_2 concentrations, oceanic gateways, or major ocean currents. Transects that sample tens of millions of years of ocean crust formed at the same mid-ocean ridge (MOR) can provide important information about the duration of hydrothermal exchange. However, sampling both the sediment and the underlying basaltic basement in a specific ocean region has rarely been undertaken in a systematic manner, and the few transects accomplished cover relatively short intervals of Earth history (e.g., Juan de Fuca Ridge, 0–3.5 Ma [Shipboard Scientific Party, 1997; Expedition 301 Scientists, 2005; Expedition 327 Scientists, 2011] and Costa Rica Rift, 0–7 Ma [Anderson, Honnorez, Becker, et al., 1985]).

On average, there is a discernible conductive heat flow deficit out to 65 Ma crust (e.g., Stein and Stein, 1994), indicating that there is significant advection of heat from the cooling of the oceanic lithosphere out to this age. However, basement hydrological flow can occur in crust of all ages if sufficient hydrologic heads can be established because crustal age is only one of a suite of interlinked parameters that includes spreading rate; basement roughness; volcanic stratigraphy and flow morphology; and sediment type, thickness, and completeness of basement blanketing. These parameters influence the duration, depth, and intensity of off-axis hydrothermal fluid flow. Simple relationships may not exist between crustal age, fluid flow, thermal and chemical exchange, and biological activity.

Development of the South Atlantic Transect drilling project

The South Atlantic Transect (SAT) drilling project was developed through IODP Proposal 853 (853-Pre, 853-Full1, IODP 853-Full2, and 853-Add), which originated following discussions at two workshops. U.S. scientists met at the Building U.S. Strategies for 2013–2023 Scientific Ocean Drilling workshop (Denver, Colorado, April 2012) with the purpose of prioritizing the 14 challenges of the IODP Science Plan for 2013–2023, "Illuminating Earth's Past, Present, and Future," and identifying new approaches for more efficient planning of drilling expeditions. This workshop identified and adapted a key strategy described in Science Plan Challenge 10 to drill crustal age transects that provide opportunities to combine diverse scientific objectives (**http://usoceandiscovery.org/wp-content/uploads/2016/05/Workshop_BuildingUSStrategies_Report.pdf**). This concept was further developed during the Transect Drilling During Transits workshop (College Station, Texas; November 2013), which convened to explore opportunities for multidisciplinary drilling transects exploiting likely drill ship transits to maxi-

mize the scientific output in relation to cost and time (**http://usoceandiscovery.org/wp-content/uploads/2016/05/Workshop_TransectDrilling_Report.pdf**). The South Atlantic was identified as a region where multiple Science Plan challenges could be addressed by drilling an age transect of sediment–basement holes.

IODP Expeditions 390 and 393, which are derived from IODP Proposals 853-Full2 and 853-Add, will drill a SAT along a crustal flow line across the western flank of the southern Mid-Atlantic Ridge (MAR) to investigate the hydrothermal evolution of the aging ocean crust, sediment- and basement-hosted microbial community variation with increasing substrate age, the paleoceanographic evolution of the South Atlantic Ocean, and the deep-ocean and subtropical gyre responses to changing global climate. The expeditions' strategy exploits drilling targets that can simultaneously advance scientific objectives across all four themes of the Science Plan.

In 1968, Deep Sea Drilling Project (DSDP) Leg 3 accomplished one of the great achievements of scientific ocean drilling: recovering sediments from a transect of spot cored holes across the South Atlantic between ~28° and 30°S (Figure **F1**) to demonstrate that basal sediment age increases with distance from the ridge axis. This provided definitive proof for the theory of seafloor spreading (Scientific Party, 1970). In celebration of the recent fiftieth anniversary of this achievement, we will return to the Leg 3 transect area to recover complete sedimentary sections and core the uppermost ~250 m of ocean crust produced between ~7 and 61 Ma at the slow/intermediate-spreading MAR.

The SAT expeditions will target six primary sites on 7, 15, 31, 49, and 61 Ma ocean crust (Figure **F1**), filling critical gaps in our sampling of intact in situ ocean crust with regards to crustal age, spreading rate, and sediment thickness (Figures **F2**, **F3**). These sections of upper ocean crust along a crustal flow line will enable us to quantify the magnitude and duration of low chemical exchange with the overlying oceans; investigate the impact of changing ocean conditions on hydrothermal exchange; determine the critical thermal, hydrogeologic, chemical, and microbial transitions across the ridge flank; and evaluate hydrothermal contributions to global biogeochemical cycles (Science Plan Challenge 10). Sampling the sedimentary and upper crustal deep biosphere along the transect will allow exploration of the microbial ecosystems' responses to variations in habitat conditions in a low-energy gyre and aging ocean crust (Challenges 5 and 7). Recovered sediments will include Cenozoic stratigraphic sections required to investigate the Earth system's past responses to high atmospheric CO_2 and temperatures and better predict the impacts of projected future anthropogenic increases in atmospheric CO_2 (Challenges 1, 2, and 4). The transect will also provide a paleoceanographic record near World Ocean Circulation Experiment (WOCE) Line A10, enabling reconstruction of the history of the deep western boundary current and the sources of deep water formation in the Atlantic basins (Challenge 1). In addition, knowledge of the controls on the extent, rate, and duration of natural CO_2 sequestration along the SAT will assist in assessing the properties and processes that govern the flow and storage of carbon in the subseafloor (Challenge 13). Expeditions 390 and 393 will recover complete sediment sections and the uppermost basaltic ocean crust along the SAT to achieve the following objectives:

1. Quantify the timing, duration, and extent of ridge flank hydrothermal fluid-rock exchange;
2. Investigate sediment- and basement-hosted microbial community variation with substrate composition and age; and
3. Investigate the responses of Atlantic Ocean circulation patterns and the Earth's climate system to rapid climate change, including elevated atmospheric CO_2 during the Cenozoic.

Background

Geological setting

Scientific ocean drilling provides the only means to sample igneous basement across the sedimented western flank of the southern MAR and recover the high-quality stratigraphic sections required to achieve our scientific objectives. Expeditions 390 and 393 will operate near the Leg 3 transect (~31°S), but a new transect will be drilled with sites that have been selected to (1) target basement formed along the same crustal flow line at similar rates (~13–25 mm/y half rate; Table **T1**) and (2) recover sections of slow-spreading crust of comparable ages to the ocean crust reference sections in Ocean Drilling Program (ODP) Holes 504B (7 Ma; Shipboard Scientific Party, 1993) and 1256D (15 Ma; Expedition 309/312 Scientists, 2006; Expedition 335 Scientists, 2012), which are hosted by intermediate- and superfast-spreading crust, respectively.

The locations of the six sites to be drilled during Expeditions 390 and 393 are targeted to optimize the recovery of material required to achieve our multidisciplinary objectives. Thick sediment cover is often targeted by scientific ocean drilling to maximize the resolution of paleoceanographic records. Also, such thick sequences are often required to install the seafloor infrastructure required for deep-ocean drilling. This has led to a bias in DSDP/ODP/IODP sampling of in situ upper ocean crust (for depths >100 m into basement) toward regions with anomalously thick sediment (Figure **F3**). Rapid deposition of sediment in such areas seals the crust from the oceans, results in anomalously hot basement temperatures, and may result in premature cessation of hydrothermal circulation. Consequently, most sites on the SAT target locations where the sediment cover is close to the global average for each crustal age (Spinelli et al., 2004), and we accept that this will reduce the resolution of the paleoceanographic records. However, because seafloor roughness is greater in slow-spreading ocean basins than in fast-spreading basins (Spinelli et al., 2004), there are significant variations in sediment thickness and the continuity of coverage along the SAT. Basement crops out at all ages along our transect (Estep et al., 2019), and these topographic variations likely impact the crustal hydrogeology. A second 61 Ma site (Proposed Site SATL-54A) would lie ~2.5 km west of 61 Ma Proposed Site SATL-53B (Figure **F4**) in a more thickly sedimented portion of the same basin to investigate the variability in duration and extent of hydrothermal alteration due to basement topography. Proposed Site SATL-54A will also provide a higher resolution paleoceanographic record at this age, the oldest among our drill sites.

The sediment sections cored at the 61 Ma sites are expected to capture key Paleogene hyperthermals, including the Paleocene/Eocene Thermal Maximum (PETM), and the underlying basement will record the cumulative hydrothermal alteration of the uppermost crust across the entire SAT. The 7 Ma site provides the young endmember for investigating the evolution of hydrothermal and microbiological systems with crustal age and allows comparison with similar-aged intermediate spreading rate crust from Hole 504B (Shipboard Scientific Party, 1993). The 31 and 49 Ma sites fill critical gaps in our ocean crust and deep biosphere sampling with respect to basement age and major changes in ocean chemistry (Coggon et al., 2010). The 15 Ma site was chosen for comparison to

Hole 1256D (Expedition 309/312 Scientists, 2006; Expedition 335 Scientists, 2012).

Leg 3 drilling results provide an indication of what to expect in the sedimentary columns of the SAT sites (Scientific Party, 1970). Leg 3 drilled ten sites in the equatorial and South Atlantic Ocean between Senegal and Brazil, including seven sites along a transect across the MAR that penetrated to basement (Sites 14–20). The basal sediment ages were within a few million years of the inferred magnetic anomaly ages, which is consistent with a half spreading rate of ~20 mm/y since 76 Ma. Recovery in the cored intervals was typically high (>98%), but the sediments were only spot cored, and there are significant gaps between cored intervals. The recovered cores make up an almost continuous Lower Cretaceous to Pleistocene composite stratigraphic section. All sites yielded calcareous sediments with calcareous nannoplankton and planktic foraminifers. Chert occurred only in association with siliceous microfossils, which were recovered only from the eastern MAR flank (Sites 17 and 18) in lower Tertiary and Quaternary sediments. There was no evidence of turbidity currents or mass slide debris. Basalts (0.05–2 m penetration) were recovered from each site, and they comprise variably altered extrusive rocks with common glass and some calcium carbonate veins.

Depth of basement drilling

Expeditions 390 and 393 will establish legacy basement boreholes with reentry cones and casing to near basement. Our target is to core ~250 m into the uppermost basaltic ocean crust at each site. To fully quantify the extent and duration of hydrothermal exchange, we need our sampling to be as representative as possible of the entire extrusive crust. A systematic downward decrease in the extent of oxidative hydrothermal alteration is not observed through all previously drilled upper crustal sections (Wilson et al., 2003), and the permeability of the extrusive crust is highly heterogeneous and not always greatest at the top of the basement (Becker et al., 2013). Commonly, fluid flow in the upper crust is channeled along specific horizons of enhanced permeability (Harris et al., 2015; Neira et al., 2016). At many drill sites globally, the fluid temperature–depth distribution recorded by hydrothermal carbonate veins, typically one of the last hydrothermal phases to form, indicates the circulation of cool (<70°C) ridge flank fluids through at least the upper 300 m (Coggon et al., 2010). If there is a depth limit to off-axis fluid circulation, sufficient basement drilling is required to establish what it is and how it varies across the ridge flanks; therefore, we need to achieve the maximum possible basement penetration. Consequently, we will establish legacy holes that can be deepened during subsequent operations if drilling on these combined expeditions is insufficient to describe the hydrothermal alteration in the uppermost crust at each age.

Seismic studies/site survey data

The supporting site survey data for Expeditions 390 and 393 are archived at the IODP Site Survey Data Bank (**https://ssdb.iodp.org/SSDBquery/SSDBquery.php**; select 853 for proposal number).

The SAT is located where fracture zones are far apart, magnetic lineations are clear, and there is little disruption in seafloor bathymetry (Figure **F1**). In January–February 2016, the Crustal Reflectivity Experiment Southern Transect (CREST) cruise (**http://dx.doi.org/10.1594/IEDA/500255**) aboard the R/V *Marcus G. Langseth* conducted a detailed geophysical survey across the western MAR flank along a crustal flow line at ~31°S (Figure **F1**) that included a 1500 km multichannel seismic reflection profile from the ridge crest to the Rio Grande Rise (RGR) spanning 0–70 Ma crust, two shorter ridge-crossing profiles spanning 0–7 Ma crust, and five ridge-parallel profiles. Ocean bottom seismometer profiles were acquired coincident with the ridge-parallel profiles. Gravity, magnetics, multibeam bathymetry, and backscatter data were also acquired.

The present-day MAR axis at 30°–32°S has a well-defined axial valley with two inferred active vents (Schmid et al., 2019). The CREST seismic survey crossed a ridge segment that is ~100 km long and bounded to the north and south by ridge offsets ~16–22 km in width. The absence of domal structures near the ridge axis that represent oceanic core complexes (OCCs) formed by detachment faulting and the well-defined marine magnetic anomalies on the ridge flanks (Cande and Kent, 1995) are consistent with the accretion of Penrose-type layered magmatic crust.

Kardell et al. (2019) calculated ages and spreading rates from magnetic data acquired during the CREST cruise (Figure **F5**). Ages of the primary sites are estimated at 6.6, 15.2, 30.6, 49.2, and 61.2 Ma with half spreading rates of 17.0, 25.5, 24.0, 19.5, and 13.5 mm/y, respectively (Table **T1**). If 20 mm/y is used to separate slow and intermediate spreading rates (Perfit and Chadwick, 1998), then the primary sites were emplaced at both slow and intermediate spreading rates.

Seismic imaging along the CREST transect shows, at all ages from 0–65 Ma, an abundance of unsedimented, exposed basement outcrops that may allow the ingress and egress of seawater and ridge flank hydrothermal fluids. This suggests that the crust is never fully sealed by sediment at these ages (Estep et al., 2019) and that there may be long-lived and ongoing connection between the oceans and uppermost basaltic crust with implications for biogeochemical exchanges and subsurface microbial activity. Seismic Layer 2A is imaged in 0–48 Ma crust but not in older crust (Estep et al., 2019). Velocities at the top of basement increase rapidly from 2.4 km/s at 0 Ma to 4.2 km/s at 6 Ma and then continue to increase gradually to 4.9 km/s at 58 Ma (Kardell et al., 2019). The presence of unsedimented basement outcrops, persistent imaging of Layer 2A, and continued velocity increase at the top of basement are consistent with fluid circulation within the upper crust that continues to at least 48–58 Ma (Estep et al., 2019; Kardell et al., 2019). The seismic transect ends just east of the eastern margin of the RGR, which may have affected the thermal history of the lithosphere and the structure of the crust some distance to the east. Careful reconstruction of the Tristan de Cunha hotspot history (O'Connor and Duncan, 1990) indicates that ~70 My ago the spreading axis migrated westward, terminating formation of the RGR, and normal spreading resumed directly to the east of the RGR between 30° and 34°S.

All primary and alternate sites are positioned in localized sedimentary basins that are imaged on seismic reflection profiles. Unsedimented basement ridges are within 1–2 km of most primary sites (Figure **F4**). Sediment thicknesses are calculated using a constant sediment velocity of 1800 m/s and vary from 50 m at Proposed Site SATL-13A to 639 m at Proposed Site SATL-54A (Table **T1**).

Scientific objectives

1. *Objective 1 (primary): quantify the timing, duration, and extent of ridge flank hydrothermal fluid-rock exchange.*

Scientific justification

Hydrothermal circulation at MORs and across their vast ridge flanks influences tectonic, magmatic, and microbial processes on a global scale; is a fundamental component of global biogeochemical cycles of key elements and isotopes (e.g., O, S, Mg, Fe, Li, B, Tl, and ^{87}Sr); and facilitates geological CO_2 sequestration within the ocean crust. The chemical and isotopic composition of seawater reflects the dynamic balance between riverine inputs from the continents, burial of marine sediments, and hydrothermal exchanges with the ocean crust (e.g., Palmer and Edmond, 1989). Ocean crust is young and chemically relatively homogeneous compared to continental crust, and its chemical exchanges with seawater are limited to a few relatively well known reactions. Consequently, hydrothermal contributions to ocean chemistry are simpler to reconstruct than riverine inputs (Coggon and Teagle, 2011; Davis et al., 2003; Vance et al., 2009). Knowledge of the rates and magnitudes of hydrothermal exchanges will help us to decipher the changing global conditions responsible for past variations in seawater chemistry, such as mountain building, changes in seafloor spreading rate, large igneous province emplacement, changing climate, and evolution of biological systems. Science Plan Challenge 10 (Earth Connections theme) therefore asks, "What are the mechanisms, magnitude, and history of chemical exchanges between the oceanic crust and seawater?" and recognizes the answer requires ocean basin–wide transects across ridge flanks with different hydrogeologic histories.

Conductive heat flow deficits indicate that, on average, hydrothermal exchange persists at low temperatures (<<100°C) to 65 Ma on the ridge flanks (Stein and Stein, 1994). Given the vast extent of the ridge flanks, the hydrothermal fluid flux through them is many orders of magnitude greater than that through high-temperature (≤400°C) axial systems (Mottl, 2003) and is likely important for elements for which fluid-rock exchange occurs at low temperatures (e.g., Mg, K, S, Li, B, C, and H_2O). Hydrothermally altered ocean crust provides a time-integrated record of geochemical exchange with seawater manifested through changes in its chemical and isotopic composition, mineral assemblages, and physical properties (e.g., porosity, permeability, and seismic properties). The intensity of seawater-basalt exchange depends on the crustal age, architectural and thermal history, and spreading rate. Consequently, hydrothermal contributions to global geochemical cycles depend on the global length of slow-, intermediate-, and fast-spreading ridges and the age-area distribution of the ridge flanks, which have varied significantly throughout the Phanerozoic (Müller et al., 2008). However, the impact of these variations on geochemical cycles is uncertain because the magnitude and spatial and temporal distribution of crust-seawater hydrothermal exchanges are poorly quantified. For example, the role of MOR spreading in controlling past atmospheric CO_2 and hence climate remains controversial (Alt and Teagle, 1999; Berner et al., 1983; Gillis and Coogan, 2011; Staudigel et al., 1989) because of uncertainties regarding the rate, extent, and duration of hydrothermal $CaCO_3$ precipitation due to our sparse sampling of intermediate age ocean crust (Figure **F2**). The hydrothermal carbonates that sequester CO_2 in the ocean crust also record the composition of the fluids from which they precipitate (Coggon et al., 2004) and provide an exciting opportunity to develop medium-resolution records of past ocean chemistry (e.g., Mg/Ca and Sr/Ca) (Coggon and Teagle, 2011; Coggon et al., 2010; Rausch et al., 2013), which integrates past changes in major Earth system processes such as plate tectonics, mountain building, and climate. However, this approach is limited by the poor sampling of ocean crust of a variety of ages.

Drilling experiments on the Juan de Fuca Ridge flank were a key investigation of hydrothermal evolution across a ridge flank but were restricted to young (<3.6 Ma), intermediate-spreading (29 mm/y half spreading rate) crust (Davis et al., 1997; Expedition 301 Scientists, 2005; Expedition 327 Scientists, 2011). There is a dearth of holes in 20–100 Ma intact in situ MOR crust and no significant penetrations (>100 m) of 46–120 Ma crust (Figure **F2**) (Expedition 335 Scientists, 2012). Consequently, the critical thermal, hydrogeologic, chemical, and microbial transitions across the ridge flanks remain unknown (Figure **F6**). Our current sampling of in situ upper ocean crust (>100 m) is biased toward areas with anomalously thick sediment for their crustal ages (Figure **F3**), and the majority of holes in ocean crust >35 Ma penetrate intermediate- or fast-spreading crust. The recovery of uppermost basement sections along the SAT across slow/intermediate-spreading MAR crust will address these sampling gaps with respect to age, spreading rate, and sediment thickness.

Crustal accretion along the northern MAR is complex, with significant regions where spreading is accommodated by amagmatic extension by detachment faults that exhume sections of deep lithosphere to form OCCs (Mallows and Searle, 2012). However, a recent survey of the modern southern MAR during Cruise MSM25 of the R/V *Maria S. Merian* (2013) found no OCCs between 25° and 33°S (Devey, 2014). This, combined with the relatively well defined marine magnetic anomalies on the southern MAR flanks (Maus et al., 2009), is consistent with accretion of intact magmatic crust. Because the ~31°S SAT follows a crustal flow line through a relatively long spreading segment (~100 km) away from major transform faults, we expect a Penrose-type stratigraphy of lavas overlying dikes and gabbros to have been accreted along the transect (Penrose Conference Participants, 1972).

Expected outcomes

Hydrothermal alteration of basement cores will be investigated using a combination of petrological and geochemical analyses, radiometric dating, and detailed quantitative core logging of rock types, alteration features, and veins. The recovery of thinly sedimented slow/intermediate-spreading ocean crust along the proposed SAT will provide the following opportunities:

- To determine the nature, rates, magnitudes, distribution, and duration of hydrothermal alteration across the ridge flank;
- To investigate the effect of titanomagnetite/titanomaghemite alteration on the magnetic anomaly signal to elucidate its origin;
- To compare hydrothermal alteration of the uppermost slow/intermediate-spreading crust with crust of similar ages produced at faster spreading ridges (e.g., Holes 504B and 1256D);
- To evaluate the effect of changes in global spreading rates and the age-area distribution of the seafloor on hydrothermal contributions to global biogeochemical cycles; and
- To investigate signatures of changing ocean chemistry in the hydrothermal record and develop medium-resolution records of past ocean chemistry using hydrothermal minerals (following Coggon et al., 2010).

It will also allow us to test the following hypotheses:

- Hydrothermal chemical exchange ceases within 20 My of crustal formation.
- Basement topography and sedimentation history affect the rate and duration of hydrothermal alteration.

Relationship to the IODP Science Plan

Challenge 10: What are the mechanisms, magnitude, and history of chemical exchanges between the oceanic crust and seawater?

Recently there has been a dramatic shift in appreciation of the value and application of studies of hydrothermally altered ocean crust, which can be used to both reconstruct records of past ocean chemistry and decipher the changes to global conditions responsible for variations in these records. The ultimate goal, as stated in Challenge 10, is to drill a series of ocean-wide transects along plate tectonic flow lines, from zero-age MOR crust to >100 Ma, with transects required across a range of spreading rates and tectonic styles. Drilling the SAT during Expeditions 390 and 393 will constitute a major contribution to this effort and significantly advance our understanding of how the ocean crust ages and the influence of this process on ocean chemistry through time. It will also provide better age resolution for investigations of past seawater chemistry based on crustal alteration.

Challenge 13: What properties and processes govern the flow and storage of carbon in the subseafloor?

A key goal of Challenge 13 is to investigate opportunities for geoengineered carbon sequestration in the deep sea to mitigate future climate change. The permeable upper ocean crust is of particular interest because it constitutes a vast potential reservoir for CO_2 trapping in areas where the crust is isolated from the oceans by low-permeability sediments (Marieni et al., 2013) or permanent storage through carbonate mineralization (Matter et al., 2016). Hydrothermal carbonate precipitation provides a natural analogue for potential industrial-scale CO_2 sequestration through carbonate mineralization of basalt. Knowledge of the controls on the extent, rate, and duration (Coogan et al., 2016; Harris et al., 2014) of natural CO_2 sequestration along the SAT will assist efforts to assess the feasibility of geoengineered CO_2 sequestration within the ocean crust (Marieni et al., 2013).

2. *Objective 2 (primary): investigate sediment- and basement-hosted microbial community variation with substrate composition and age*

Scientific justification

Scientific ocean drilling has revealed that microorganisms, Archaea, Bacteria, and eukaryotic fungi and protists are present, intact, and metabolically active in uncontaminated deep subsurface sediment and basalt. Knowledge about subseafloor microbial communities has grown exponentially since the initial microbial investigations by DSDP in the 1980s, but <4% of ODP/Integrated Ocean Drilling Program/IODP sites sampled have been sampled, documented, or archived for microbiological purposes (Figure **F7**) (Kallmeyer et al., 2012; Orcutt et al., 2014). Determining microbial community composition and physiological capabilities along the SAT will provide insights into the role of microbes in mineral alteration, hydrocarbon formation, and global biogeochemical cycles. The Science Plan Biosphere Frontiers theme therefore asks, "What are the origin, composition, and global significance of subseafloor communities?" (Challenge 5) and "How sensitive are ecosystems and biodiversity to environmental change?" (Challenge 7).

In sediments, the number of microbial cells present is estimated to equal that in the entire oceanic water column (Kallmeyer et al., 2012). However, the amount of biomass stored in the deep subsurface remains contentious because microbial cell abundance in subseafloor sediment varies by approximately five orders of magnitude (Figure **F7**) with significant geographic variation in the structure of subseafloor communities (Inagaki et al., 2006). The majority of studies have focused on relatively high biomass continental shelf systems. Recent efforts, including IODP Expeditions 329 (South Pacific Gyre; Expedition 329 Scientists, 2011) and 336 (North Pond; Expedition 336 Scientists, 2012), investigated lower biomass sedimentary systems underlying oceanic gyres. Crucially, no data have been collected from the South Atlantic Gyre (SAG). Such data would refine the global biomass census and improve our understanding of the global carbon cycle.

The presence or absence of oxygen in marine sediments has profound implications for the quantity, diversity, and function of microbial communities. Oxygen penetration depth varies between oceanic regions and settings, ranging from only a few millimeters in areas with high rates of microbial respiration, such as on continental shelves, to the entire sediment column in extremely low biomass sediments, such as those beneath the South Pacific Gyre (D'Hondt et al., 2015). Extrapolation of an observed global relationship between oxygen penetration and sedimentation rate and thickness indicates SAG sediment may be oxic to basement (D'Hondt et al., 2015). During Leg 3, oxygen was not measured, but sulfate was detected near the basement. However, sediment organic carbon concentrations along the SAT are intermediate to those of North Pond, where oxygen penetrated tens of meters below seafloor (mbsf) and nitrate was present to basement, and Nankai Trough, where oxygen was depleted by 3 mbsf and sulfate depleted by 19 mbsf (Figure **F8**) (Expedition 336 Scientists, 2012; Tobin et al., 2009; Orcutt et al., 2013; Reese et al., 2018). This indicates that oxygen is unlikely to extend to the basement at sites along the SAT, contrary to model predictions (D'Hondt et al., 2015), and that the classical redox succession of oxygen respiration followed by nitrate reduction, and potentially followed by metal reduction, may be present. However, we hypothesize that oxygen will be reintroduced at the bottom of the sediment column as a result of oxygenated fluid fluxing from the basement, which is the case at North Pond (Expedition 336 Scientists, 2012). The recovery of the sediment package will allow us to address this conundrum regarding oxygen penetration, biomass, and carbon limitation of microbial activity.

We will compare the phylogenetic diversity, functional structure, and metabolic activity of SAG communities with results from previously studied regions. By exploiting the variations in sediment carbon composition expected across the subsiding MOR flank, we can examine the response of autotrophy versus heterotrophy to carbonate chemistry. Additionally, previous studies of the sedimentary deep biosphere have explored community diversity based on site-to-site or downhole (age) comparisons, often implicitly assuming a similar "starter community" that colonized the seafloor and whose structure and function subsequently changed in response to evolving geochemical conditions or burial depth. However, recent work suggests energy limitation may preclude replication (Lever et al., 2015; Lomstein et al., 2012) and thus limit community changes. The proposed age-transect approach will allow us to test this assumption directly by investigating the impact of burial depth and chemical zonation on sediment of the same age and hence the same starter community.

Given the dearth of basement holes in ocean crust of intermediate age, there are no microbiological samples across the critical ridge–flank transitions in basement properties that may affect microbial communities (Figure **F6**). The majority of biological alteration of subseafloor basalts is thought to occur within 20 My of crustal formation (Bach and Edwards, 2003). However, microbiological investigations of oceanic basement have focused on young (<10 Ma) crust (Jungbluth et al., 2013; Lever et al., 2013; Mason et al., 2010; Orcutt et al., 2011) or older (>65 Ma) lava associated with hotspot volcanism along the Louisville seamount trail (Expedition 330 Scientists, 2012; Sylvan et al., 2015). Basement outcrops that penetrate the relatively impermeable sediment provide permeable conduits that facilitate subseafloor fluid circulation in older basement (Wheat and Fisher, 2008). Fluid flow across the basement–sediment interface can produce redox gradients that provide recharge of depleted electron acceptors (e.g., oxygen and nitrate) to basal sediments, as observed above 3.5 and 8 Ma ocean crust on the Juan de Fuca Ridge flank (Engelen et al., 2008) and at North Pond (Orcutt et al., 2013), respectively. However, the extent and duration of fluid flow through this interface across the ridge flanks remains unknown (Figure **F6**). The recovery of the uppermost basaltic basement from 7 to 61 Ma along the SAT will allow us to determine whether microbial populations are indeed present in basement older than 20 Ma and to investigate the nature, extent, and duration of communication between the sedimentary and crustal biosphere for the first time.

Expected outcomes

We will sample subseafloor populations of Bacteria, Archaea, and microbial eukaryotes in both the sedimentary and upper crustal ecosystems along the proposed transect, quantify their biomass by cell enumeration, identify them using molecular biology methods, measure the stable isotopic composition (C, N, and S) of sediment and basement to relate processes to geochemistry, measure their metabolic activities using a variety of incubation assays, and resolve their physiological adaptations with omics-based approaches with the following aims:

- To evaluate cell abundance and community activity in the low-energy subseafloor biosphere of the SAG and refine estimates of global subseafloor sedimentary microbial abundance;
- To resolve model predictions about the depth of oxygen penetration into sediment from overlying seawater and into the bottom of the sediment package from oxygenated fluid in basement;
- To evaluate the role of subseafloor microbes in sediment biogeochemistry and basement alteration and hence global biogeochemical cycles; and
- To investigate how aging of the ocean crust influences the composition of the crustal biosphere, in particular the effects of changing oxidation state and permeability on microbial abundance, diversity, and function.

Our samples will also allow us to test the following hypotheses:

- SAG microbial communities share membership and function with both oligotrophic sediments, like those found at North Pond, and open ocean systems with higher organic matter input, such as Nankai Trough, given the intermediate organic carbon content of the SAT sites.
- Microbial community structure and diversity depends on the starter community (and hence sediment age) rather than subsequent selection driven by burial or chemical zonation.
- Crustal biomass decreases with increasing basement age, and communication between the sedimentary and crustal biosphere ceases within 20 My.
- Microbial diversity increases within subseafloor basalts with basement age as previously demonstrated in basalts exposed on the seafloor (Lee et al., 2015; Santelli et al., 2009).

Relationship to the IODP Science Plan

Challenge 5: What are the origin, composition, and global significance of subseafloor communities?

Using modern molecular biology tools, we will be able to determine the phylogenetic and functional composition of the subseafloor communities across an age transect beneath the SAG. Crucially, we will be able to detect overlaps in community membership, if they occur, between basement and sediment communities and between younger and older sites. The SAT will fill critical gaps in our global sampling of the deep biosphere with respect to geographic location and basement age. Quantification of the biomass and rates of microbial activity in these samples will significantly advance our understanding of the global significance of the deep biosphere.

Challenge 7: How sensitive are ecosystems and biodiversity to environmental change?

We will investigate this question for both sediment- and basement-hosted ecosystems. Through the sediment sections, we will correlate paleoceanographic records with microbiological composition and activity to investigate how past environmental events have influenced current communities. This has been demonstrated for very shallow sediment communities (Hamdan et al., 2013) but never investigated in deeper sediments. Using recovered basement cores, we will investigate microbial diversity as a function of the changing hydrological, physical, and chemical conditions across the aging ridge flank. We predict an increase in diversity with distance from the MAR due to increased niche creation as basalts age.

3. *Objective 3 (secondary): investigate the responses of Atlantic Ocean circulation patterns and the Earth's climate system to rapid climate change including elevated atmospheric CO_2 during the Cenozoic*

Scientific justification

Climate change due to increased atmospheric CO_2 poses significant and imminent threats to global society and the environment. Knowledge of past ocean circulation patterns and temperatures are required to assess the skill of numerical models in simulating intervals of high pCO_2. The Science Plan Climate and Ocean Change theme therefore asks, "How does Earth's climate system respond to elevated levels of atmospheric CO_2?" (Challenge 1).

High pCO_2 intervals are often characterized by relatively shallow lysocline and calcite compensation depths (CCDs) resulting in poor preservation of $CaCO_3$ microfossils used to reconstruct paleoceanographic records. This problem can be overcome by coring sediment deposited on basement slightly older than the targeted sediment age that accumulated prior to thermal subsidence of the seafloor below the CCD. More continuous composite stratigraphic

sequences are obtained by drilling multiple sites along a crustal-age transect, a strategy successfully employed during ODP Leg 199 (Shipboard Scientific Party, 2002) and Integrated Ocean Drilling Program Expedition 320/321 (Pälike et al., 2012). The Walvis Ridge depth transect sampled during ODP Leg 208 demonstrated the dynamic nature of the Cenozoic CCD and lysocline in the southeastern Atlantic (Shipboard Scientific Party, 2004) and the value of redrilling previous transects to collect more complete records of Earth history. Although spot cored, Leg 3 sites demonstrate moderate to excellent carbonate preservation along the SAT (Scientific Party, 1970) and its suitability for high-resolution paleoclimatic and paleoceanographic reconstructions through key intervals of rapid climate change (Figure **F9**) (Cramer et al., 2009; Zachos et al., 2001, 2008), including the PETM and other short-lived hyperthermals, early and middle Eocene climatic optima, onset of Antarctic glaciation across the Eocene/Oligocene boundary (Oi1 event), multiple Oligocene and Miocene glaciation events (Oi and Mi events), Miocene climatic optimum and Monterey Carbon Excursion, Pliocene warmth, and the onset of Northern Hemisphere glaciation.

Global ocean circulation transfers heat and nutrients around the globe, both influencing and responding to changes in Earth's climate system (Broecker, 1991; Stommel, 1961; Wunsch, 2002). Fortuitously, the western intensification of ocean currents means we can substantially reconstruct deepwater mass properties and thus thermohaline circulation history by characterizing western portions of major ocean basins using drilling transects. The western South Atlantic is the main northward flow path of Antarctic Bottom Water (AABW) and southward flow path of North Atlantic Deep Water (NADW) and their precursor water masses. Consequently, the SAT cores will provide complementary data needed to constrain the evolution of thermohaline circulation patterns and climate change as the Drake Passage and Southern Ocean opened, the northern North Atlantic deepwater gateway opened, and the Tethys Ocean became restricted to thermohaline circulation. In particular, these cores will assist in establishing how high-latitude sea surface (and hence deep ocean) temperatures and the CCD varied in response to pCO_2 changes and ocean acidification (Barker and Thomas, 2004; Barrera et al., 1997; Billups, 2002; Bohaty et al., 2009; Cramer et al., 2009; Frank and Arthur, 1999; Kennett and Stott, 1991; Scher and Martin, 2006; Thomas et al., 2003; Wright et al., 1991, 1992). The SAT will yield a complementary record to western North Atlantic sediments (Expedition 342; Norris et al., 2014), and together these data will provide an exceptional record of the evolution of Atlantic overturning circulation through the Cenozoic.

A novel, direct way to compare paleoceanographic reconstructions of past high pCO_2 to modern conditions is to recover sediments along transects of water column data collected by the WOCE. The SAT constitutes a "paleo-WOCE" line following the western portion of WOCE Line A10 (Figure **F10**), providing access to paleoceanographic records of southern and northern-sourced deep and bottom waters. We will test models of bipolar deepwater evolution (e.g., Borelli et al., 2014; Cramer et al., 2009; Katz et al., 2011; Tripati et al., 2005) using stable and radiogenic isotope analyses of sediments recovered from these key western South Atlantic sites.

The Walvis Ridge depth transect (Shipboard Scientific Party, 2004) revealed a dramatic 2 km CCD shoaling during the PETM due to the acidification of the ocean from massive carbon addition followed by a gradual recovery (Figure **F11**) (Zachos et al., 2005; Zeebe et al., 2008). Given chemical weathering feedbacks, the recovery of the CCD should have resulted in a transient over-deepening of the CCD (Dickens et al., 1997). Collectively, the SAT sites will provide additional data for reconstructing changes in the position of the lysocline and CCD in the western South Atlantic that are essential for constraining the timing of gateway events and the history of Northern Component Water (NCW) and Southern Component Water (SCW), which were the precursors to NADW and AABW, and the nature of Atlantic basin responses to climate change relative to the Pacific.

Expected outcomes

Microfossils provide a critical archive of ocean and climate history including long-term changes (e.g., early Eocene warmth, Cenozoic cooling, and Pliocene warmth) and abrupt events (e.g., early Paleogene hyperthermals and multiple glaciation events). Complete sedimentary sections recovered along paleo-WOCE Line A10 will exploit thermal subsidence of the ocean crust along the transect to provide material for high-resolution proxy records including benthic and planktic foraminiferal geochemistry, micropaleontological assemblages, orbitally tuned age models, neodymium isotopes, and alkenone $\delta^{13}C$ and boron isotope pCO_2 reconstructions with the following aims:

- To reconstruct the evolution of deepwater masses over the past 61 My to assess contributions of NCW and SCW in the early Paleogene western South Atlantic (Kennett and Stott, 1990) and to document the influence of the openings of the Drake and Tasman Passages on South Atlantic deepwater circulation;
- To provide high-resolution constraints on CCD and carbonate chemistry changes of the deep western Atlantic, particularly during transient hyperthermals and other intervals of global warmth;
- To reconstruct the Cenozoic history of the South Atlantic subtropical gyre by monitoring proxies of productivity and paleobiogeography of oceanic plankton, rates of speciation/extinction relative to the equatorial zone and higher latitudes, and changes in biodiversity and subtropical ecosystem dynamics; and
- To evaluate the response of subtropical planktic and benthic biota to changing environmental conditions such as global warming, ocean acidification, or fertility patterns during intervals of rapid climate change through the Cenozoic.

They will also allow us to test the following hypotheses:

- Low latitude sites were potential sources of deep water formation at times of global warmth and high atmospheric pCO_2.
- The strength of the coupling between the climate and the carbon cycle varied through the Cenozoic.
- The lysocline and CCD responded differently on the western side of the MAR compared to the Walvis Ridge record due to changing deep/bottom water sources, gateway configurations, and flow paths.
- The subtropical gyre cut off the delivery of heat to Antarctica as the Antarctic Circumpolar Current developed through the late Eocene–Oligocene.

Relationship to the IODP Science Plan

Challenge 1: How does Earth's climate respond to elevated levels of atmospheric CO_2?

The SAT will focus on the rates and consequences of Cenozoic global warming. We will improve estimates of global climate sensitivity to higher levels of greenhouse gases and transient perturbations to the carbon cycle such as hyperthermals. SAT sites can help

us understand how tropical–subtropical temperatures and productivity responded to a high-CO_2 world and how the planktic and benthic biosphere responded to global warming and ocean acidification.

Challenge 2: How do ice sheets and sea level respond to a warming climate?

The deep Atlantic record will shed new light on where and when deep/bottom water masses formed and how these sites responded to a warming climate. The SAT will sample the primary flow paths of NCW and SCW through the South Atlantic, providing new constraints on reconstructions of ocean circulation and its response to gateway changes and abrupt cooling and warming events.

Challenge 4: How resilient is the ocean to chemical perturbations?

The SAT is uniquely situated to assess both the Atlantic basin response to global warming and changes in thermohaline circulation in the main axis of deep ocean circulation west of the MAR and document changes in the lysocline and CCD in response to ocean acidification associated with hyperthermals. The SAT will be compared with records from Walvis Ridge, which indicate very dynamic deep-sea carbonate chemistry during the Cenozoic (Figure **F11**) and other basins to investigate their variable responses. The response of planktic organisms of the biologically diverse subtropical gyre will be compared with emerging trends of ocean acidification today.

Operations plan/coring strategy

To fully achieve the SAT objectives and establish legacy boreholes for future basement experiments, we plan the following operations for each site: (1) recover a complete sediment section, (2) install a drill-in reentry cone and casing to near the sediment/basalt boundary, (3) core to ~250 m subbasement, and (4) collect wireline geophysical logging data through the basement sections.

Sedimentary intervals of particular interest include geochemical zones (e.g., oxic, nitrate reducing, Fe-reducing, and sulfate–methane transition zones) within the deep biosphere and records through key Paleogene and Neogene paleoceanographic events (Figure **F9**). The sediment–basement interface is an important target, especially because it has not previously been well studied for microbiological investigations. The sediments are expected to be predominantly calcareous ooze (Scientific Party, 1970). To recover complete stratigraphic sections, we will therefore use the advanced piston corer (APC) system when drilling conditions permit. We expect to transition to the extended core barrel (XCB) system at ~250 m in thick sediment at Proposed Site SATL-54A. The rotary core barrel (RCB) system will be used in basaltic basement. RCB coring recovery rates in basaltic basement are highly variable because they depend on the drilling conditions and the extent of brecciation/fracturing and typically average <30% (Figure **F2**). In combination with wireline logging, using detailed core-log integration following Tominaga et al. (2009), these recovery rates should be sufficient to accomplish our basement objectives.

The operations plans for Expeditions 390 and 393 are summarized in Tables **T2** and **T3**, and the time required for operations at alternate sites are summarized in Table **T4**. The time required to complete these operations was estimated assuming (1) APC/XCB recovery of sediments at ~10 m/h, which is consistent with previous drilling in similar rock types (e.g. Shipboard Scientific Party, 2004), and (2) decreasing rates of basalt penetration during RCB operations of 4.5 m/h in the uppermost 50 m, 3 m/h through the subsequent 100 m, and 2 m/h thereafter based on previous drilling results in basaltic basement. The time allocated for wireline logging includes deployment of the advanced piston corer temperature tool (APCT-3), the triple combo tool with the Ultrasonic Borehole Imager (UBI), and at least two passes of the Formation MicroScanner (FMS) at each site.

Sediment coring strategy

The SAT comprises six sites located at five different crustal ages (~7, 15, 31, 49, and 61 Ma), and two of the sites are located in the same localized sedimentary basin on 61 Ma crust where significant basement topography results in variable sediment thickness (~180 and 640 m thick at Proposed Sites SATL-53B and SATL-54A, respectively). At each of the five crustal ages, we will drill three sediment holes. This will allow compilation of complete paleoceanographic records across core breaks using stratigraphic correlation and provide sufficient material for whole-round microbiological and pore water sampling. At crustal ages of 7, 15, 31, and 49 Ma, this will be achieved by triple APC coring at a single site (SATL-13A, SATL-25A, SATL-33B, and SATL-43A, respectively). The triple coring of the sediment section on 61 Ma crust will comprise (1) an APC hole to refusal (estimated to occur at 250 mbsf depending on drilling conditions) at Proposed Site SATL-54A followed by XCB coring to basement (~639 mbsf) and (2) two APC holes to basement at Proposed Site SATL-53B (180 mbsf). This sediment coring strategy was designed to (1) ensure we recover three APC sections of the uppermost sedimentary section at a basement age of 61 Ma and (2) optimize the drilling operations that can be achieved during Expeditions 390 and 393 because it allows sedimentary coring to be completed at Proposed Sites SATL-53B and SATL-54A using a single pipe trip because they are only 1.2 nmi apart. Given the efficiency of this strategy, all sediment coring at Proposed Sites SATL-53B and SATL-54A will be conducted during Expedition 390. The basement operations at Proposed Site SATL-54A will be conducted during Expedition 393 to achieve the required balance of operations across the two expeditions and ensure that our highest priority basement coring is achieved first. Given our uncertainty regarding the sediment thickness and to ensure that the sediment–basement interface is well sampled at all crustal ages, we plan to use XCB coring to sample the uppermost basement in all sediment holes. All sediment cores will be oriented except for those from Proposed Site SATL-13A, where the sediment is only expected to be ~50 m thick. Temperature measurements will be made during sediment coring using the APCT-3 with the number of measurements taken dependent on the sediment thickness (typically three or four; Tables **T2**, **T3**, **T4**).

Basement coring strategy

At each of the six primary sites, we will install a standard "drill-in" reentry cone system with 13⅜ inch casing. Given that the sediment–basement interface is a key target for both our hydrothermal and microbiological primary objectives, we will extend the casing to just above this interface to allow us to recover the uppermost basement during RCB operations. If, however, this interface has already been successfully sampled during XCB operations, a decision may be taken to extend the casing into the basement to improve hole stability. The reentry cone systems have been designed with 13⅜ inch casing to allow for future installation of a narrower 10¾ inch casing string across the sediment–basement interface (and deeper into

basement) to stabilize this region of the holes if they are reoccupied during any future drilling investigations. Following installation of the reentry cone system, we will deploy two RCB bits in each hole. Given the expected basement penetration rates and 40–50 h rotation on each RCB bit, the expected basement penetration is 250 m using two RCB bits at each site. To ensure that the holes are left clean for any future operations, the second RCB bit will be dropped on the seafloor rather than in the hole prior to wireline logging operations.

Microbiological operations

Shipboard microbiological sampling will follow standard protocols (Lever et al., 2006; Smith et al., 2000). Perfluorocarbon tracers will be used to monitor potential contamination, and drilling fluid samples will be taken for cross-reference during postexpedition research.

Proposed drill sites

The SAT comprises six primary drill sites located at five different crustal ages. For each primary site, we have identified one or two alternate sites (Table **T1**). It was not possible to exactly match sediment thickness between primary and alternate sites. Multiple alternate sites for each primary site with varying sediment thickness were therefore chosen to provide a range of options dependent on the desired scientific outcomes and/or operational requirements that necessitate operations at an alternate site.

1. Proposed Site SATL-13A (primary) is located nearest to the MAR on 6.6 Ma crust formed at a half spreading rate of 17 mm/y and overlain by ~50 m of sediment. This site provides a comparison to young ocean crust drilled at reference Hole 504B (6.9 Ma; spreading rate of 36 mm/y; 275 m of sediment). Alternate Proposed Sites SATL-11B (~4 km north) and SATL-12A (~17 km north) formed at the same age and spreading rate but have sediment thicknesses of 104 and 96 m, respectively.
2. Proposed Site SATL-25A (primary) is located on 15.2 Ma crust formed at 25.5 mm/y and overlain by ~104 m of sediment. This site provides a comparison to reference ocean crust at Site 1256 (15 Ma; spreading rate of 220 mm/y; 250 m of sediment). Alternate Proposed Site SATL-24A is located ~1 km to the west and has a similar sediment thickness (~94 m). Alternate Proposed Site SATL-23A is located ~5 km to the east and has a sediment thickness of ~162 m.
3. Proposed Site SATL-33B (primary) is located on 30.6 Ma crust formed at 24 mm/y and overlain by ~138 m of sediment. Alternate Proposed Sites SATL-31A (~5.5 km south) and SATL-35A (~8 km north) formed at the same age and spreading rate and have sediment thicknesses of 183 and 93 m, respectively.
4. Proposed Site SATL-43A (primary) is located on 49.2 Ma crust formed at 19.5 mm/y and overlain by ~148 m of sediment. Alternate proposed sites are SATL-41A (~11 km south; ~203 m sediment) and SATL-44A (~3 km west; ~176 m sediment).
5. Proposed Site SATL-53B (primary) is located on 61.2 Ma crust formed at 13.5 mm/y and overlain by ~180 m of sediment. Alternate Proposed Site SATL-55A is ~22 km to the north and has a sediment thickness of ~126 m.
6. Proposed Site SATL-54A (primary) is located on 61 Ma crust formed at 13.5 mm/y and overlain by ~639 m of sediment. Alternate Proposed Site SATL-56A is ~10 km to the east and has a sediment thickness of ~510 m.

Wireline logging/downhole measurements strategy

Wireline logging is planned with two tool strings at all six of the SAT sites principally to characterize features of the basaltic ocean crust such as lava morphology, structure, fractures, veins, porosity, and sonic velocity. Logging data provide in situ formation characterization that are unaffected by core expansion. These will be complementary to descriptions and analyses of the core itself and will provide continuous observations throughout the basement intervals as well as the only information on the unrecovered intervals across core gaps. The tools will be deployed in the rotary-drilled basement hole at each site. Because these holes will be cased down to close to the basement/sediment contact, only natural gamma radiation logs will be useful for the sediment section. The possible exception to this is the 639 m deep sediment hole at Proposed Site SATL-54A, drilled early in Expedition 390, which could be logged as a contingency operation during Expedition 393.

The operational plans (Tables **T2**, **T3**) include deployment of two tool strings during logging operations. The triple combo tool string provides formation resistivity, density, porosity, natural (spectral) gamma radiation, and borehole diameter data. We plan to add the UBI tool to this tool string for an oriented 360° image of the sonic reflection amplitude and radius of the borehole wall. The FMS-sonic tool string will provide oriented resistivity images of the borehole wall as well as formation acoustic velocity, natural gamma radiation, and borehole diameter data. We will run two passes of this tool so that the coverage of FMS images can be increased. Details of the logging tools are available at **http://iodp.tamu.edu/tools/logging**.

Proposed Sites SATL-53B and SATL-54A are situated in ~5 km deep water where the longer variants of the tool strings (e.g., quad combo) are too heavy to deploy safely. We do not plan to run check shot surveys because the basement contact will be clear in the core and drilling data, and this depth can be correlated to the basement reflection in the seismic profiles.

Directly after each logging operation, the downhole logging data will be sent to the Lamont-Doherty Earth Observatory Borehole Research Group at Columbia University (New York, USA) for data reduction, which includes depth correlation between logging runs and speed adjustments to the downhole images. The data will then be returned to the shipboard downhole logging scientists for interpretation within days (**http://iodp.tamu.edu/tools/logging**).

Temperature measurements are planned at all six sites to reconstruct the thermal gradient and heat flow at each site. Typically, ~3–5 measurements will be made in one hole per site using the APCT-3. Fewer APCT-3 measurements will be made at Proposed Site SATL-13A because the sediment there is only 50 m thick.

The temperature of the fluid in the borehole is measured in the cable head section in both downhole tool strings, although the fluid temperature is not usually equilibrated to the formation temperature. However, we note the possibility of taking downhole temperature profiles during Expedition 393 at a site or sites already drilled during Expedition 390 when the temperature will have had time to equilibrate. Similarly, it may be possible to sample formation fluids that have entered the borehole during the ~6 months between expeditions using either the JRSO water sampling temperature probe (WSTP) or the third-party Kuster Flow Through Sampler. However, these operations would take time, and they are not included in the operations schedule presented here.

Risks and contingency

Our priority is to achieve the greatest possible basement penetration at each site following the recovery of complete sedimentary sections and sampling of the sediment–basement transition. This will require flexibility in our operational plans to counter any unexpected eventualities. Stable weather is expected in the subtropical SAT region, and the piracy risk is low. The greatest risk to the SAT project is therefore the loss of time, for example as a result of personal, medical, or mechanical incidents. Other risks to the completion of the planned operations include (1) operational problems, for example difficulties installing casing into basement or stuck pipe, (2) lower than predicted penetration rates, which would affect the penetration that could be achieved in the allotted time, and (3) hiatuses in the sediments that would result in incomplete recovery of paleoceanographic records. The latter is considered a low risk because hiatuses were only encountered at RGR sites during Leg 3 and would not affect our operational plans.

The two-expedition nature of the SAT project, with both expeditions transiting along the same transect, allows for additional operational flexibility compared to normal single-expedition IODP projects. This gives us the option to adapt the operational plan of Expedition 393 in response to the operations completed during Expedition 390. The highest priority sites are deliberately scheduled during Expedition 390 to give us an opportunity to revisit these sites during Expedition 393 if key operational objectives have not been met. The Co-Chief Scientists will therefore work with the Operations Superintendent to review Expedition 390 and revise the operations plan for Expedition 393 as needed.

In the event of a loss of operational time, the operation plans (Tables **T2**, **T3**, **T4**) will have to be adjusted. The nature of any changes would depend on the circumstances, amount of time lost, and operations already completed. Possible changes we could make to the operation plans include

- Reducing the number of APC holes at selected sites,
- Reducing the number of RCB bits used at selected sites,
- Reducing the basement penetration depth at selected sites,
- Deploying free-fall rather than drill-in reentry cones,
- Adjusting the frequency of additional operations (e.g., core orientation measurements),
- Adjusting the wireline logging schedule,
- Reallocating the basement drilling time from the lower priority site (SATL-25A), and
- Reallocating the sediment and basement drilling time from the lower priority site (SATL-25A).

In the event that we have additional time available, for example through failure of a hole, that time would be reallocated. Additional operations could include

- Deeper RCB basement coring at priority sites;
- APC coring of sediments at alternate sites with thicker (higher resolution) sediment sections (Table **T1**);
- Revisiting Expedition 390 sites during Expedition 393 to measure basement temperatures, in particular at Proposed Site SATL-53B, where operations could be conducted in combination with the scheduled Expedition 393 operations at nearby Proposed Site SATL-54A without requiring an additional pipe trip; and
- Logging of the sediment section at Proposed Site SATL-54A.

In addition to the above contingency plans, we will further increase our operational flexibility as follows:

- We will carry sufficient spare hardware, including an extra reentry cone system, additional casing, and free-fall reentry cones.
- We will carry a spare, lighter reentry cone system with 10¾ inch casing for use at Proposed Site SATL-54A where deployment of the weight of 600 m of 13⅜ inch casing would be prohibited by heave in excess of 0.5 m. In other words, very calm sea conditions will be required. A further fallback plan for this deep site in the case that heave conditions exceed the limit for 10¾ inch casing would be to core without casing through a free-fall reentry cone.
- The half-length APC (HLAPC) coring system will be available.

Sampling and data sharing strategy

Shipboard and shore-based researchers should refer to the IODP Sample, Data, and Obligations Policy and Implementation Guidelines at **http://www.iodp.org/top-resources/program-documents/policies-and-guidelines**. This document outlines the policy for distributing IODP samples and data to research scientists, curators, and educators. The document also defines the obligations that sample and data recipients incur. The Sample Allocation Committee (SAC; composed of the Co-Chief Scientists and Expedition Project Managers/Staff Scientists from both expeditions, the IODP Curator on shore, and curatorial representatives on board) will work with the entire scientific party to formulate a formal expedition-specific sampling plan for shipboard and postcruise sampling.

Every member of the science party is obligated to carry out scientific research for the expedition and publish their results. Shipboard scientists are expected to submit sample requests (at **http://iodp.tamu.edu/curation/samples.html**) ~6 months before the beginning of the expedition. Based on sample requests (shore based and shipboard) submitted by this deadline, the SAC will prepare a tentative sampling plan, which will be revised on the ship as dictated by core recovery and expedition objectives. The sampling plan will be subject to modification depending upon the actual material recovered and collaborations that may evolve between scientists during the expedition. Modification of the strategy during the expedition must be approved by the Co-Chief Scientists, Staff Scientists, and curatorial representative on board ship.

Great care will be taken to maximize shared sampling to promote integration of data sets and enhance scientific collaboration among members of the scientific party so that our scientific objectives are met and each scientist has the opportunity to contribute. The minimum permanent archive will be the standard archive half of each core. All sample frequencies and sizes must be justified on a scientific basis and will depend on core recovery, the full spectrum of other requests, and the expedition objectives. Some redundancy of measurement is unavoidable, but minimizing the duplication of measurements among the shipboard party and identified shore-based collaborators will be a factor in evaluating sample requests.

Personal shipboard sampling will be restricted to acquiring ephemeral data types (e.g., microbial samples and pore water geochemistry) needed for shipboard measurements and personal, postcruise research. Whole-round samples may be taken for interstitial water, microbiology, geochemistry, and physical property measurements as dictated by the shipboard sampling plan that will be formulated before the expedition and finalized during the first few days on board. At the discretion of the SAC, limited low-resolution

sampling for pilot studies that are required to define plans for the postcruise sampling meeting may be approved.

During both expeditions, all archive halves will become permanent archives and will not be sampled. Following both expeditions, the IODP Curator will determine the archive halves designated as permanent over any intervals recovered from multiple holes at a site and those that are outside of the working splice. The archive halves of single holes will become permanent archives.

If some critical intervals are recovered, there may be considerable demand for samples from a limited amount of cored material. These intervals may require special handling, a higher sampling density, reduced sample size, or continuous core sampling by a single investigator. A sampling plan coordinated by the SAC may be required before critical intervals are sampled.

All shipboard microbiological sampling will follow standard protocols (Lever et al., 2006; Smith et al., 2000) using perfluorocarbon tracers to monitor potential contamination and taking drilling fluid samples for cross-reference during postcruise research. Sediments will be sampled on the catwalk prior to core splitting or handling by other scientists. Basement samples will be selected through the core liner when possible or after the core is poured onto cleaned (with ethanol) half-core liners in the core splitting room. Microbiological samples will be taken prior to any other sampling for basement objectives but only under the guidance of the Co-Chiefs or a delegated shipboard scientist knowledgeable enough to help select samples that are not unique and critical for other basement objectives while still being of high value for biosphere objectives. All scientists participating in the basement sample selection will wear surgical masks and gloves so that they do not contaminate the samples. Once a sample is chosen, with preference toward samples at least 10 cm long and with visible veins and/or alteration, the sample will immediately be transferred into a sterile Whirl-Pak bag or similar sample bag and transported to the microbiology laboratory. Shipboard microbiology sample processing will occur using one or both of the KOACH tabletop clean zone systems and a purpose-built clean room area for handling microbiological samples similar to that provided for IODP Expedition 360 (Dick et al., 2017). Following microbiological sample processing, any remaining core material will be returned to allow detailed petrographic description and sampling as appropriate.

We plan to postpone nearly all personal sampling for postcruise research until a shore-based sampling meeting. Following Expeditions 390 and 393, cores will be delivered to the IODP Bremen Core Repository at MARUM/University of Bremen in Bremen, Germany, for the postcruise sampling meeting and permanent storage. One combined sampling meeting will be held for both expeditions and will take place ~3–5 months after the end of Expedition 393. All of the data and samples collected will be protected by a 1 y moratorium period following the completion of the postcruise sampling meeting. During this moratorium, all Expeditions 390 and 393 data and samples will be available only to the expedition shipboard and approved shore-based scientists. Selected cores (mostly archive halves) may be shipped at the end of each expedition to the IODP Gulf Coast Repository in College Station, Texas (USA), for programmatic X-ray fluorescence measurements if the SAC considers this a scientific priority.

Expedition scientists and scientific participants

The current list of participants for Expedition 390 and 393 can be found at **http://iodp.tamu.edu/scienceops/expeditions/south_atlantic_transect.html**.

References

Alt, J.C., and Teagle, D.A.H., 1999. The uptake of carbon during alteration of ocean crust. *Geochimica et Cosmochimica Acta,* 63(10):1527–1535. **https://doi.org/10.1016/S0016-7037(99)00123-4**

Anderson, R.N., Honnorez, J., Becker, K., et al., 1985. *Initial Reports of the Deep Sea Drilling Project,* 83: Washington, DC (U.S. Government Printing Office). **https://doi.org/10.2973/dsdp.proc.83.1985**

Andrén, T., Jørgensen, B.B., Cotterill, C., Green, S., Andrén, E., Ash, J., Bauersachs, T., Cragg, B., Fanget, A.-S., Fehr, A., Granoszewski, W., Groeneveld, J., Hardisty, D., Herrero-Bervera, E., Hyttinen, O., Jensen, J.B., Johnson, S., Kenzler, M., Kotilainen, A., Kotthoff, U., Marshall, I.P.G., Martin, E., Obrochta, S., Passchier, S., Quintana Krupinski, N., Riedinger, N., Slomp, C., Snowball, I., Stepanova, A., Strano, S., Torti, A., Warnock, J., Xiao, N., and Zhang, R., 2015. Expedition 347 summary. *In* Andrén, T., Jørgensen, B.B., Cotterill, C., Green, S., and the Expedition 347 Scientists, *Proceedings of the Integrated Ocean Drilling Program,* 347: College Station, TX (Integrated Ocean Drilling Program). **https://doi.org/10.2204/iodp.proc.347.101.2015**

Bach, W., and Edwards, K.J., 2003. Iron and sulfide oxidation within the basaltic ocean crust: implications for chemolithoautotrophic microbial biomass production. *Geochimica et Cosmochimica Acta,* 67(20):3871–3887. **https://doi.org/10.1016/S0016-7037(03)00304-1**

Barker, P.F., and Thomas, E., 2004. Origin, signature and palaeoclimatic influence of the Antarctic Circumpolar Current. *Earth-Science Reviews,* 66(1–2):143–162. **https://doi.org/10.1016/j.earscirev.2003.10.003**

Barrera, E., Savin, S.M., Thomas, E., and Jones, C.E., 1997. Evidence for thermohaline-circulation reversals controlled by sea- level change in the latest Cretaceous. *Geology,* 25(8):715–718. **https://doi.org/10.1130/0091-7613(1997)025<0715:EFTCRC>2.3.CO;2**

Becker, K., Fisher, A.T., and Tsuji, T., 2013. New packer experiments and borehole logs in upper oceanic crust: evidence for ridge-parallel consistency in crustal hydrogeological properties. *Geochemistry, Geophysics, Geosystems,* 14(8):2900–2915. **https://doi.org/10.1002/ggge.20201**

Berner, R.A., Lasaga, A.C., and Garrels, R.M., 1983. The carbonate-silicate geochemical cycle and its effect on atmospheric carbon dioxide over the past 100 million years. *American Journal of Science,* 283(7):641–683. **https://doi.org/10.2475/ajs.283.7.641**

Billups, K., 2002. Late Miocene through early Pliocene deep water circulation and climate change viewed from the sub-Antarctic South Atlantic. *Palaeogeography, Palaeoclimatology, Palaeoecology,* 185(3–4):287–307. **https://doi.org/10.1016/S0031-0182(02)00340-1**

Bohaty, S.M., Zachos, J.C., Florindo, F., and Delaney, M.L., 2009. Coupled greenhouse warming and deep-sea acidification in the middle Eocene. *Paleoceanography,* 24(2):PA2207. **https://doi.org/10.1029/2008PA001676**

Borrelli, C., Cramer, B.S., and Katz, M.E., 2014. Bipolar Atlantic deepwater circulation in the middle-late Eocene: effects of Southern Ocean gateway openings. *Paleoceanography,* 29(4):308–327. **https://doi.org/10.1002/2012PA002444'**

Broecker, W.S., 1991. The great ocean conveyor. *Oceanography,* 4:79–89. **https://doi.org/10.5670/oceanog.1991.07**

Cande, S.C., and Kent, D.V., 1995. Revised calibration of the geomagnetic polarity timescale for the Late Cretaceous and Cenozoic. *Journal of Geo-*

physical Research: Solid Earth, 100(B4):6093–6095. **https://doi.org/10.1029/94JB03098**

Coggon, R.M., and Teagle, D.A.H., 2011. Hydrothermal calcium-carbonate veins reveal past ocean chemistry. *TrAC Trends in Analytical Chemistry,* 30(8):1252–1268. **https://doi.org/10.1016/j.trac.2011.02.011**

Coggon, R.M., Teagle, D.A.H., Cooper, M.J., and Vanko, D.A., 2004. Linking basement carbonate vein compositions to porewater geochemistry across the eastern flank of the Juan de Fuca Ridge, ODP Leg 168. *Earth and Planetary Science Letters,* 219(1–2):111–128. **https://doi.org/10.1016/S0012-821X(03)00697-6**

Coggon, R.M., Teagle, D.A.H., Smith-Duque, C.E., Alt, J.C., and Cooper, M.J., 2010. Reconstructing past seawater Mg/Ca and Sr/Ca from mid-ocean ridge flank calcium carbonate veins. *Science,* 327(5969):1114–1117. **https://doi.org/10.1126/science.1182252**

Coogan, L.A., Parrish, R.R., and Roberts, N.M.W., 2016. Early hydrothermal carbon uptake by the upper oceanic crust: insight from in situ U-Pb dating. *Geology*, 44(2):147–150. **https://doi.org/10.1130/G37212.1**

Cramer, B.S., Toggweiler, J.R., Wright, J.D., Katz, M.E., and Miller, K.G., 2009. Ocean overturning since the Late Cretaceous: inferences from a new benthic foraminiferal isotope compilation. *Paleoceanography,* 24(4). **https://doi.org/10.1029/2008PA001683**

Davis, A.C., Bickle, M.J., and Teagle, D.A.H., 2003. Imbalance in the oceanic strontium budget. *Earth and Planetary Science Letters*, 211(1–2):173–187. **https://doi.org/10.1016/S0012-821X(03)00191-2**

Devey, C.W., 2014. SoMARTherm: the Mid-Atlantic Ridge 13–33°S – Cruise No. MSM25 – January 24–March 5, 2013 – Cape Town (South Africa) – Mindelo (Cape Verde). *MARIA S. MERIAN-Berichte,* MSM25:80. **https://doi.org/10.2312/cr_msm25**

D'Hondt, S., Inagaki, F., Alvarez Zarikian, C., Abrams, L.J., Dubois, N., Engelhardt, T., Evans, H., et al., 2015. Presence of oxygen and aerobic communities from sea floor to basement in deep-sea sediments. *Nature Geoscience,* 8(4):299–304. **https://doi.org/10.1038/ngeo2387**

Dick, H.J.B., MacLeod, C.J., Blum, P., Abe, N., Blackman, D.K., Bowles, J.A., Cheadle, M.J., Cho, K., Ciążela, J., Deans, J.R., Edgcomb, V.P., Ferrando, C., France, L., Ghosh, B., Ildefonse, B.M., Kendrick, M.A., Koepke, J.H., Leong, J.A.M., Liu, C., Ma, Q., Morishita, T., Morris, A., Natland, J.H., Nozaka, T., Pluemper, O., Sanfilippo, A., Sylvan, J.B., Tivey, M.A., Tribuzio, R., and Viegas, L.G.F., 2017. Expedition 360 summary. *In* MacLeod, C.J., Dick, H.J.B., Blum, P., and the Expedition 360 Scientists, *Southwest Indian Ridge Lower Crust and Moho*. Proceedings of the International Ocean Discovery Program, 360: College Station, TX (International Ocean Discovery Program). **https://doi.org/10.14379/iodp.proc.360.101.2017**

Dickens, G.R., Castillo, M.M., and Walker, J.C.G., 1997. A blast of gas in the latest Paleocene: simulating first-order effects of massive dissociation of oceanic methane hydrate. *Geology,* 25(3):259–262. **https://doi.org/10.1130/0091-7613(1997)025<0259:ABOGIT>2.3.CO;2**

Engelen, B., Ziegelmüller, K., Wolf, L., Köpke, B., Gittel, A., Cypionka, H., Treude, T., Nakagawa, S., Inagaki, F., Lever, M.A., and Steinsbu, B.O., 2008. Fluids from the ocean crust support microbial activities within the deep biosphere. *Geomicrobiology Journal,* 25(1):56–66. **https://doi.org/10.1080/01490450701829006**

Estep, J.D., Reece, R., Kardell, D.A., Christeson, G.L., and Carlson, R.L., 2019. Seismic layer 2A: evolution and thickness from 0–70 Ma crust in the slow-intermediate spreading South Atlantic. *Journal of Geophysical Research: Solid Earth*, 124(8):7633–7651. **https://doi.org/10.1029/2019JB017302**

Expedition 301 Scientists, 2005. Expedition 301 summary. *In* Fisher, A.T., Urabe, T., Klaus, A., and the Expedition 301 Scientists, *Proceedings of the Integrated Ocean Drilling Program,* 301: College Station, TX (Integrated Ocean Drilling Program Management International, Inc.). **https://doi.org/10.2204/iodp.proc.301.101.2005**

Expedition 308 Scientists, 2006. Expedition 308 summary. *In* Flemings, P.B., Behrmann, J.H., John, C.M., and the Expedition 308 Scientists, *Proceedings of the Integrated Ocean Drilling Program,* 308: College Station, TX (Integrated Ocean Drilling Program Management International, Inc.). **https://doi.org/10.2204/iodp.proc.308.101.2006**

Expedition 309/312 Scientists, 2006. Expedition 309/312 summary. *In* Teagle, D.A.H., Alt, J.C., Umino, S., Miyashita, S., Banerjee, N.R., Wilson, D.S., and the Expedition 309/312 Scientists. *Proceedings of the Integrated Ocean Drilling Program,* 309/312: Washington, DC (Integrated Ocean Drilling Program Management International, Inc.). **https://doi.org/10.2204/iodp.proc.309312.101.2006**

Expedition 313 Scientists, 2010. Expedition 313 summary. *In* Mountain, G., Proust, J.-N., McInroy, D., Cotterill, C., and the Expedition 313 Scientists, *Proceedings of the Integrated Ocean Drilling Program,* 313: Tokyo (Integrated Ocean Drilling Program Management International, Inc.). **https://doi.org/10.2204/iodp.proc.313.101.2010**

Expedition 325 Scientists, 2011. Expedition 325 summary. *In* Webster, J.M., Yokoyama, Y., Cotterill, C., and the Expedition 325 Scientists, *Proceedings of the Integrated Ocean Drilling Program,* 325: Tokyo (Integrated Ocean Drilling Program Management International, Inc.). **https://doi.org/10.2204/iodp.proc.325.101.2011**

Expedition 327 Scientists, 2011. Expedition 327 summary. *In* Fisher, A.T., Tsuji, T., Petronotis, K., and the Expedition 327 Scientists, *Proceedings of the Integrated Ocean Drilling Program,* 327: Tokyo (Integrated Ocean Drilling Program Management International, Inc.). **http:/doi.org/10.2204/iodp.proc.327.101.2011**

Expedition 329 Scientists, 2011. Expedition 329 summary. *In* D'Hondt, S., Inagaki, F., Alvarez Zarikian, C.A., and the Expedition 329 Scientists, *Proceedings of the Integrated Ocean Drilling Program,* 329: Tokyo (Integrated Ocean Drilling Program Management International, Inc.). **https://doi.org/10.2204/iodp.proc.329.101.2011**

Expedition 330 Scientists, 2012. Expedition 330 summary. *In* Koppers, A.A.P., Yamazaki, T., Geldmacher, J., and the Expedition 330 Scientists, *Proceedings of the Integrated Ocean Drilling Program,* 330: Tokyo (Integrated Ocean Drilling Program Management International, Inc.). **https://doi.org/10.2204/iodp.proc.330.101.2012**

Expedition 335 Scientists, 2012. Expedition 335 summary. *In* Teagle, D.A.H., Ildefonse, B., Blum, P., and the Expedition 335 Scientists, *Proceedings of the Integrated Ocean Drilling Program,* 335: Tokyo (Integrated Ocean Drilling Program Management International, Inc.). **https://doi.org/10.2204/iodp.proc.335.101.2012**

Expedition 336 Scientists, 2012. Expedition 336 summary. *In* Edwards, K.J., Bach, W., Klaus, A., and the Expedition 336 Scientists, *Proceedings of the Integrated Ocean Drilling Program,* 336: Tokyo (Integrated Ocean Drilling Program Management International, Inc.). **https://doi.org/10.2204/iodp.proc.336.101.2012**

Frank, T.D., and Arthur, M.A., 1999. Tectonic forcings of Maastrichtian ocean-climate evolution. *Paleoceanography,* 14(2):103–117. **https://doi.org/10.1029/1998PA900017**

Gillis, K.M., and Coogan, L.A., 2011. Secular variation in carbon uptake into the ocean crust. *Earth and Planetary Science Letters*, 302(3–4):385–392. **https://doi.org/10.1016/j.epsl.2010.12.030**

Hamdan, L.J., Coffin, R.B., Sikaroodi, M., Greinert, J., Treude, T., and Gillevet, P.M., 2013. Ocean currents shape the microbiome of Arctic marine sediments. *ISME Journal*, 7(4):685–696. **https://doi.org/10.1038/ismej.2012.143**

Harris, M., Coggon, R.M., Smith-Duque, C.E., Cooper, M.J., Milton, J.A., and Teagle, D.A.H., 2015. Channelling of hydrothermal fluids during the accretion and evolution of the upper oceanic crust: Sr isotope evidence from ODP Hole 1256D. *Earth and Planetary Science Letters,* 416:56–66. **https://doi.org/10.1016/j.epsl.2015.01.042**

Harris, M., Coggon, R.M., Teagle, D.A.H., Roberts, N.M.W., and Parrish, R.R., 2014. Laser ablation MC-ICP-MS U/Pb geochronology of ocean basement calcium carbonate veins [presented at the 2014 American Geophysical Union Fall Meeting, San Francisco, CA, 15–19 December 2014]. (Abstract V31B-4740. **https://abstractsearch.agu.org/meetings/2014/FM/V31B-4740.html**

Inagaki, F., Nunoura, T., Nakagawa, S., Teske, A., Lever, M., Lauer, A., Suzuki, M., et al., 2006. Biogeographical distribution and diversity of microbes in methane hydrate-bearing deep marine sediments on the Pacific Ocean margin. *Proceedings of the National Academy of Sciences of the United States of America,* 103(8):2815–2820. **https://doi.org/10.1073/pnas.0511033103**

Jungbluth, S.P., Grote, J., Lin, H.-T., Cowen, J.P., and Rappe, M.S., 2013. Microbial diversity within basement fluids of the sediment-buried Juan de Fuca Ridge flank. *ISME Journal,* 7(1):161–172. **https://doi.org/10.1038/ismej.2012.73**

Kallmeyer, J., Pockalny, R., Adhikari, R.R., Smith, D.C., and D'Hondt, S., 2012. Global distribution of microbial abundance and biomass in subseafloor sediment. *Proceedings of the National Academy of Sciences of the United States of America,* 109(40):16213–16216. **https://doi.org/10.1073/pnas.1203849109**

Kardell, D.A., Christeson, G.L., Estep, J.D., Reece, R.S., and Carlson, R.L., 2019. Long-lasting evolution of Layer 2A in the western South Atlantic: evidence for low-temperature hydrothermal circulation in old oceanic crust. *Journal of Geophysical Research: Solid Earth*, 124(3):2252–2273. **https://doi.org/10.1029/2018JB016925**

Katz, M.E., Cramer, B.S., Toggweiler, J.R., Esmay, G., Liu, C., Miller, K.G., Rosenthal, Y., Wade, B.S., and Wright, J.D., 2011. Impact of Antarctic Circumpolar Current development on late Paleogene ocean structure. *Science*, 332(6033):1076–1079. **https://doi.org/10.1126/science.1202122**

Kennett, J.P., and Stott, L.D., 1990. Proteus and Proto-oceanus: ancestral Paleogene oceans as revealed from Antarctic stable isotopic results: ODP Leg 113. *In* Barker, P.F., Kennett, J.P., et al., *Proceedings of the Ocean Drilling Program, Scientific Results,* 113: College Station, TX (Ocean Drilling Program), 865–880. **https://doi.org/10.2973/odp.proc.sr.113.188.1990**

Kennett, J.P., and Stott, L.D., 1991. Abrupt deep-sea warming, palaeoceanographic changes and benthic extinctions at the end of the Palaeocene. *Nature*, 353(6341):225–229. **https://doi.org/10.1038/353225a0**

Lee, H.J., Jeong, S.E., Kim, P.J., Madsen, E.L., and Jeon, C.O., 2015. High resolution depth distribution of Bacteria, Archaea, methanotrophs, and methanogens in the bulk and rhizosphere soils of a flooded rice paddy. *Frontiers in Microbiology*, 6:639. **https://doi.org/10.3389/fmicb.2015.00639**

Lever, M.A., Alperin, M., Engelen, B., Inagaki, F., Nakagawa, S., Steinsbu, B.O., Teske A., and IODP Expedition 301 Scientists, 2006. Trends in basalt and sediment core contamination during IODP Expedition 301. *Geomicrobiology Journal,* 23(7):517–530. **https://doi.org/10.1080/01490450600897245**

Lever, M.A., Rogers, K.L., Lloyd, K.G., Overmann, J., Schink, B., Thauer, R.K., Hoehler, T.M., and Jørgensen, B.B., 2015. Life under extreme energy limitation: a synthesis of laboratory- and field-based investigations. *FEMS Microbiology Reviews*, 39(5):688-728. **https://doi.org/10.1093/femsre/fuv020**

Lever, M.A., Rouxel, O., Alt, J.C., Shimizu, N., Ono, S., Coggon, R.M., Shanks, W.C., III, et al., 2013. Evidence for microbial carbon and sulfur cycling in deeply buried ridge flank basalt. *Science,* 339(6125):1305–1308. **https://doi.org/10.1126/science.1229240**

Lomstein, B.A., Langerhuus, A.T., D'Hondt, S., Jørgensen, B.B., and Spivack, A., 2012. Endospore abundance, microbial growth and necromass turnover in deep sub-seafloor sediment. *Nature,* 484(7392):101–104. **https://doi.org/10.1038/nature10905**

Mallows, C., and Searle, R.C., 2012. A geophysical study of oceanic core complexes and surrounding terrain, Mid-Atlantic Ridge 13°N–14°N. *Geochemistry, Geophysics, Geosystems*, 13(6):Q0AG08. **https://doi.org/10.1029/2012GC004075**

Marieni, C., Henstock, T.J., and Teagle, D.A.H., 2013. Geological storage of CO_2 within the oceanic crust by gravitational trapping. *Geophysical Research Letters,* 40(23):6219–6224. **https://doi.org/10.1002/2013GL058220**

Mason, O.U., Nakagawa, T., Rosner, M., Van Nostrand, J.D., Zhou, J., Maruyama, A., Fisk, M.R., and Giovannoni, S.J., 2010. First investigation of the microbiology of the deepest layer of ocean crust. *PLoS One,* 5(11):e15399. **https://doi.org/10.1371/journal.pone.0015399**

Matter, J.M., Stute, M., Snæbjörnsdottir, S.O., Oelkers, E.H., Gislason, S.R., Aradottir, E.S., Sigfusson, B., et al., 2016. Rapid carbon mineralization for permanent disposal of anthropogenic carbon dioxide emissions. *Science*, 352(6291):1312–1314. **https://doi.org/10.1126/science.aad8132**

Maus, S., Barckhausen, U., Berkenbosch, H., Bournas, N., Brozena, J., Childers, V., Dostaler, F., et al., 2009. EMAG2: a 2-arc min resolution Earth Magnetic Anomaly Grid compiled from satellite, airborne, and marine magnetic measurements. *Geochemistry, Geophysics, Geosystems,* 10(8):Q08005. **https://doi.org/10.1029/2009GC002471**

Michibayashi, K., Tominaga, M., Ildefonse, B., and Teagle, D.A.H., 2019. What lies beneath: the formation and evolution of oceanic lithosphere. *Oceanography*, 32(1):126–137. **https://doi.org/10.5670/oceanog.2019.136**

Mollenhauer, G., R. R. Schneider, T. Jennerjahn, Müller, P.J., and Wefer., G., 2004. Organic carbon accumulation in the South Atlantic Ocean: its modern, mid-Holocene and last glacial distribution. *Global and Planetary Change*, 40(3–4):249–266. **https://doi.org/10.1016/j.gloplacha.2003.08.002**

Mottl, M.J., 2003. Partitioning of energy and mass fluxes between mid-ocean ridge axes and flanks at high and low temperature. *In* Halbach, P.E., Tunnicliffe, V., and Hein, J.R. (Eds.), *Energy and Mass Transfer in Marine Hydrothermal Systems:* Berlin (Dahlem University Press), 271–286.

Müller, R.D., Sdrolias, M., Gaina, C., Steinberger, B., and Heine, C., 2008. Long-term sea-level fluctuations driven by ocean basin dynamics. *Science,* 319(5868):1357–1362. **https://doi.org/10.1126/science.1151540**

Neira, N.M., Clark, J.F., Fisher, A.T., Wheat, C.G., Haymon, R.M., and Becker, K., 2016. Cross-hole tracer experiment reveals rapid fluid flow and low effective porosity in the upper oceanic crust. *Earth and Planetary Science Letters,* 450:355–365. **https://doi.org/10.1016/j.epsl.2016.06.048**

Norris, R.D., Wilson, P.A., Blum, P., Fehr, A., Agnini, C., Bornemann, A., Boulila, S., Bown, P.R., Cournede, C., Friedrich, O., Ghosh, A.K., Hollis, C.J., Hull, P.M., Jo, K., Junium, C.K., Kaneko, M., Liebrand, D., Lippert, P.C., Liu, Z., Matsui, H., Moriya, K., Nishi, H., Opdyke, B.N., Penman, D., Romans, B., Scher, H.D., Sexton, P., Takagi, H., Turner, S.K., Whiteside, J.H., Yamaguchi, T., and Yamamoto, Y., 2014. Expedition 342 summary. *In* Norris, R.D., Wilson, P.A., Blum, P., and the Expedition 342 Scientists, *Proceedings of the Integrated Ocean Drilling Program,* 342: College Station, TX (Integrated Ocean Drilling Program). **https://doi.org/10.2204/iodp.proc.342.101.2014**

O'Connor, J.M., and Duncan, R.A., 1990. Evolution of the Walvis Ridge–Rio Grande Rise hotspot system: implications for African and South American plate motions over plumes. *Journal of Geophysical Research: Solid Earth,* 95(B11):17475–17502. **https://doi.org/10.1029/JB095iB11p17475**

Orcutt, B.N., Bach, W., Becker, K., Fisher, A.T., Hentscher, M., Toner, B.M., Wheat, C.G., and Edwards, K.J., 2011. Colonization of subsurface microbial observatories deployed in young ocean crust. *ISME Journal,* 5(4):692–703. **https://doi.org/10.1038/ismej.2010.157**

Orcutt, B.N., LaRowe, D.E., Lloyd, K.G., Mills, H., Orsi, W., Reese, B.K., Sauvage, J., Huber, J.A., and Amend, J., 2014. IODP Deep Biosphere Research Workshop report—a synthesis of recent investigations, and discussion of new research questions and drilling targets. *Scientific Drilling,* 17:61–66. **https://doi.org/10.5194/sd-17-61-2014**

Orcutt, B.N., Wheat, C.G., Rouxel, O., Hulme, S., Edwards, K.J., and Bach, W., 2013. Oxygen consumption rates in subseafloor basaltic crust derived from a reaction transport model. *Nature Communications,* 4:2539. **https://doi.org/10.1038/ncomms3539**

Pälike, H., Lyle, M.W., Nishi, H., Raffi, I., Ridgwell, A., Gamage, K., Klaus, A., et al., 2012. A Cenozoic record of the equatorial Pacific carbonate compensation depth. *Nature,* 488(7413):609–614. **https://doi.org/10.1038/nature11360**

Palmer, M.R., and Edmond, J.M., 1989. The strontium isotope budget of the modern ocean. *Earth and Planetary Science Letters,* 92(1):11–26. **https://doi.org/10.1016/0012-821X(89)90017-4**

Penrose Conference Participants, 1972. Report of the Penrose field conference on ophiolites. *Geotimes*, 17:24–25.

Perfit, M.R., and Chadwick, W.W., Jr., 1998. Magmatism at mid-ocean ridges: constraints from volcanological and geochemical investigations. *In* Buck, W.R., Delaney, P.T., Karson, J.A., and Lagabrielle, Y. (Eds.), *Faulting and Magmatism at Mid-Ocean Ridges*. Geophysical Monograph, 106:59–115. **https://doi.org/10.1029/GM106p0059**

Rausch, S., Böhm, F., Bach, W., Klügel, A., and Eisenhauer, A., 2013. Calcium carbonate veins in ocean crust record a threefold increase of seawater Mg/Ca and Sr/Ca in the past 30 million years. *Earth and Planetary Science Letters*, 362:215–224. **https://doi.org/10.1016/j.epsl.2012.12.005**

Reese, B.K., Zinke, L.A., Sobol, M.S., LaRowe, D.E., Orcutt, B.N., Zhang, X., Jaekel, U., et al., 2018. Nitrogen cycling of active bacteria within oligotrophic sediment of the Mid-Atlantic Ridge Flank. *Geomicrobiology Journal,* 35(6):468–483. **https://doi.org/10.1080/01490451.2017.1392649**

Ryan, W.B.F., Carbotte, S.M., Coplan, J.O., O'Hara, S., Melkonian, A., Arko, R., Weissel, R.A., et al., 2009. Global multi-resolution topography synthesis. *Geochemistry, Geophysics, Geosystems,* 10(3):Q03014. **https://doi.org/10.1029/2008GC002332**

Santelli, C.M., Edgcomb, V.P., Bach, W., and Edwards, K.J., 2009. The diversity and abundance of bacteria inhabiting seafloor lavas positively correlate with rock alteration. *Environmental Microbiology,* 11(1):86–98. **https://doi.org/10.1111/j.1462-2920.2008.01743.x**

Scher, H.D., and Martin, E.E., 2006. Timing and climatic consequences of the opening of Drake Passage. *Science,* 312(5772):428–430. **https://doi.org/10.1126/science.1120044**

Schmid, F., Peters, M., Walter, M., Devey, C., Petersen, S., Yeo, I., Köhler, J., Jamieson, J.W., Walker, S., and Sültenfuß, J., 2019. Physico-chemical properties of newly discovered hydrothermal plumes above the Southern Mid-Atlantic Ridge (13°–33°S). *Deep Sea Research Part I: Oceanographic Research Papers*, 148:34–52. **https://doi.org/10.1016/j.dsr.2019.04.010**

Scientific Party, 1970. Introduction. *In* Maxwell A.E., et al., *Initial Reports of the Deep Sea Drilling Project,* 83: Washington, DC (U.S. Government Printing Office), 7–9. **https://doi.org/10.2973/dsdp.proc.3.101.1970**

Shipboard Scientific Party, 1993. Explanatory notes. *In* Alt, J.C., Kinoshita, H., Stokking, L.B., et al., *Proceedings of the Ocean Drilling Program, Initial Reports,* 148: College Station, TX (Ocean Drilling Program), 5–24. **https://doi.org/10.2973/odp.proc.ir.148.101.1993**

Shipboard Scientific Party, 1997. Introduction and summary: hydrothermal circulation in the oceanic crust and its consequences on the eastern flank of the Juan de Fuca Ridge. *In* Davis, E.E., Fisher, A.T., Firth, J.V., et al., *Proceedings of the Ocean Drilling Program, Initial Reports,* 168: College Station, TX (Ocean Drilling Program), 7–21. **https://doi.org/10.2973/odp.proc.ir.168.101.1997**

Shipboard Scientific Party, 2002. Leg 199 summary. *In* Lyle, M., Wilson, P.A., Janecek, T.R., et al., *Proceedings of the Ocean Drilling Program, Initial Reports,* 199: College Station, TX (Ocean Drilling Program), 1–87. **https://doi.org/10.2973/odp.proc.ir.199.101.2002**

Shipboard Scientific Party, 2003. Leg 201 summary. *In* D'Hondt, S.L., Jørgensen, B.B., Miller, D.J., et al., *Proceedings of the Ocean Drilling Program, Initial Reports,* 201: College Station, TX (Ocean Drilling Program), 1–81. **https://doi.org/10.2973/odp.proc.ir.201.101.2003**

Shipboard Scientific Party, 2004. Leg 208 summary. *In* Zachos, J.C., Kroon, D., Blum, P., et al., *Proceedings of the Ocean Drilling Program, Initial Reports,* 208: College Station, TX (Ocean Drilling Program), 1–112. **https://doi.org/10.2973/odp.proc.ir.208.101.2004**

Smith, D.C., Spivack, A.J., Fisk, M.R., Haveman, S.A., Staudigel, H., and the Leg 185 Shipboard Scientific Party, 2000. *Technical Note 28: Methods for Quantifying Potential Microbial Contamination during Deep Ocean Coring.* Ocean Drilling Program. **https://doi.org/10.2973/odp.tn.28.2000**

Spinelli, G.A., Giambalvo, E.R., and Fisher, A.T., 2004. Sediment permeability, distribution, and influence on fluxes in oceanic basement. *In* Davis, E.E., and Elderfield, H. (Eds.), *Hydrogeology of the Oceanic Lithosphere:* Cambridge, United Kingdom (Cambridge University Press), 151–188.

Staudigel, H., Hart, S.R., Schmincke, H.-U., and Smith, B.M., 1989. Cretaceous ocean crust at DSDP Sites 417 and 418: carbon uptake from weathering versus loss by magmatic outgassing. *Geochimica et Cosmochimica Acta,* 53(11):3091–3094. **https://doi.org/10.1016/0016-7037(89)90189-0**

Stein, C.A., and Stein, S., 1994. Constraints on hydrothermal heat flux through the oceanic lithosphere from global heat flow. *Journal of Geophysical Research: Solid Earth,* 99(B2):3081–3095. **https://doi.org/10.1029/93JB02222**

Stommel, H., 1961. Thermohaline convection with two stable regimes of flow. *Tellus,* 13:224–230. **https://onlinelibrary.wiley.com/doi/pdf/10.1111/j.2153-3490.1961.tb00079.x**

Sylvan, J.B., Hoffman, C.L., Momper, L.M., Toner, B.M., Amend, J.P., and Edwards, K.J., 2015. *Bacillus rigiliprofundi* sp. nov., an endospore-forming, Mn-oxidizing, moderately halophilic bacterium isolated from deep subseafloor basaltic crust. *International Journal of Systematic and Evolutionary Microbiology,* 65:1992–1998. **https://doi.org/10.1099/ijs.0.000211**

Thomas, D.J., Bralower, T.J., and Jones, C.E., 2003. Neodymium isotopic reconstruction of late Paleocene–early Eocene thermohaline circulation. *Earth and Planetary Science Letters,* 209(3–4):309–322. **https://doi.org/10.1016/S0012-821X(03)00096-7**

Tobin, H., Kinoshita, M., Ashi, J., Lallemant, S., Kimura, G., Screaton, E.J., Moe, K.T., Masago, H., Curewitz, D., and the Expedition 314/315/316 Scientists, 2009. NanTroSEIZE Stage 1 expeditions: introduction and synthesis of key results. *In* Kinoshita, M., Tobin, H., Ashi, J., Kimura, G., Lallemant, S., Screaton, E.J., Curewitz, D., Masago, H., Moe, K.T., and the Expedition 314/315/316 Scientists, *Proceedings of the Integrated Ocean Drilling Program,* 314/315/316: Washington, DC (Integrated Ocean Drilling Program Management International, Inc.). **https://doi.org/10.2204/iodp.proc.314315316.101.2009**

Tominaga, M., Teagle, D.A.H., Alt, J.C., and Umino, S., 2009. Determination of the volcanostratigraphy of the oceanic crust formed at superfast spreading ridge: electrofacies analyses of ODP/IODP Hole 1256D. *Geochemistry, Geophysics, Geosystems,* 10(1):Q01003. **https://doi.org/10.1029/2008GC002143**

Tripati, A., Backman, J., Elderfield, H., and Ferretti, P., 2005. Eocene bipolar glaciation associated with global carbon cycle changes. *Nature,* 436(7049):341–346. **https://doi.org/10.1038/nature03874**

Vance, D., Teagle, D.A.H., and Foster, G.L., 2009. Variable Quaternary chemical weathering fluxes and imbalances in marine geochemical budgets. *Nature,* 458(7237):493–496. **https://doi.org/10.1038/nature07828**

Wheat, C.G., and Fisher, A.T., 2008. Massive, low-temperature hydrothermal flow from a basaltic outcrop on 23 Ma seafloor of the Cocos plate: chemical constraints and implications. *Geochemistry, Geophysics, Geosystems,* 9(12):Q12O14. **https://doi.org/10.1029/2008GC002136**

Wilson, D.S., Teagle, D.A.H., Acton, G.D., et al., 2003. *Proceedings of the Ocean Drilling Program, Initial Reports,* 206: College Station, TX (Ocean Drilling Program). **https://doi.org/10.2973/odp.proc.ir.206.2003**

Wright, J.D., Miller, K.G., and Fairbanks, R.G., 1991. Evolution of modern deepwater circulation: evidence from the late Miocene Southern Ocean. *Paleoceanography,* 6(2):275–290. **https://doi.org/10.1029/90PA02498**

Wunsch, C., 2002. What is the thermohaline circulation? *Science,* 298(5596):1179–1181. **https://doi.org/10.1126/science.1079329**

Zachos, J., Pagani, M., Sloan, L., Thomas, E., and Billups, K., 2001. Trends, rhythms, and aberrations in global climate 65 Ma to present. *Science,* 292(5517):686–693. **https://doi.org/10.1126/science.1059412**

Zachos, J.C., Dickens, G.R., and Zeebe, R.E., 2008. An early Cenozoic perspective on greenhouse warming and carbon-cycle dynamics. *Nature,* 451(7176):279–283. **https://doi.org/10.1038/nature06588**

Zachos, J.C., Röhl, U., Schellenberg, S.A., Sluijs, A., Hodell, D.A., Kelly, D.C., Thomas, E., et al., 2005. Rapid acidification of the ocean during the Paleocene–Eocene Thermal Maximum. *Science,* 308(5728):1611–1615. **https://doi.org/10.1126/science.1109004**

Zeebe, R.E., Zachos, J.C., Caldeira, K., and Tyrrell, T., 2008. Oceans: carbon emissions and acidification. *Science*, 321(5885):51–52. **https://doi.org/10.1126/science.1159124**

Table T1. Primary and alternate site details, Expeditions 390 and 393. CDP = common depth point.

Site	Primary/Alternate	Latitude (°)	Longitude (°)	Water depth (m)	Sediment thickness (m)	Age (Ma)	Half spreading rate (mm/y)	Profile	CDP
11B	Alternate	−30.22233	−15.03817	3057	104	6.6	17.0	CREST01	12603
12A	Alternate	−30.10376	−15.04832	3373	96	6.6	17.0	CREST01	14712
13A	Primary	−30.26056	−15.0349	3047	50	6.6	17.0	CREST01	11923
23A	Alternate	−30.39535	−16.87974	3819	162	15.2	25.5	CREST1E	8724
24A	Alternate	−30.40021	−16.93053	3676	94	15.2	25.5	CREST1DE	3434
25A	Primary	−30.40344	−16.92282	3691	104	15.2	25.5	CREST02	12770
31A	Alternate	−30.76406	−20.43255	4188	183	30.6	24.0	CREST03	11346
33B	Primary	−30.71029	−20.4339	4193	138	30.6	24.0	CREST03	12300
35A	Alternate	−30.63251	−20.43586	4157	93	30.6	24.0	CREST03	13680
41A	Alternate	−31.00332	−24.81913	4408	203	49.2	19.5	CREST04	10926
43A	Primary	−30.89618	−24.84162	4323	148	49.2	19.5	CREST1BC	3252
44A	Alternate	−30.89703	−24.86951	4283	176	49.2	19.5	CREST1BC	2825
53B	Primary	−30.94207	−26.69912	4985	180	61.2	13.5	CREST1AB	3410
54A	Primary	−30.94242	−26.72188	4991	639	61.2	13.5	CREST1AB	3062
55A	Alternate	−30.72151	−26.69525	4857	126	61.2	13.5	CREST05	16750
56A	Alternate	−30.94091	−26.62983	4998	510	61.2	13.5	CREST1AB	4470

Table T2. Operations and time estimates for primary sites, Expedition 390.

Site No.	Location (Latitude Longitude)	Seafloor Depth (mbrf)	Operations Description	Transit (days)	Drilling Coring (days)	Logging (days)
Rio de Janeiro			Begin Expedition 5.0	port call days		
			Transit ~1002 nmi to SATL-54A @ 11.0 kt	3.8		
SATL-54A	30° 56.5452' S	5002	Hole A: APC/XCB to 639 mbsf (basement)		6.0	
	26° 43.3128' W					
			Sub-Total Days On-Site: 6.0			
			Transit ~1.2 nmi to SATL-53B @ 1.5 kt	0.0		
SATL-53B	30° 56.5242' S	4996	Hole A - APC to 180 mbsf with orientation and APCT-3 measurements		1.5	
	26° 41.9472' W		Hole B - APC to 180 mbsf (basment)		1.7	
			Hole C - Reentry system to ~175 mbsf		1.9	
			Hole C - RCB core to 430 mbsf and log with triple combo and FMS sonic		8.1	1.0
			Sub-Total Days On-Site: 14.2			
			Transit ~505 nmi to SATL-25A @ 11.0 kt	1.9		
SATL-25A	30° 24.2064' S	3702	Hole A - APC to 104 mbsf with orientation and APCT-3 measurements		1.1	
	16° 55.3692' W		Hole B - APC to 104 mbsf (basement)		0.6	
			Hole C - APC to 104 mbsf (basement)		1.0	
			Hole D - Reentry system to ~99 mbsf		1.6	
			Hole D - RCB core to 354 mbsf and log with triple combo and FMS sonic		7.2	0.9
			Sub-Total Days On-Site: 12.4			
			Transit ~98 nmi to SATL-13A @ 11.0 kt	0.4		
SATL-13A	30° 15.6336' S	3058	Hole A - APC to 50 mbsf with orientation and APCT-3 measurements		0.6	
	15° 2.0940' W		Hole B - APC to 50 mbsf (basement)		0.3	
			Hole C - APC to 50 mbsf (basement)		0.6	
			Hole D - Reentry system to ~45 mbsf		1.4	
			Hole D - RCB core to 300 mbsf and log with triple combo and FMS sonic		6.8	0.9
			Sub-Total Days On-Site: 10.6			
			Transit ~1708 nmi to Cape Town @ 10.5 kt	6.7		
Cape Town			End Expedition	12.8	40.4	2.8

Port Call:	5.0	Total Operating Days:	56.0
Sub-Total On-Site:	43.2	Total Expedition:	61.0

Table T3. Operations and time estimates for primary sites, Expedition 393.

Site No.	Location (Latitude Longitude)	Seafloor Depth (mbrf)	Operations Description	Transit (days)	Drilling Coring (days)	Logging (days)
Cape Town			Begin Expedition 5.0	port call days		
			Transit ~1969 nmi to SATL-33B @ 11.0 kt	7.5		
SATL-33B	30° 42.6174' S	4204	Hole A - APC to 138 mbsf with orientation and APCT-3 measurements		1.7	
	20° 26.0340' W		Hole B - APC to 138 mbsf (basement)		0.9	
			Hole C - APC to 138 mbsf (basement)		1.3	
			Hole D - Reentry system to ~133 mbsf		1.8	
			Hole D - RCB core to 388 mbsf and log with triple combo and FMS sonic		8.3	1.0
			Sub-Total Days On-Site: 15.0			
			Transit ~227 nmi to SATL-43A @ 11.0 kt	0.9		
SATL-43A	30° 53.7708' S	4334	Hole A - APC to 148 mbsf with orientation and APCT-3 measurements		1.5	
	24° 50.4972' W		Hole B - APC to 148 mbsf (basement)		0.9	
			Hole C - APC to 148 mbsf (basement)		1.4	
			Hole D - Reentry system to ~143 mbsf		1.8	
			Hole D - RCB core to 398 mbsf and log with triple combo and FMS sonic		8.3	1.0
			Sub-Total Days On-Site: 14.9			
			Transit ~97 nmi to SATL-54A @ 11.0 kt	0.4		
SATL-54A	30° 56.5452' S	5002	Hole B - Reentry system to ~600 mbsf		2.9	
	26° 43.3128' W		Hole B - RCB core to 879 mbsf and log with triple combo and FMS sonic		9.3	1.1
			Sub-Total Days On-Site: 13.3			
			Transit ~1708 nmi to Rio de Janeiro @ 10.5 kt	4.0		
Rio de Janeiro			End Expedition	12.8	40.1	3.1

Port Call:	5.0	Total Operating Days:	56.0
Sub-Total On-Site:	43.2	Total Expedition:	61.0

Table T4. Time estimates for alternate sites, Expeditions 390 and 393.

Site No.	Latitude	Longitude	Seafloor Depth (mbrf)	Operations Description	Drilling Coring (days)	Logging (days)	Days on Site
SATL-11B	30° 13.3398' S	15° 2.2902' W	3068	Hole A - APC to 104 mbsf with orientation and APCT-3 measurements	1.0		
				Hole B - APC to 104 mbsf (basement)	0.5		
				Hole C - APC to 104 mbsf (basement)	0.9		
				Hole D - Reentry system to ~99 mbsf	1.5		
				Hole D - RCB core to 354 mbsf and log with triple combo and FMS sonic	7.1	0.9	11.9
				Sediment Thickness: 104 m Basement Penetration: 250 m			
SATL-12A	30° 6.2256' S	15° 2.8992' W	3384	Hole A - APC to 96 mbsf with orientation and APCT-3 measurements	1.0		
				Hole B - APC to 96 mbsf (basement)	0.5		
				Hole C - APC to 96 mbsf (basement)	0.9		
				Hole D - Reentry system to ~91 mbsf	1.6		
				Hole D - RCB core to 346 mbsf and log with triple combo and FMS sonic	7.3	0.9	12.2
				Sediment Thickness: 96 m Basement Penetration 250 m			
SATL-23A	30° 23.7210' S	16° 52.7844' W	3830	Hole A - APC to 162 mbsf with orientation and APCT-3 measurements	1.4		
				Hole B - APC to 162 mbsf (basement)	0.9		
				Hole C - APC to 162 mbsf (basement)	1.2		
				Hole D - Reentry system to ~157 mbsf	1.7		
				Hole D - RCB core to 412 mbsf and log with triple combo and FMS sonic	7.7	1.0	13.9
				Sediment Thickness: 162 m Basement Penetration 250 m			
SATL-24A	30° 24.0126' S	16° 55.8318' W	3687	Hole A - APC to 94 mbsf with orientation and APCT-3 measurements	1.1		
				Hole B - APC to 94 mbsf (basement)	0.6		
				Hole C - APC to 94 mbsf (basement)	0.9		
				Hole D - Reentry system to ~89 mbsf	1.6		
				Hole D - RCB core to 344 mbsf and log with triple combo and FMS sonic	7.5	1.0	12.7
				Sediment Thickness: 94 m Basement Penetration 250 m			
SATL-31A	30° 45.8436' S	20° 25.9530' W	4199	Hole A - APC to 183 mbsf with orientation and APCT-3 measurements	1.4		
				Hole B - APC to 183 mbsf (basement)	1.1		
				Hole C - APC to 183 mbsf (basement)	1.6		
				Hole D - Reentry system to ~178 mbsf	1.8		
				Hole D - RCB core to 433 mbsf and log with triple combo and FMS sonic	7.9	1.0	14.8
				Sediment Thickness: 183 m Basement Penetration 250 m			
SATL-35A	30° 37.9506' S	20° 26.1516' W	4168	Hole A - APC to 93 mbsf with orientation and APCT-3 measurements	1.1		
				Hole B - APC to 93 mbsf (basement)	0.6		
				Hole C - APC to 93 mbsf (basement)	1.0		
				Hole D - Reentry system to ~88 mbsf	1.7		
				Hole D - RCB core to 343 mbsf and log with triple combo and FMS sonic	7.8	1.0	13.2
				Sediment Thickness: 93 m Basement Penetration 250 m			
SATL-41A	31° 0.1992' S	24° 49.1478' W	4419	Hole A - APC to 203 mbsf with orientation and APCT-3 measurements	1.5		
				Hole B - APC to 203 mbsf (basement)	1.2		
				Hole C - APC to 203 mbsf (basement)	1.7		
				Hole D - Reentry system to ~198 mbsf	1.9		
				Hole D - RCB core to 453 mbsf and log with triple combo and FMS sonic	8.1	1.0	15.4
				Sediment Thickness: 203 m Basement Penetration 250 m			
SATL-44A	30° 53.8218' S	24° 52.1706' W	4294	Hole A - APC to 176 mbsf with orientation and APCT-3 measurements	1.3		
				Hole B - APC to 176 mbsf (basement)	1.1		
				Hole C - APC to 176 mbsf (basement)	1.5		
				Hole D - Reentry system to ~171 mbsf	1.9		
				Hole D - RCB core to 426 mbsf and log with triple combo and FMS sonic	8.0	1.0	14.8
				Sediment Thickness: 178 m Basement Penetration 250 m			
SATL-55A	30° 43.2906' S	26° 41.7150' W	4868	Hole A - APC to 126 mbsf with orientation and APCT-3 measurements	1.5		
				Hole B - APC to 126 mbsf (basement)	0.9		
				Hole C - APC to 126 mbsf (basement)	1.3		
				Hole D - Reentry system to ~121 mbsf	1.8		
				Hole D - RCB core to 376 mbsf and log with triple combo and FMS sonic	8.4	1.0	14.9
				Sediment Thickness: 126 m Basement Penetration 250 m			
SATL-56A	30° 56.4546' S	26° 37.7898' W	5009	Hole A - APC/XCB to 510 mbsf with orientation and APCT-3 measurements	4.7		
				Hole B - Reentry system to ~500 mbsf	2.6		
				Hole B - RCB core to 760 mbsf and log with triple combo and FMS sonic	8.9	1.1	17.3
				Sediment Thickness: 510 m Basement Penetration 250 m			

Figure F1. South Atlantic study region. Top: topography (Ryan et al., 2009). Bottom: magnetic anomalies (Maus et al., 2009). Inset shows regional setting. Black lines indicate locations of CREST seismic reflection profiles, and proposed drill sites are displayed with black (primary) and gray (alternate) circles. White dashed line = WOCE Line A10, white circles = DSDP Leg 3 sites.

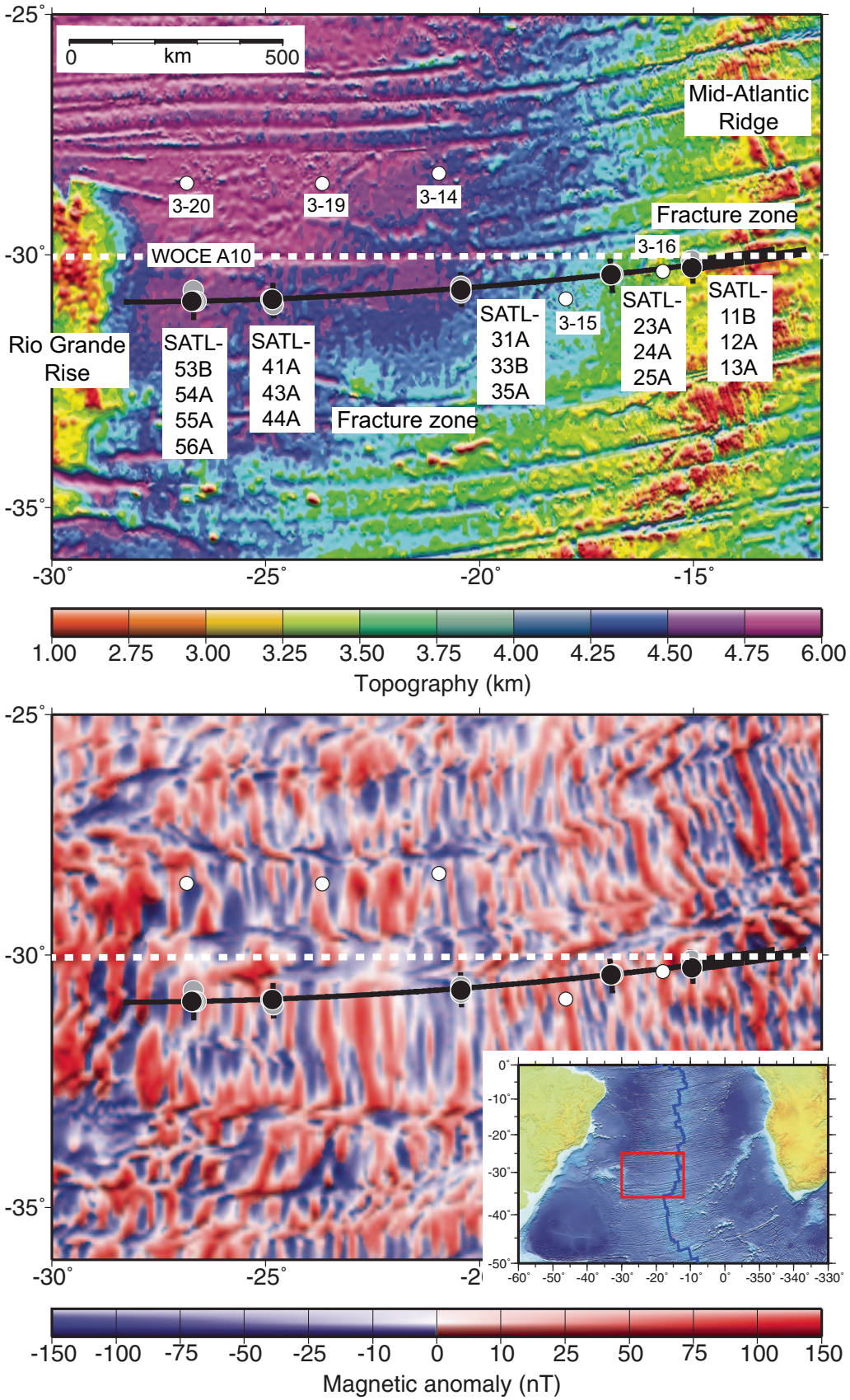

Figure F2. A. Compilation of all scientific ocean drilling holes that penetrate >100 m into the basement of intact oceanic crust and tectonically exposed lower crust/upper mantle, excluding drill holes that penetrated seamounts, oceanic plateaus, back-arc basement, hydrothermal mounds, or passive continental margins (after Michibayashi et al., 2019). Colored portions of each hole indicate the average core recovery. B. Compilation of all scientific ocean drilling holes that penetrate >100 m into intact upper (basaltic) ocean crust versus crustal age. The spreading rates at which the drilled sections formed are shown, and the colored portions of each hole indicate the average core recovery.

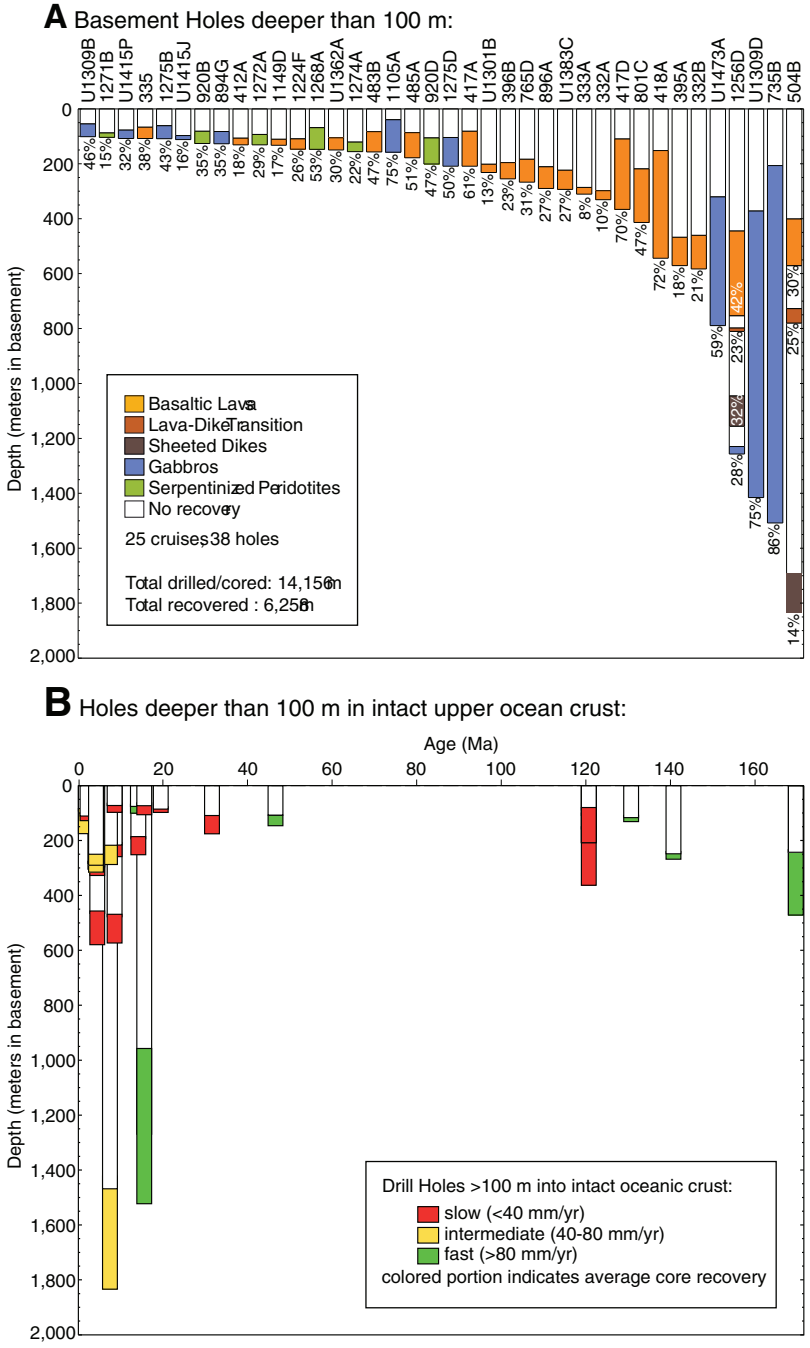

Figure F3. Sediment cover versus crustal age for Expedition 390 and 393 primary (yellow) and alternate (orange) sites. The sediment thicknesses at all DSDP/ODP/Integrated Ocean Drilling Program/IODP drill holes that cored more than 100 m into basement of intact oceanic crust and tectonically exposed lower crust/upper mantle are shown for comparison (blue diamonds). The red line indicates the global average sediment thickness versus age (red dashed line = ±1σ variation) (after Spinelli et al., 2004).

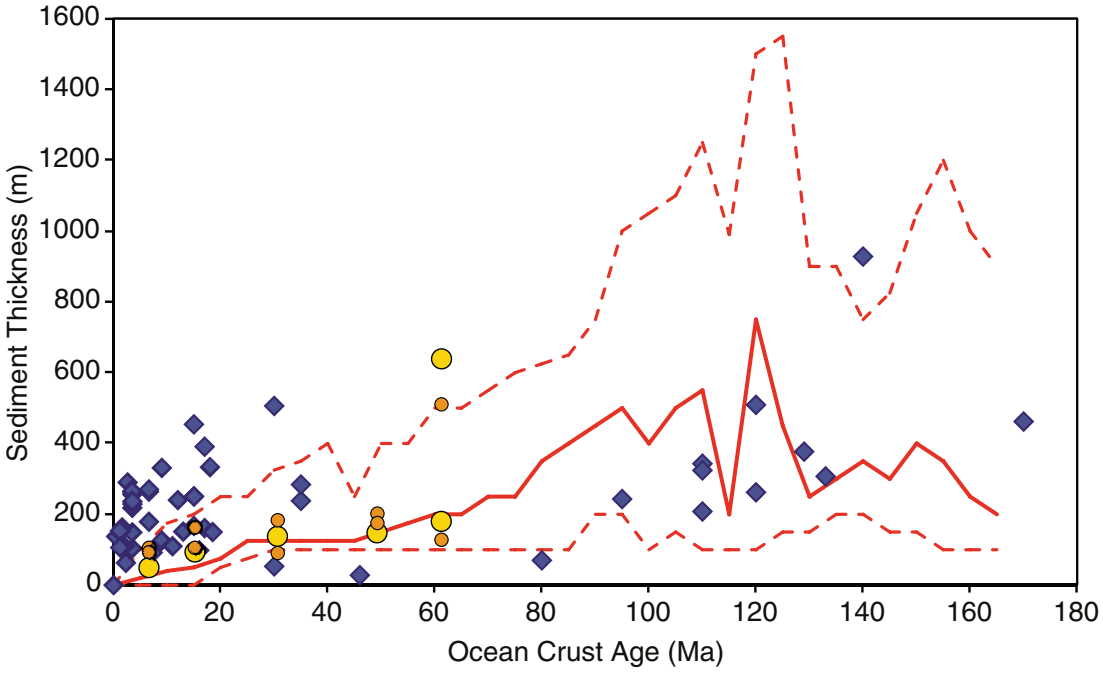

Figure F4. Seismic reflection profiles for all primary sites. Green line = interpreted basement.

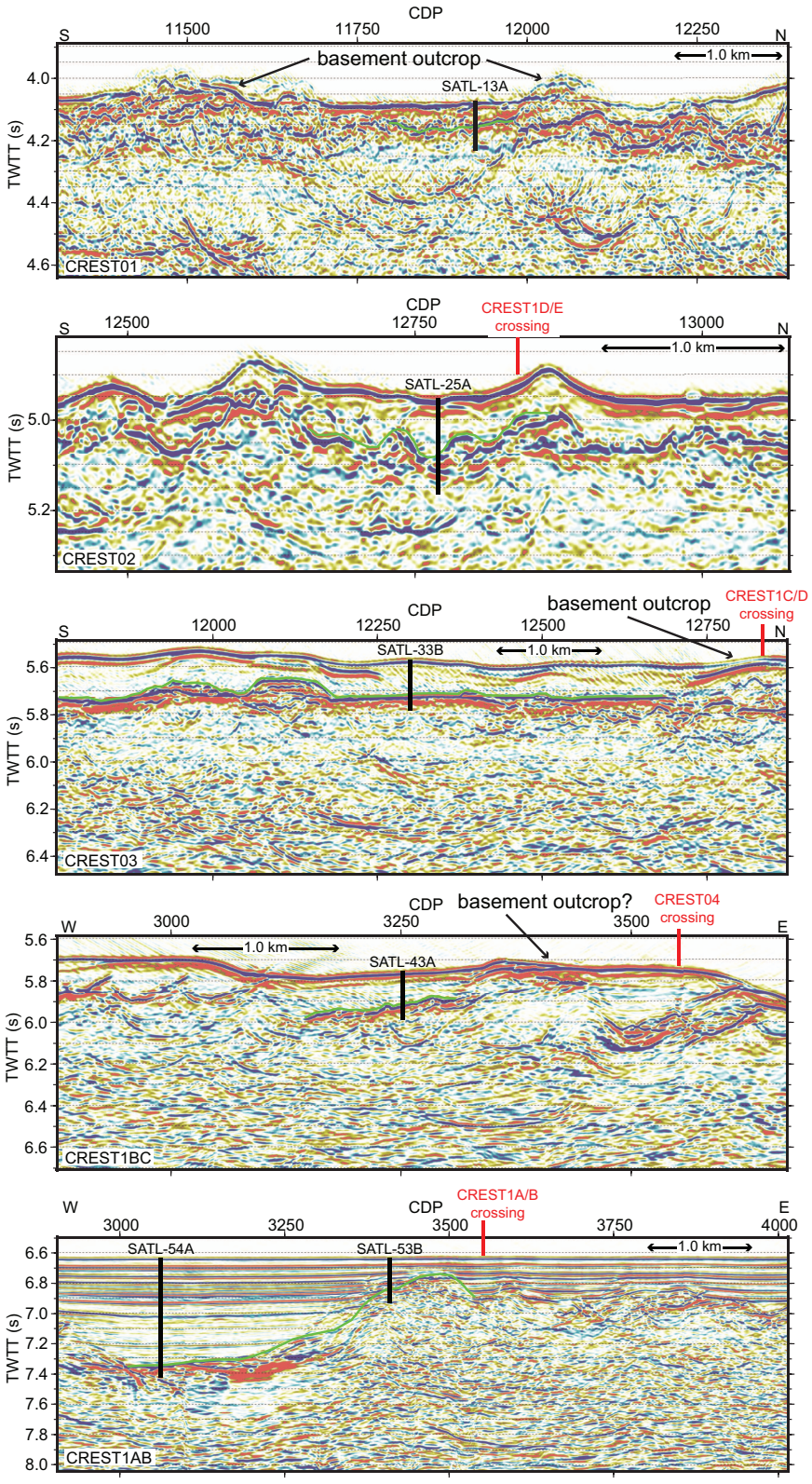

Figure F5. Ages and spreading rates along the CREST transect. Blue line = cubic interpolation of rates calculated from Table S1 of Kardell et al. (2019), orange squares = estimated values at primary drill sites.

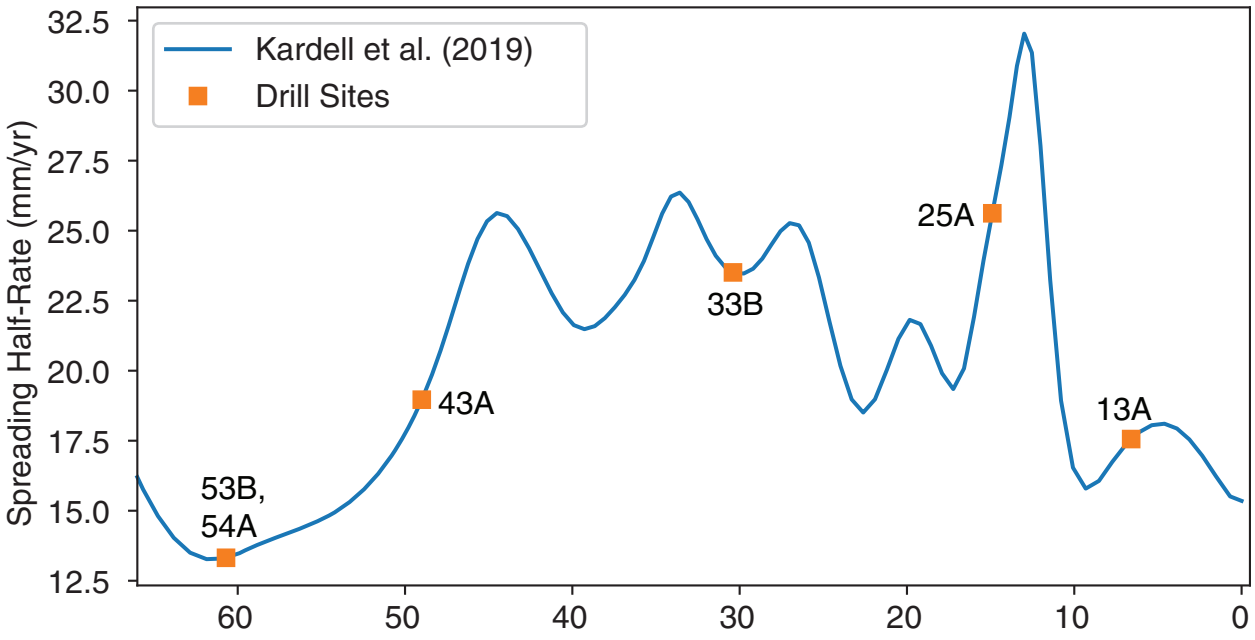

Figure F6. A. Schematic architecture of a mid-ocean ridge flank (not to scale) illustrating parameters that may influence the intensity and style of hydrothermal alteration and the hypothetical trajectory of the 120°C isotherm with crustal age. Arrows indicate heat (red) and fluid (blue) flow. B. Calculated global hydrothermal heat flow anomaly, which decreases to 0 by 65 Ma on average, and hypothetical variations in fluid flow and chemical exchange and crustal properties that could be measured to investigate the intensity and style of ridge flank hydrothermal circulation (e.g., porosity, permeability, and two possible scenarios for alteration intensity). (After Coggon and Teagle, 2011; Expedition 335 Scientists, 2012; and an original figure by K. Nakamura, AIST.)

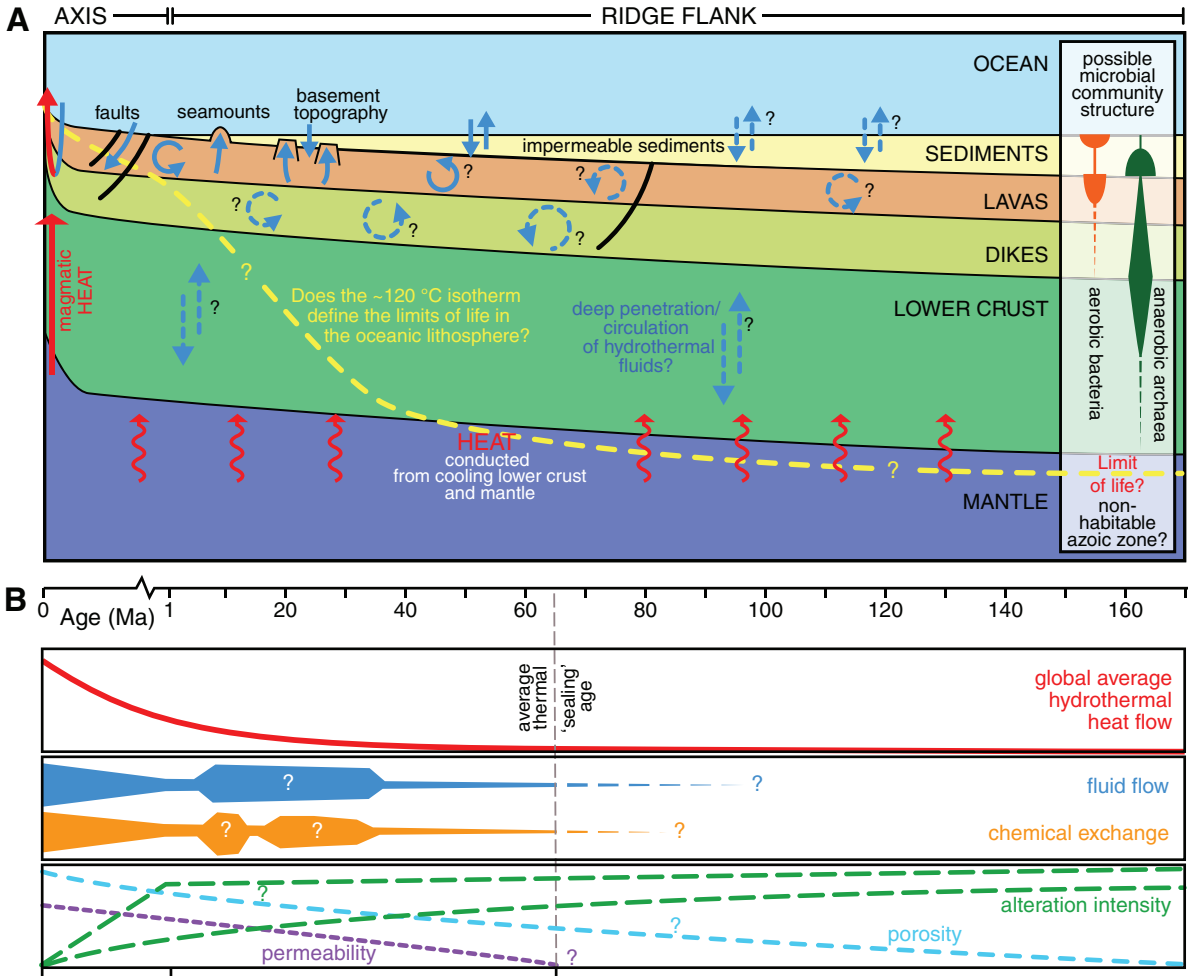

Figure F7. Left: global distribution of ODP (green circles) and IODP (red circles) drill sites. Sites where microbiological samples were taken are indicated by larger circles. Right: microbial cell abundance versus depth (meters below seafloor) at sampled sites, which reveal over five orders of magnitude of variation in biomass-depth trends, depending on the geographic origin of samples (after Kallmeyer et al., 2012; Orcutt et al., 2014). The South Atlantic represents a crucial gap in knowledge, and the sampling proposed here will be used to groundtruth models predicted from the current biomass database. Note that the symbol colors in (A) and (B) are not related because these diagrams are derived from different sources.

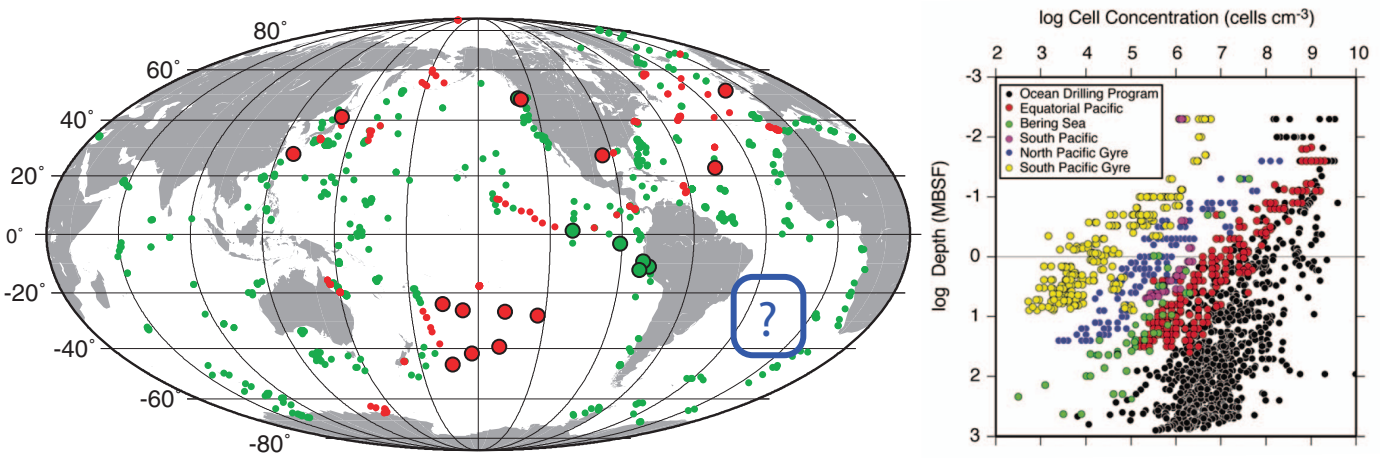

Figure F8. A. Weight percent total organic carbon (TOC) in surface sediments in the southern Atlantic Ocean (adapted from Mollenhauer et al., 2004). B. Comparison of the predicted range of weight percent TOC for the proposed SAT study area with other areas where scientific ocean drilling has conducted microbiological investigations (expedition numbers in brackets; data following Andrén et al., 2015; Shipboard Scientific Party, 2003; Expedition 329 Scientists, 2011; Expedition 336 Scientists, 2012; Expedition 308 Scientists, 2006; Tobin et al., 2009; Expedition 313 Scientists, 2010; Expedition 325 Scientists, 2011). The proposed drill sites have higher TOC concentrations than North Pond, where oxygen penetrates tens of meters into the seafloor in Holes U1383D, U1383E, and U1384A, but lower than the Nankai Trough, where pore-water oxygen is consumed less than 3 meters below seafloor.

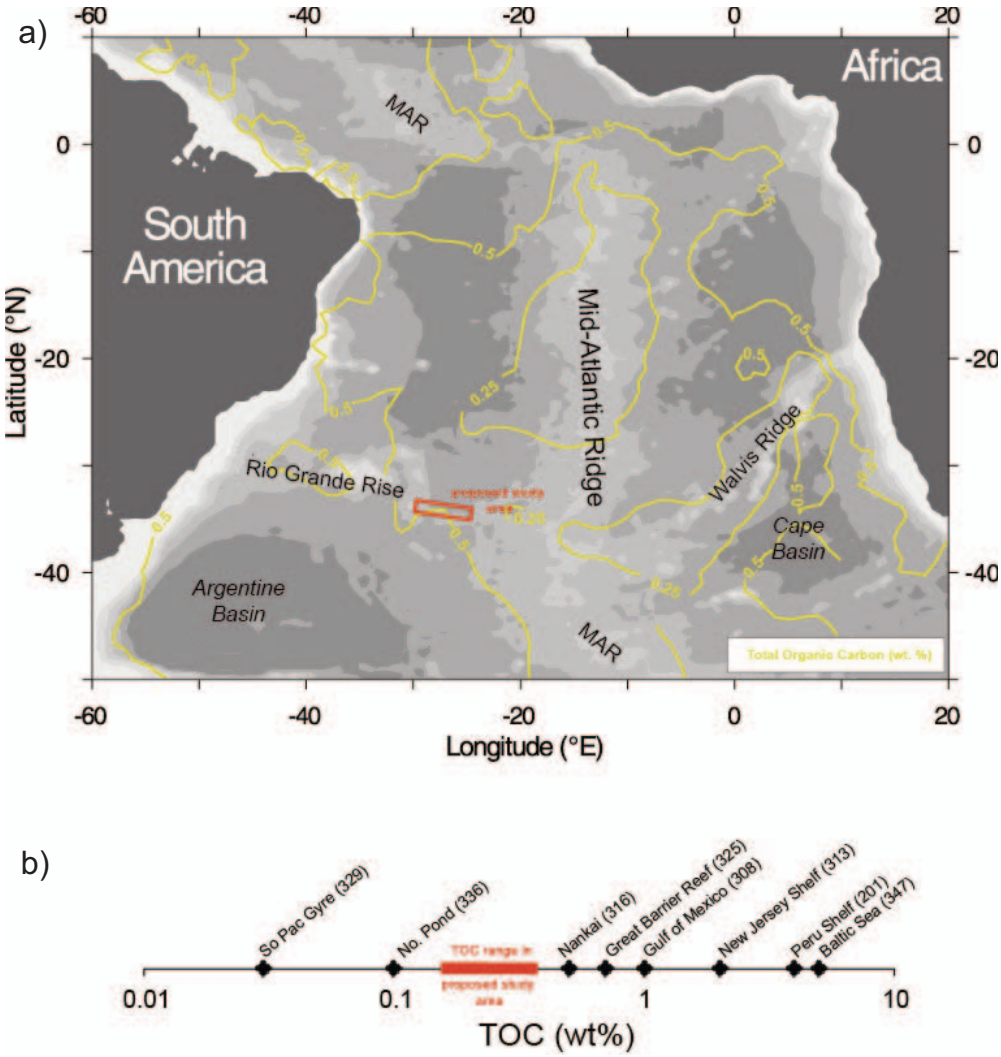

Figure F9. Composite deep-sea benthic foraminiferal $\delta^{13}C$ and $\delta^{18}O$ records showing both gradual and abrupt changes in global climate during the Cenozoic (modified from Cramer et al., 2009). A rich paleoceanographic record will be accessed by drilling the SAT sites, as demonstrated by DSDP Leg 3 spot coring on the western flank of the Mid-Atlantic Ridge. The bars to the right show the five primary SAT sites, present water depth, and key ocean history objectives. The deepest sites will generally contain carbonate-rich sediments in the older part (blue), deposited when a site was closer to the ridge crest and shallower than the CCD, transitioning up to carbonate-poor sediment (red) in the younger part as each site subsided below the CCD.

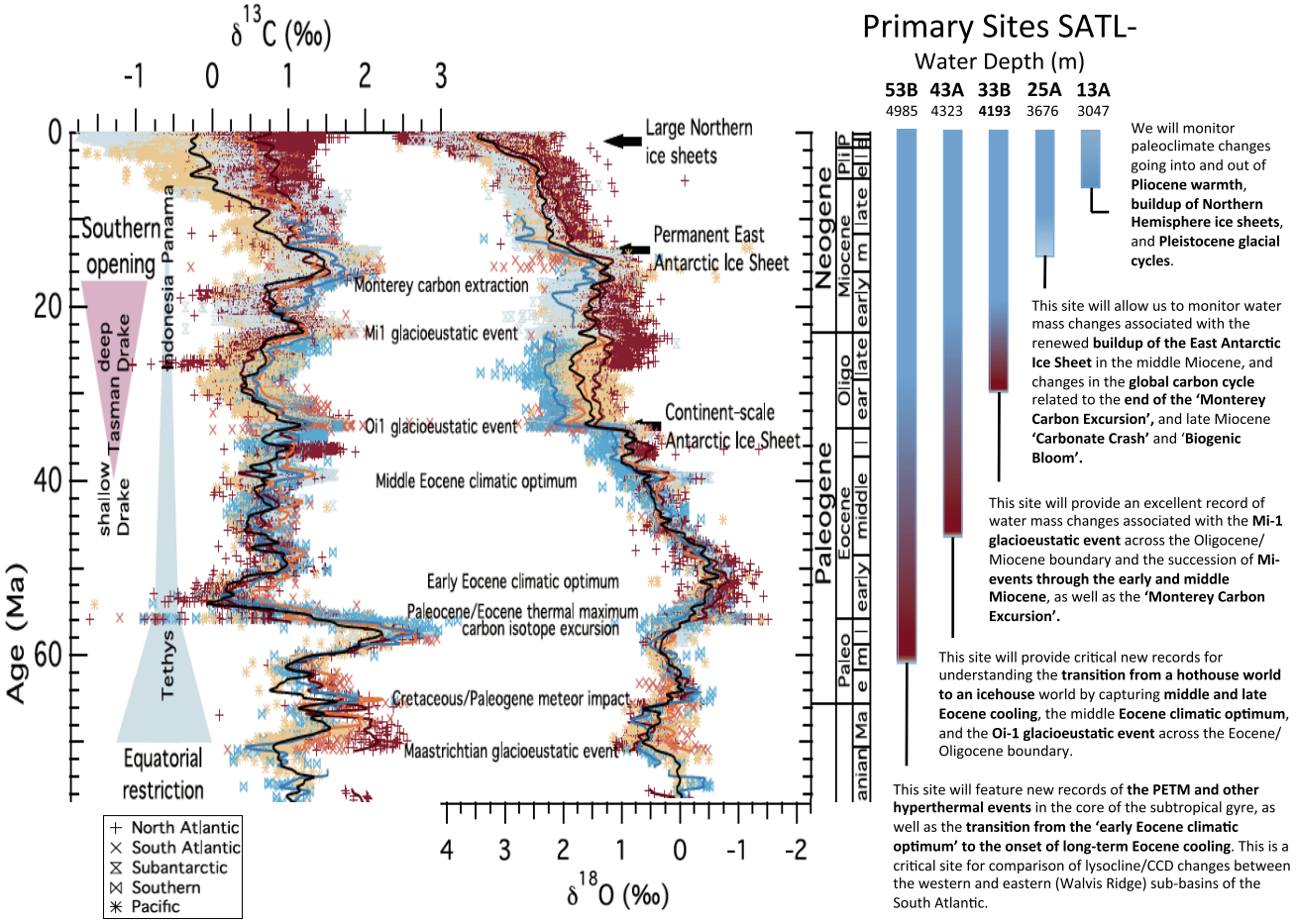

Figure F10. WOCE temperature, salinity, and phosphorus profiles along south–north Transect A-16 through the western South Atlantic Basin and west–east Transect A-10 at 30°S near the location of the SAT (data from World Ocean Circulation Experiment; **http://www.ewoce.org**). White rectangles show the approximate coverage of the SAT.

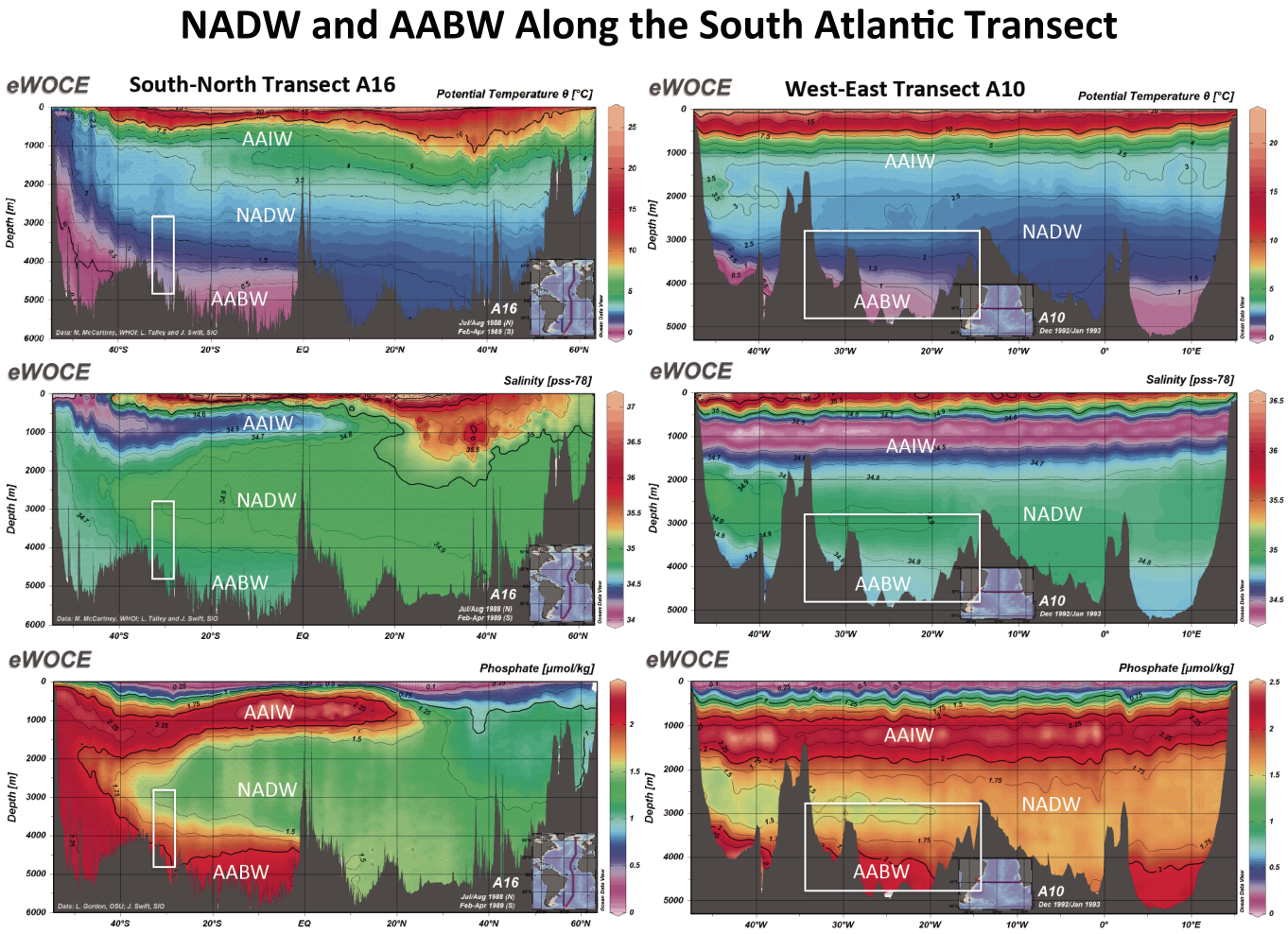

Figure F11. Top: percent carbonate in depth transect of drill sites recovered during ODP Leg 208 on the Walvis Ridge, eastern South Atlantic (Shipboard Scientific Party, 2004). The position of the lysocline and CCD were dynamic during the Cenozoic related to changing deepwater circulation, productivity, and ocean acidification associated with the PETM. Bottom: modeled relative water mass age during mid-Miocene climatic optimum (Coggon et al., 2016). Red oval = correlative changes in carbonate chemistry on Walvis Ridge. Colors represent benthic "age," which is a $\delta^{13}C$-like tracer; red = old water, blue = young water. Left: mode with Northern Component Water (NCW) "on." Right: NCW "off." The SAT, near 31°S, would capture changes in these two modes of deepwater formation. SCW = Southern Component Water.

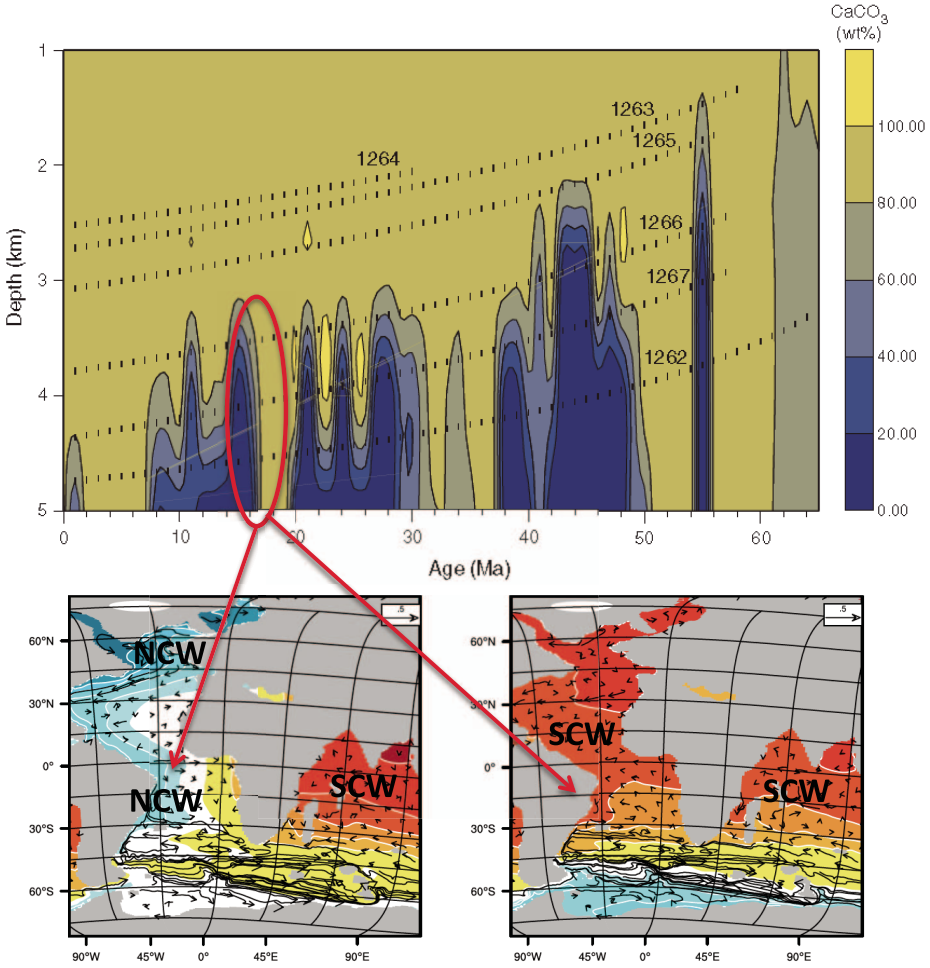

Site summaries

Site SATL-13A

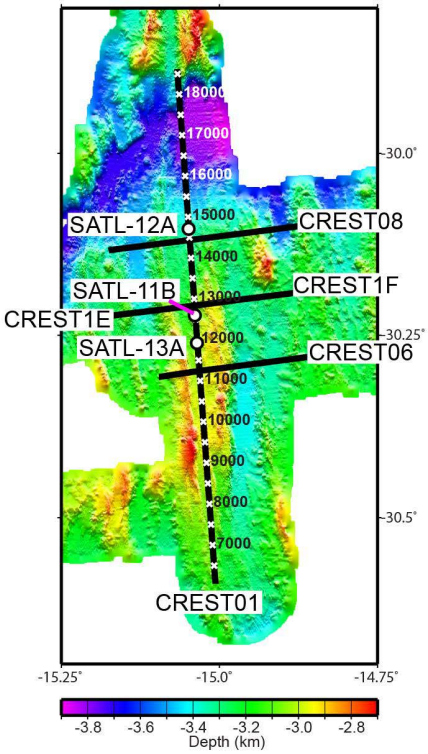

Site	SATL-13A
Priority	Primary
Latitude	-30.26056
Longitude	-15.0349
Water Depth (m)	3047
Sediment Thickness (m)	50
Age (Ma)	6.6
Half Spreading Rate (mm/yr)	17.0
Seismic Location	CREST01 CDP 11923

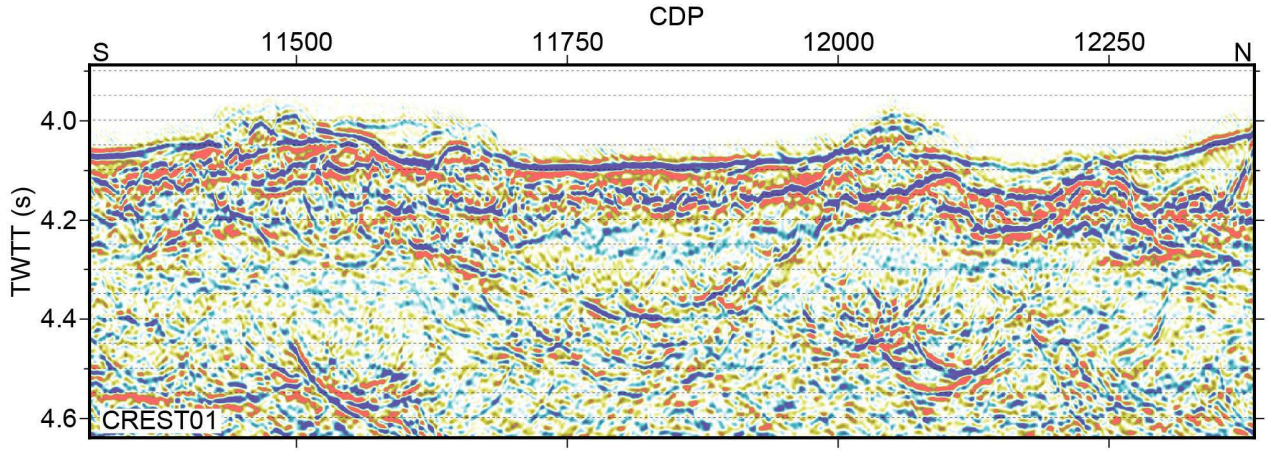

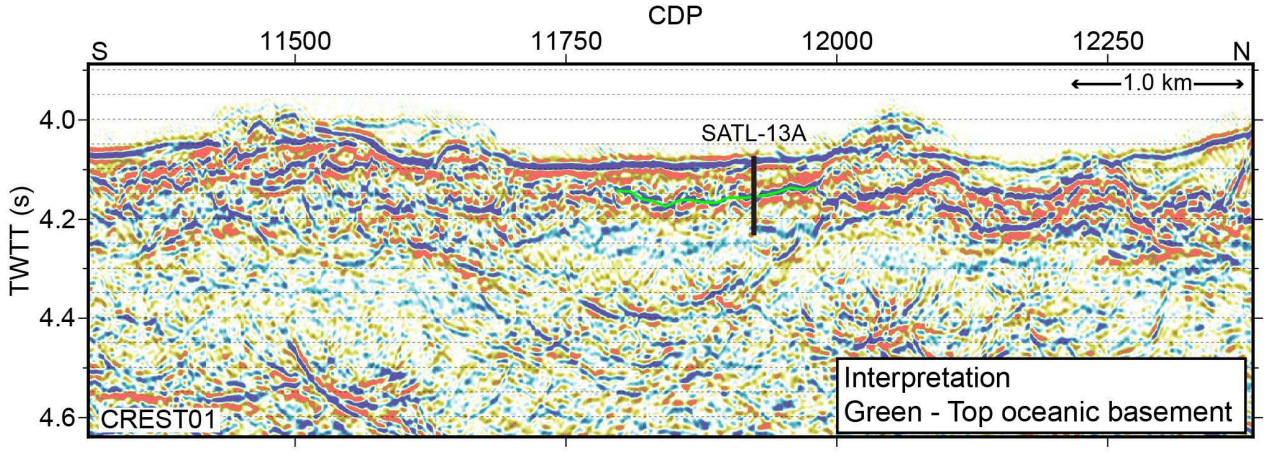

Site SATL-25A

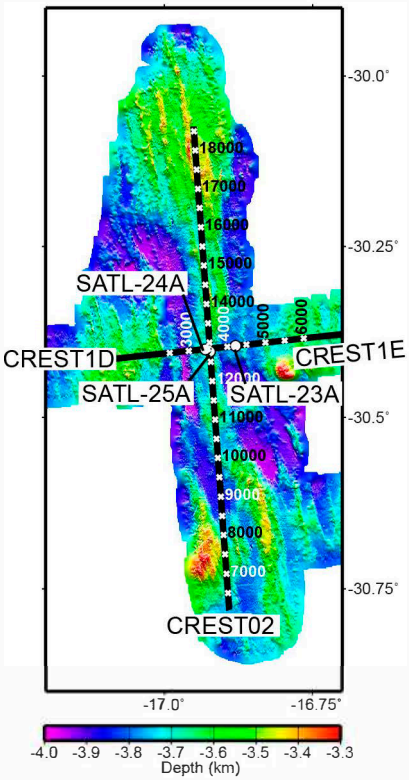

Site	SATL-25A
Priority	Primary
Latitude	-30.40344
Longitude	-16.92282
Water Depth (m)	3691
Sediment Thickness (m)	104
Age (Ma)	15.2
Half Spreading Rate (mm/yr)	25.5
Seismic Location	CREST02 CDP 12770

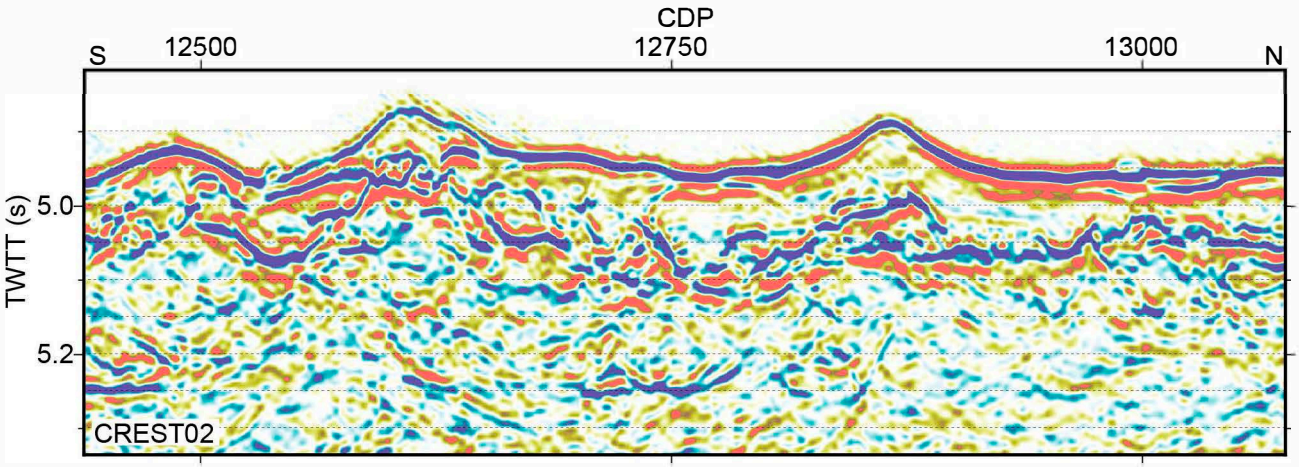

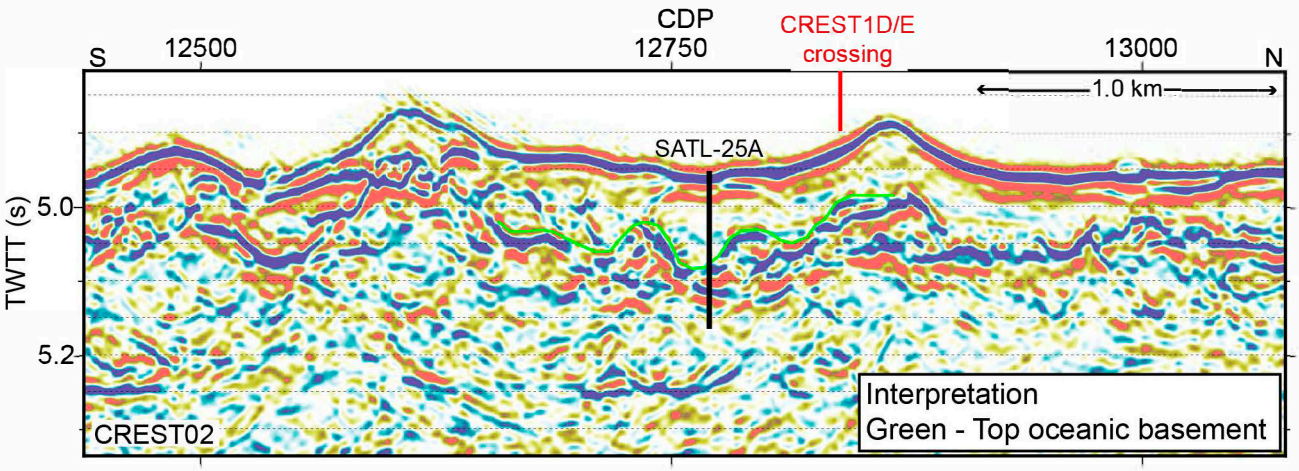

Site SATL-33B

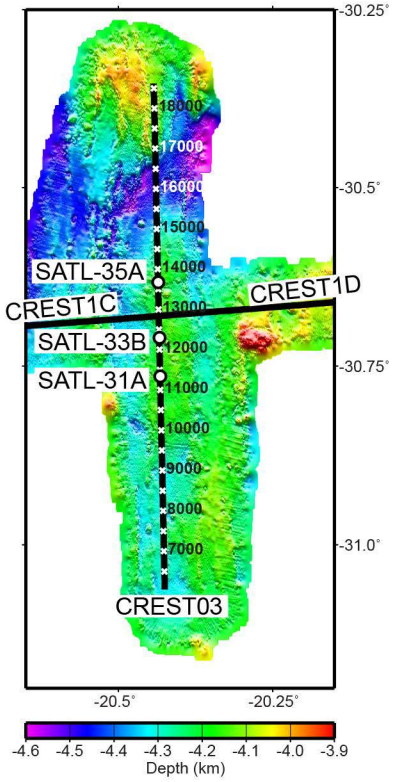

Site	SATL-33B
Priority	Primary
Latitude	-30.71029
Longitude	-20.4339
Water Depth (m)	4193
Sediment Thickness (m)	138
Age (Ma)	30.6
Half Spreading Rate (mm/yr)	24.0
Seismic Location	CREST03 CDP 12300

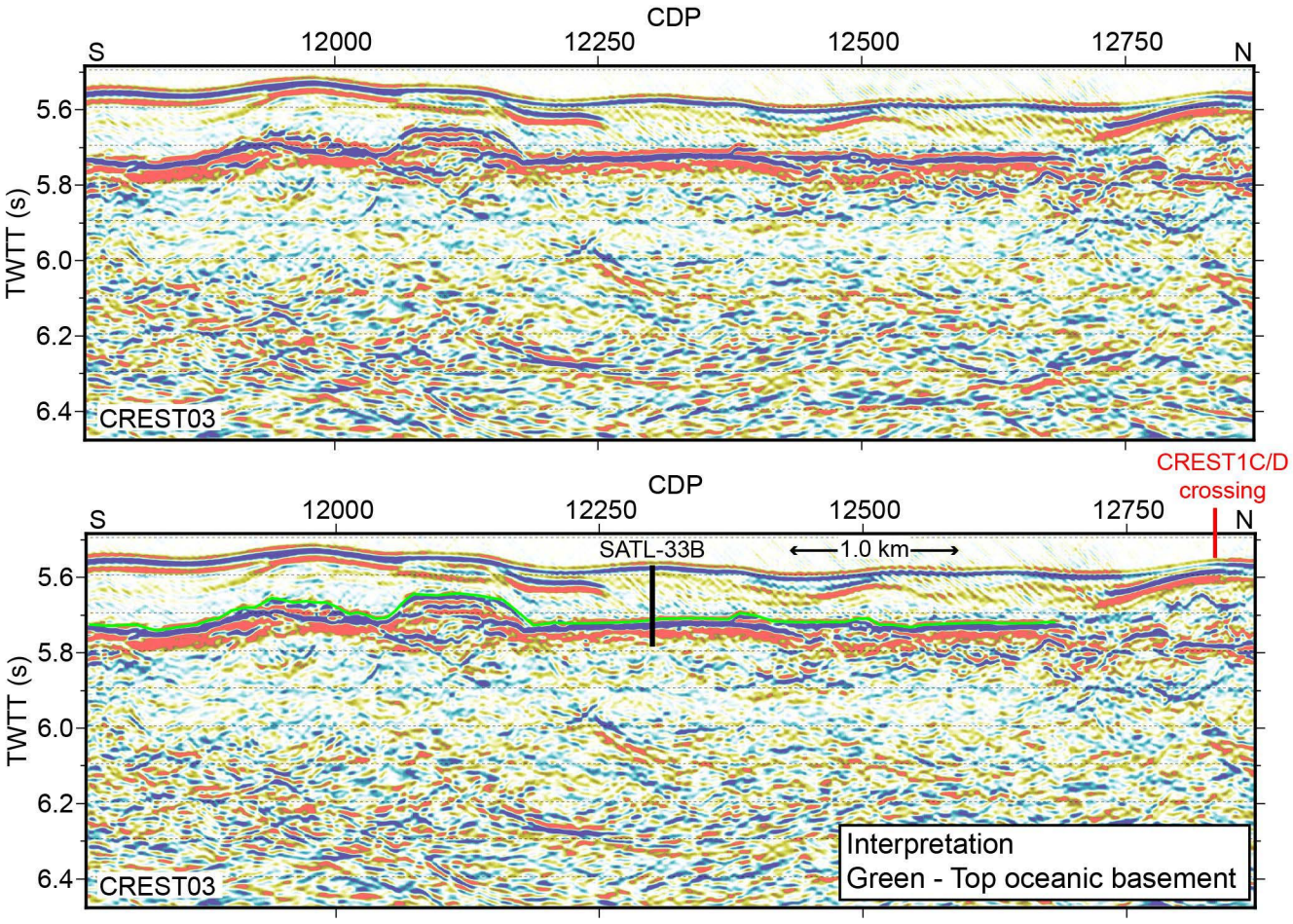

Site SATL-43A

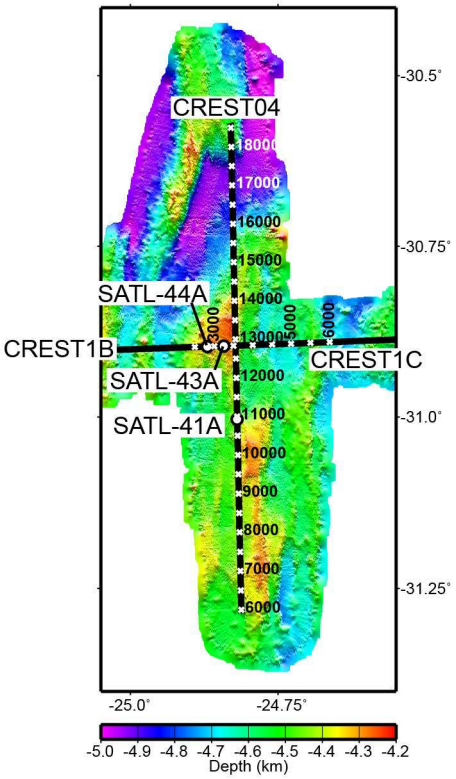

Site	SATL-43A
Priority	Primary
Latitude	-30.89618
Longitude	-24.84162
Water Depth (m)	4323
Sediment Thickness (m)	148
Age (Ma)	49.2
Half Spreading Rate (mm/yr)	19.5
Seismic Location	CREST1BC CDP 3252

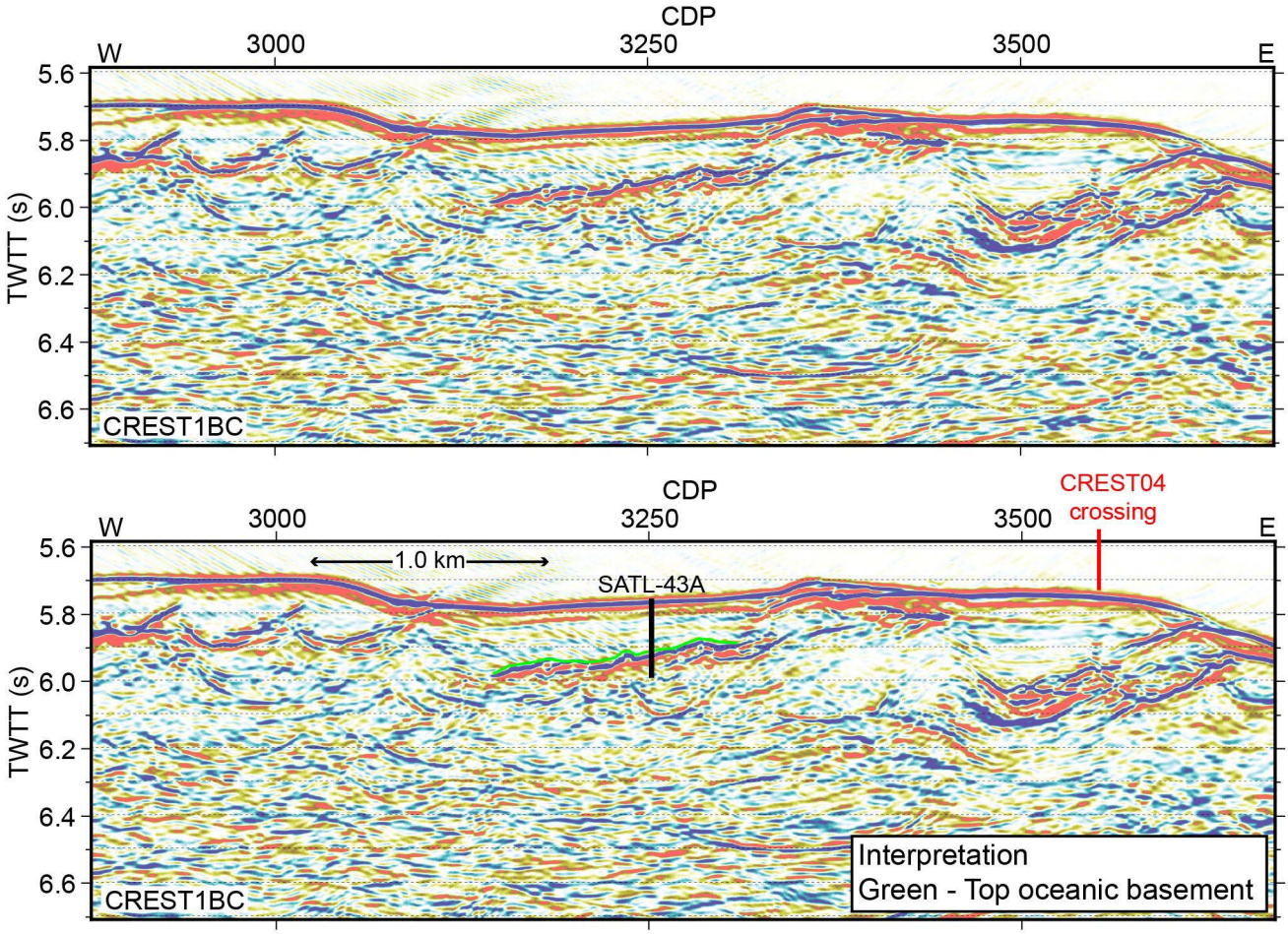

Site SATL-53B

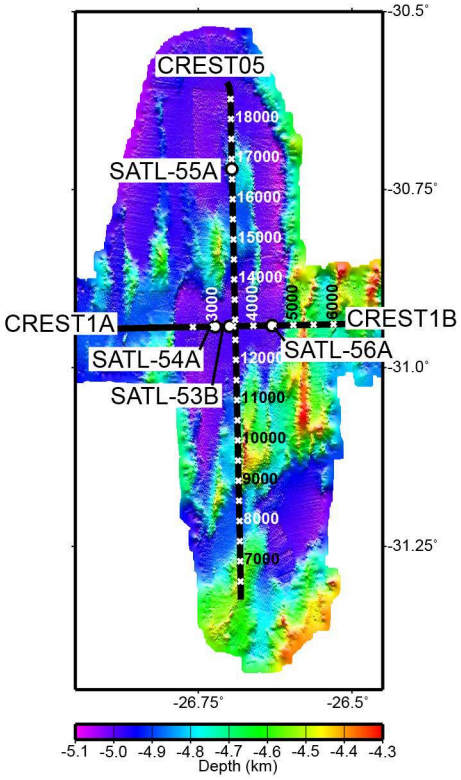

Site	SATL-53B
Priority	Primary
Latitude	-30.94207
Longitude	-26.69912
Water Depth (m)	4985
Sediment Thickness (m)	180
Age (Ma)	61.2
Half Spreading Rate (mm/yr)	13.5
Seismic Location	CREST1AB CDP 3410

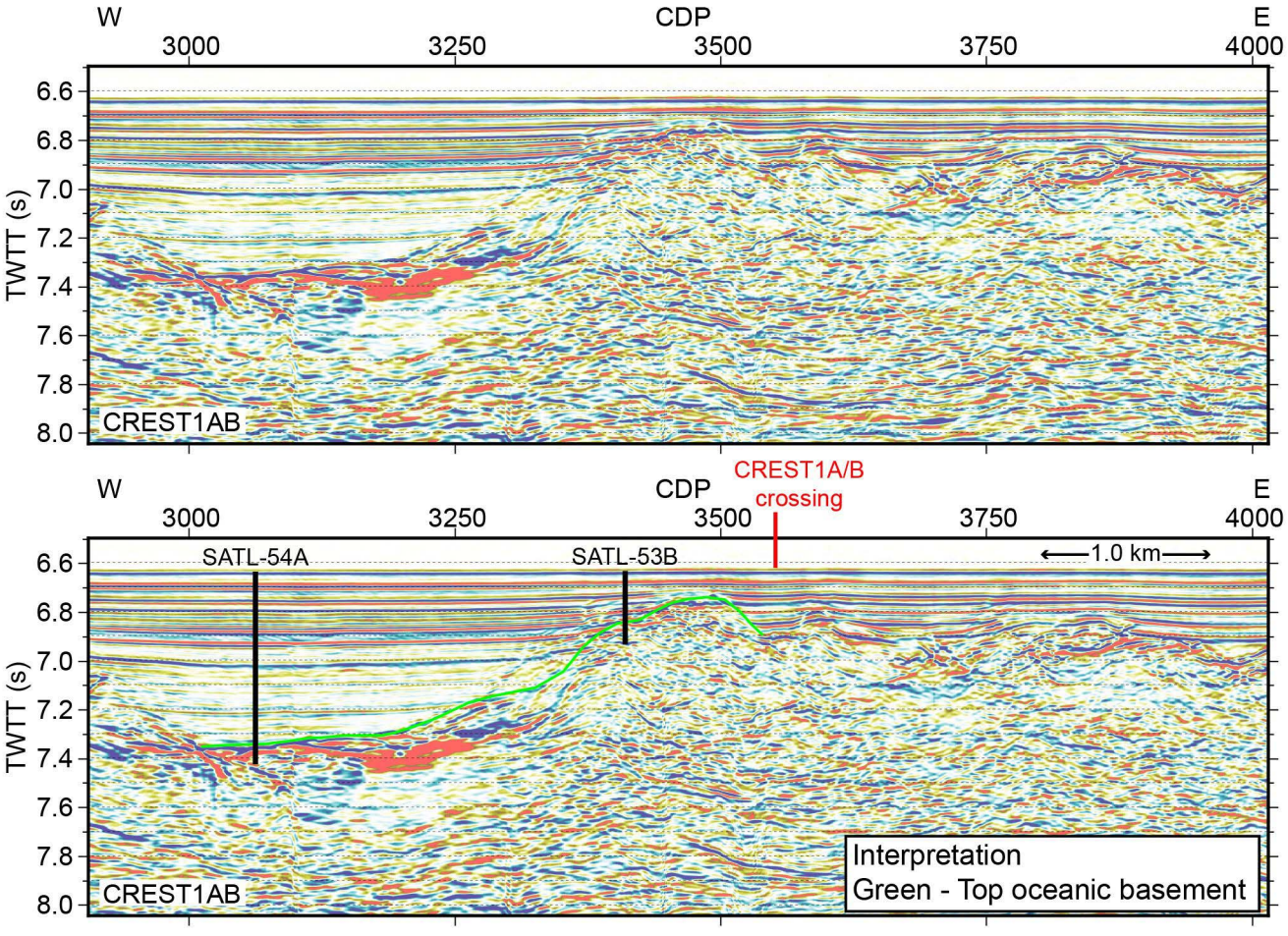

Site SATL-54A

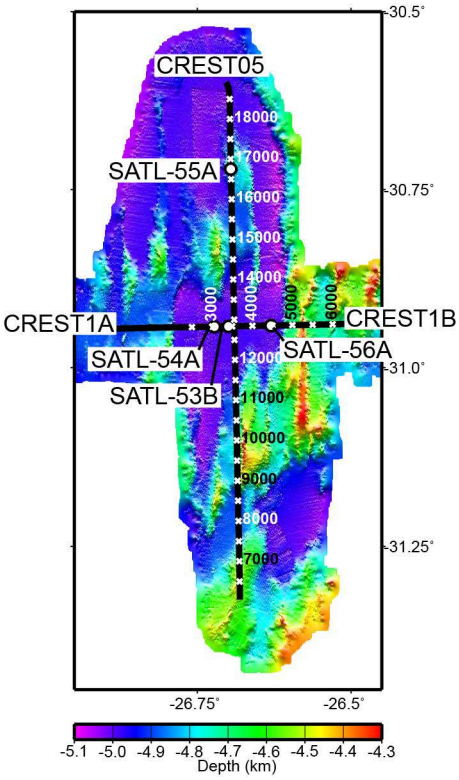

Site	SATL-54A
Priority	Primary
Latitude	-30.94242
Longitude	-26.72188
Water Depth (m)	4991
Sediment Thickness (m)	639
Age (Ma)	61.2
Half Spreading Rate (mm/yr)	13.5
Seismic Location	CREST1AB CDP 3062

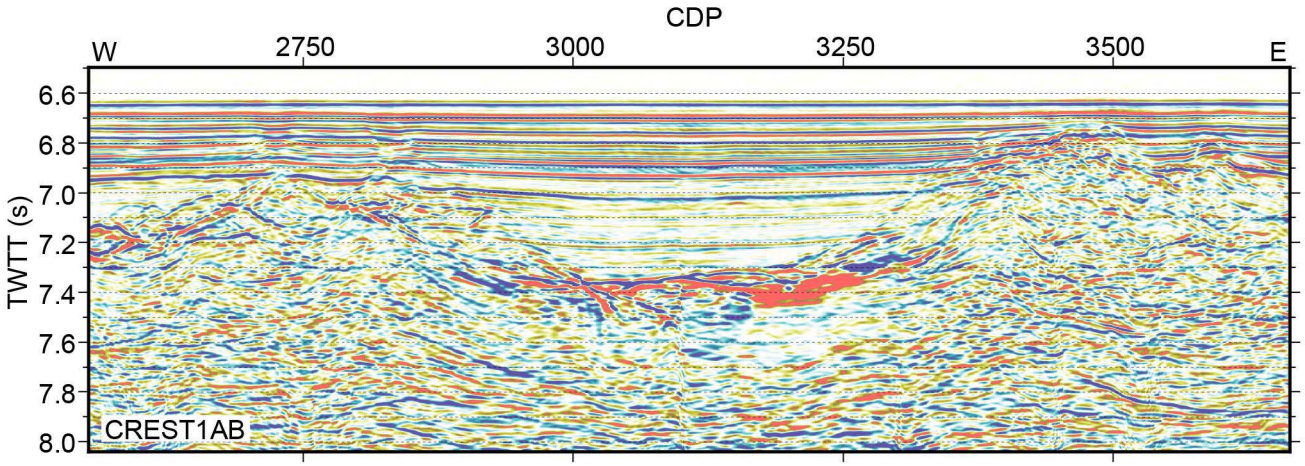

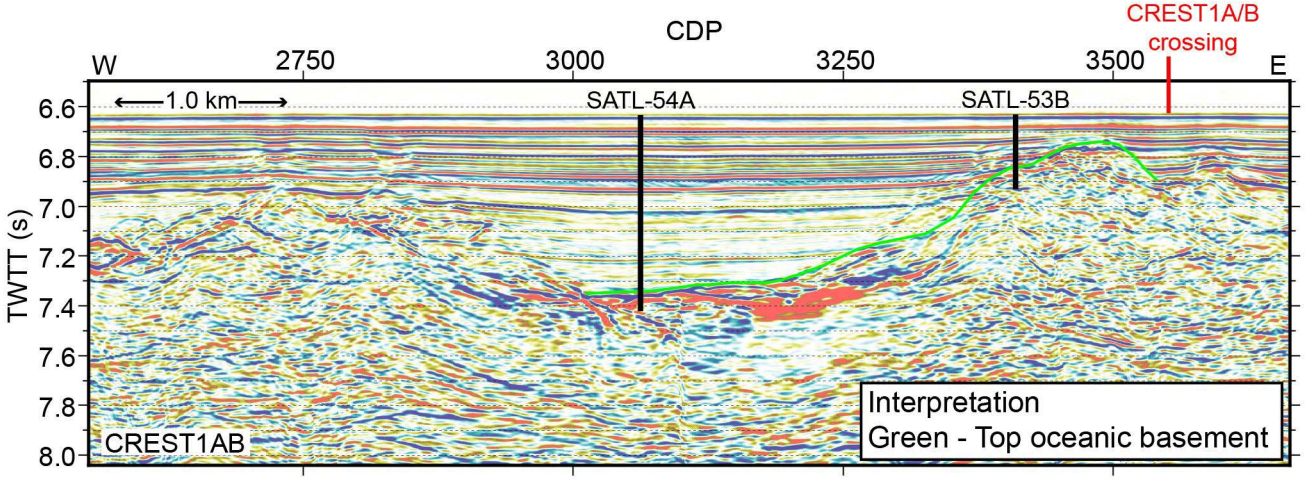

Site SATL-11B

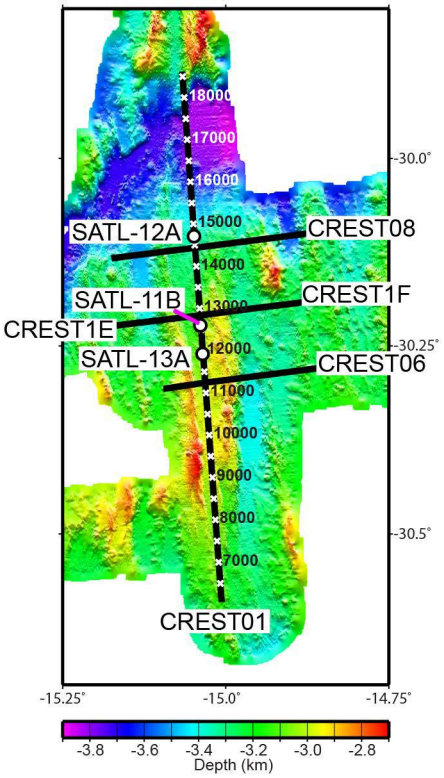

Site	SATL-11B
Priority	Alternate
Latitude	-30.22233
Longitude	-15.03817
Water Depth (m)	3057
Sediment Thickness (m)	104
Age (Ma)	6.6
Half Spreading Rate (mm/yr)	17.0
Seismic Location	CREST01 CDP 12603

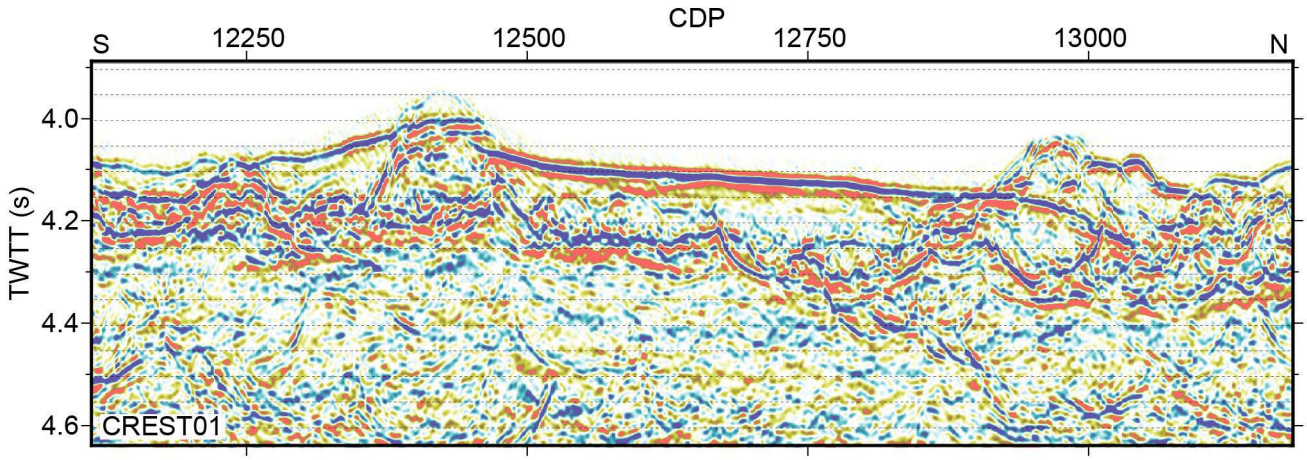

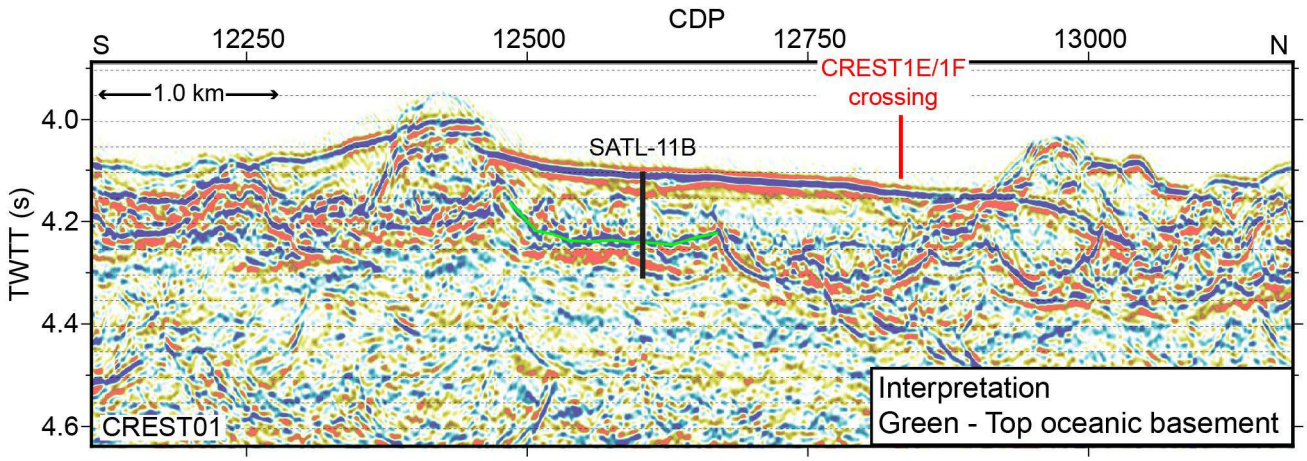

Site SATL-12A

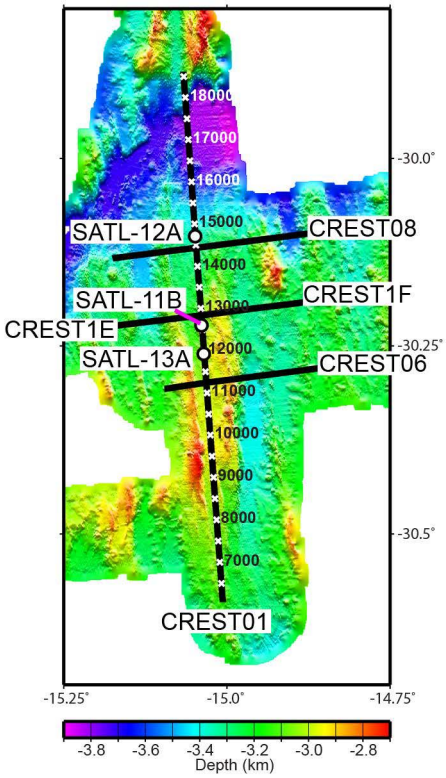

Site	SATL-12A
Priority	Alternate
Latitude	-30.10376
Longitude	-15.04832
Water Depth (m)	3373
Sediment Thickness (m)	96
Age (Ma)	6.6
Half Spreading Rate (mm/yr)	17.0
Seismic Location	CREST01 CDP 14712

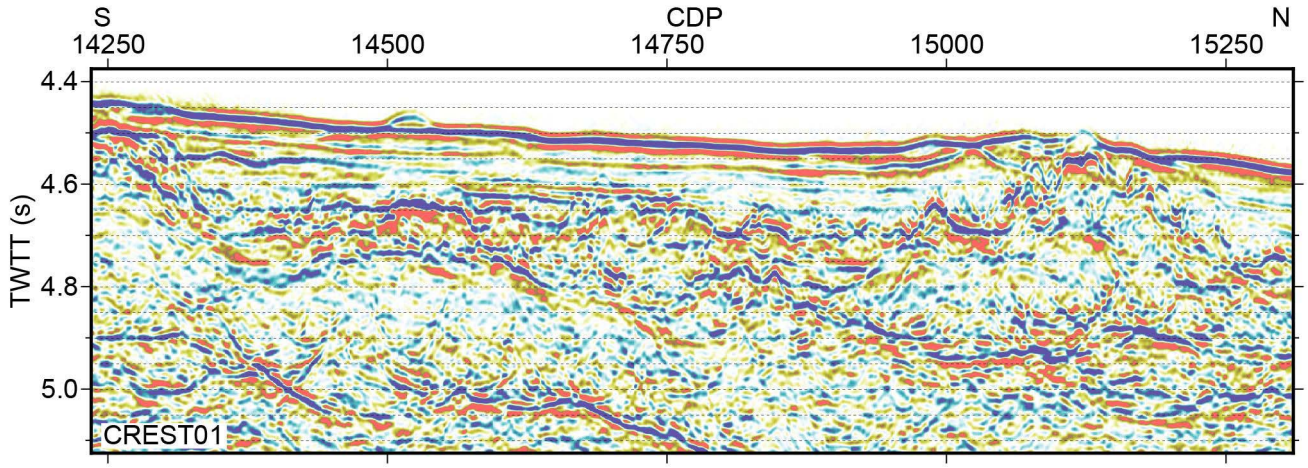

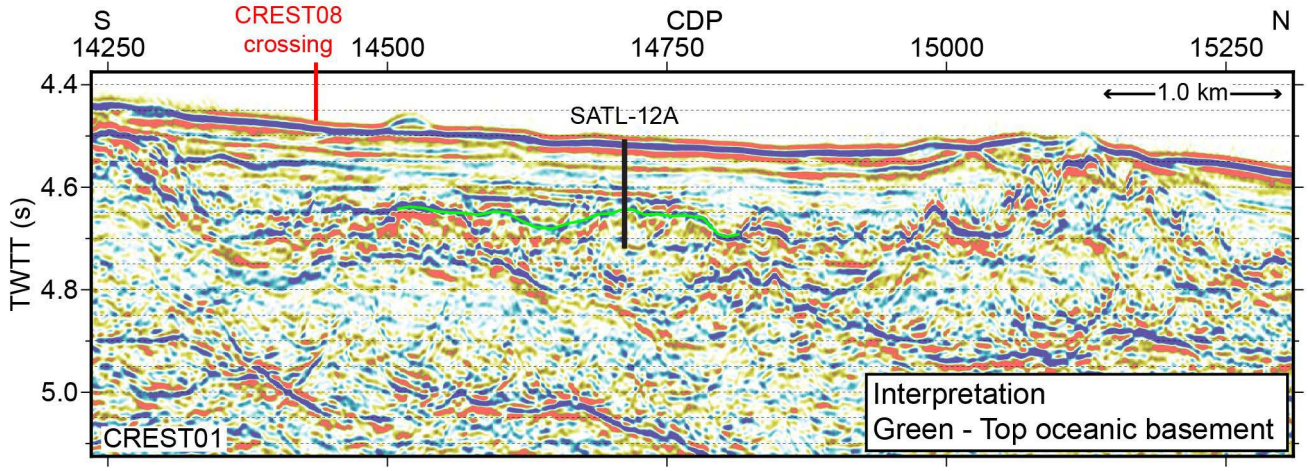

Site SATL-23A

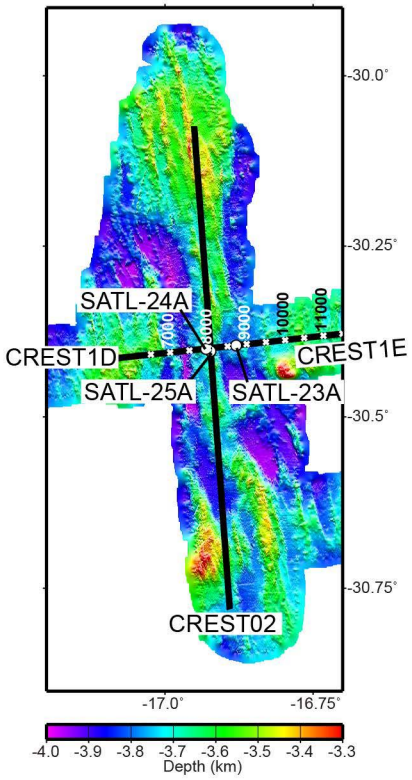

Site	SATL-23A
Priority	Alternate
Latitude	-30.39535
Longitude	-16.87974
Water Depth (m)	3819
Sediment Thickness (m)	162
Age (Ma)	15.2
Half Spreading Rate (mm/yr)	25.5
Seismic Location	CREST1E CDP 8724

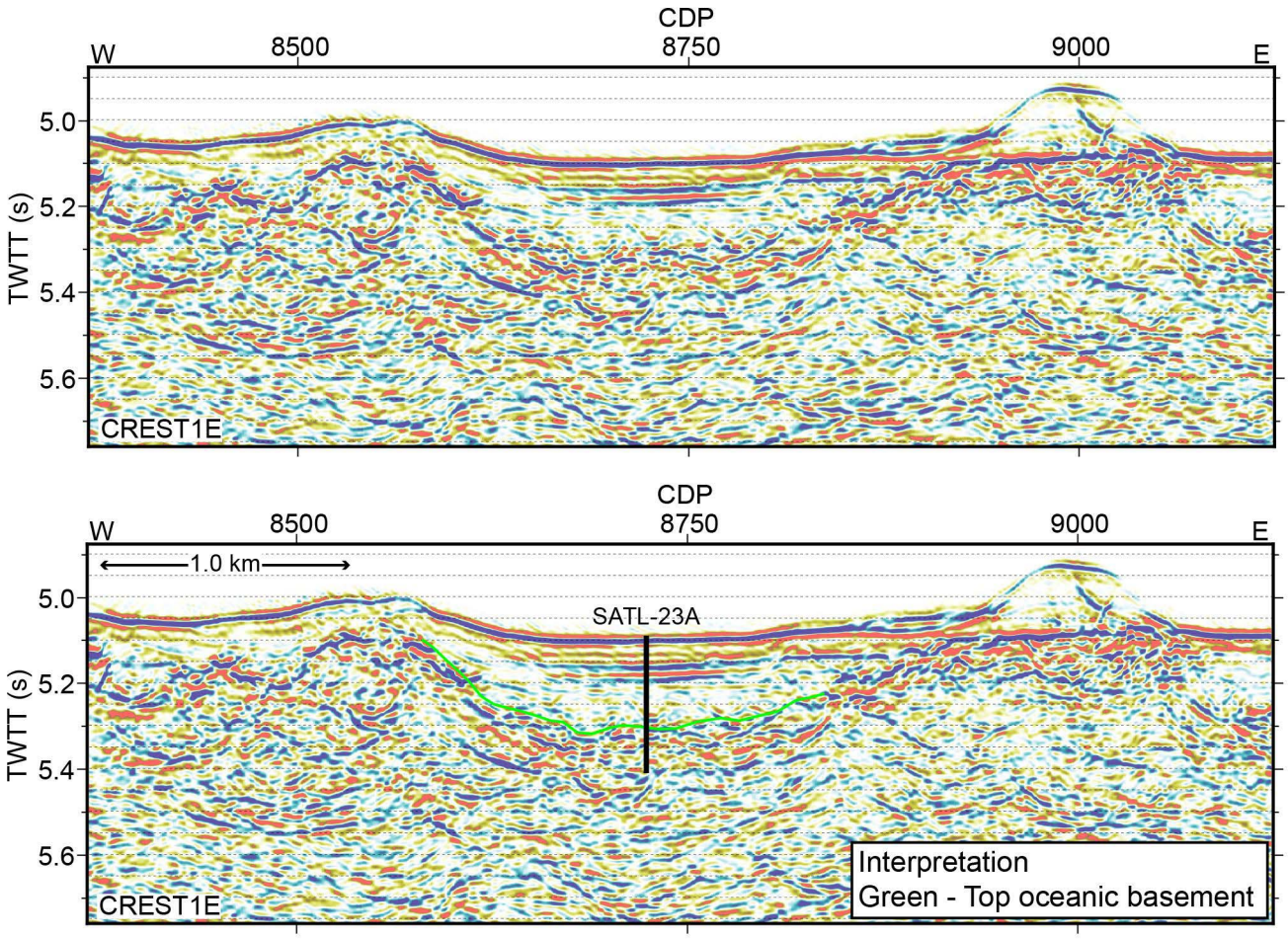

Site SATL-24A

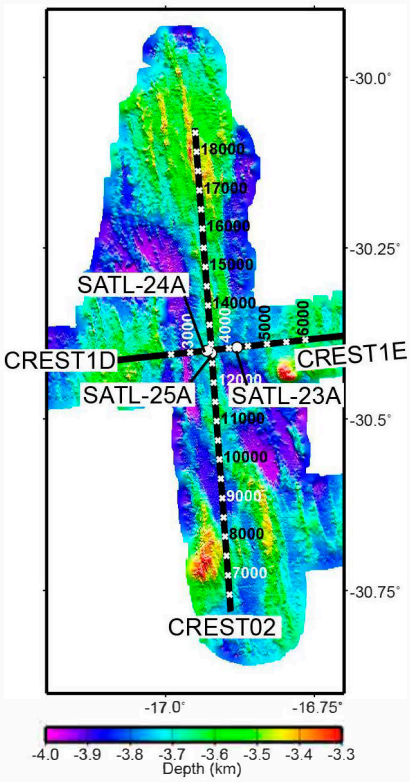

Site	SATL-24A
Priority	Alternate
Latitude	-30.40021
Longitude	-16.93053
Water Depth (m)	3676
Sediment Thickness (m)	94
Age (Ma)	15.2
Half Spreading Rate (mm/yr)	25.5
Seismic Location	CREST1DE CDP 3434

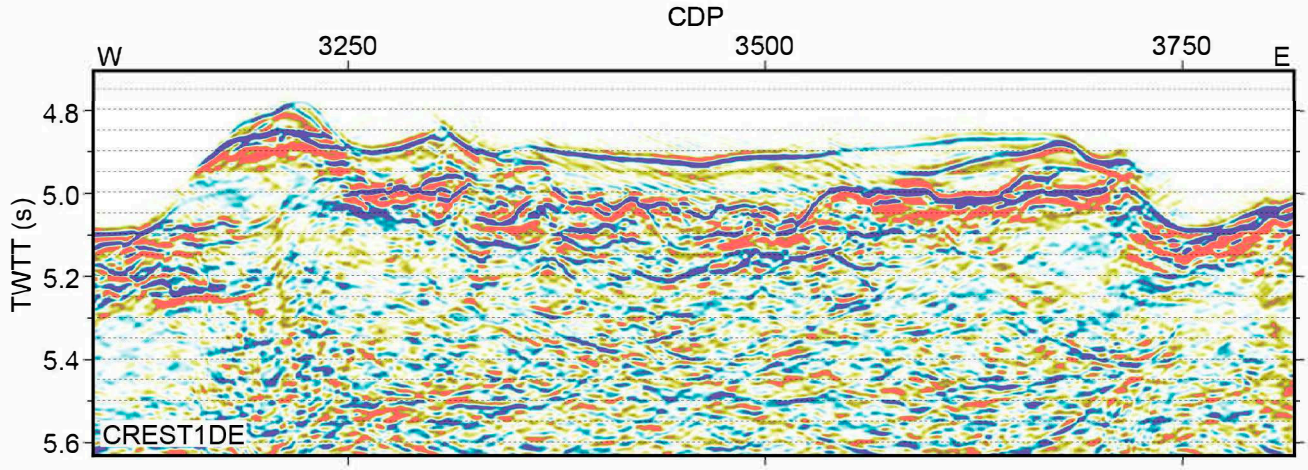

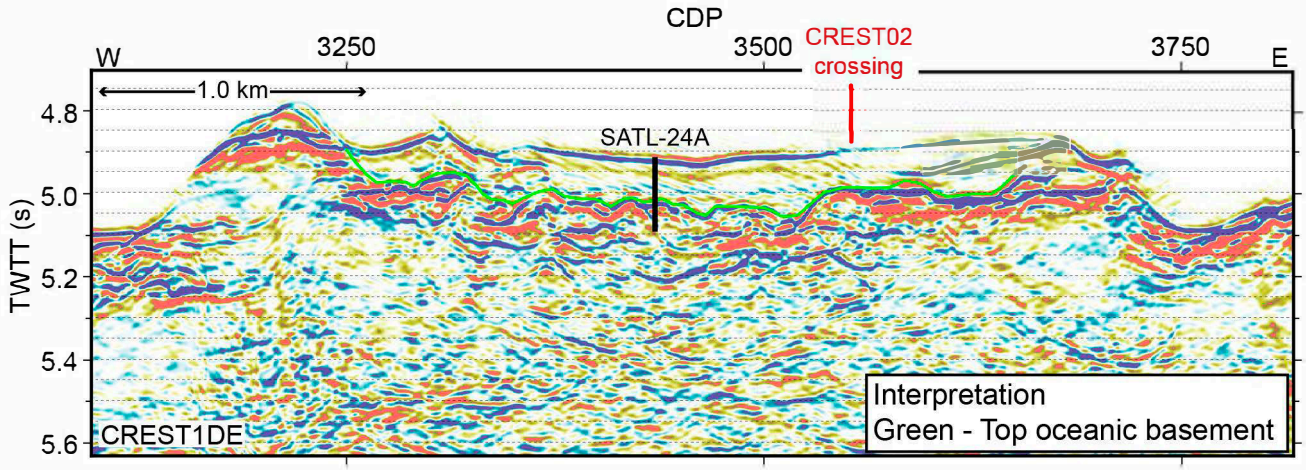

Site SATL-31A

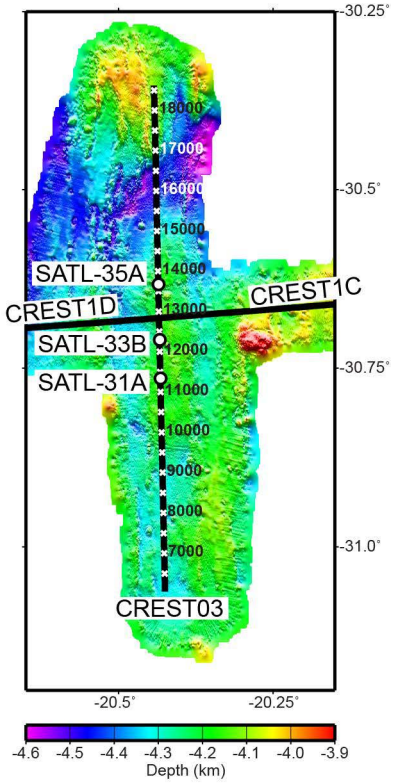

Site	SATL-31A
Priority	Alternate
Latitude	-30.76406
Longitude	-20.43255
Water Depth (m)	4188
Sediment Thickness (m)	183
Age (Ma)	30.6
Half Spreading Rate (mm/yr)	24.0
Seismic Location	CREST03 CDP 11346

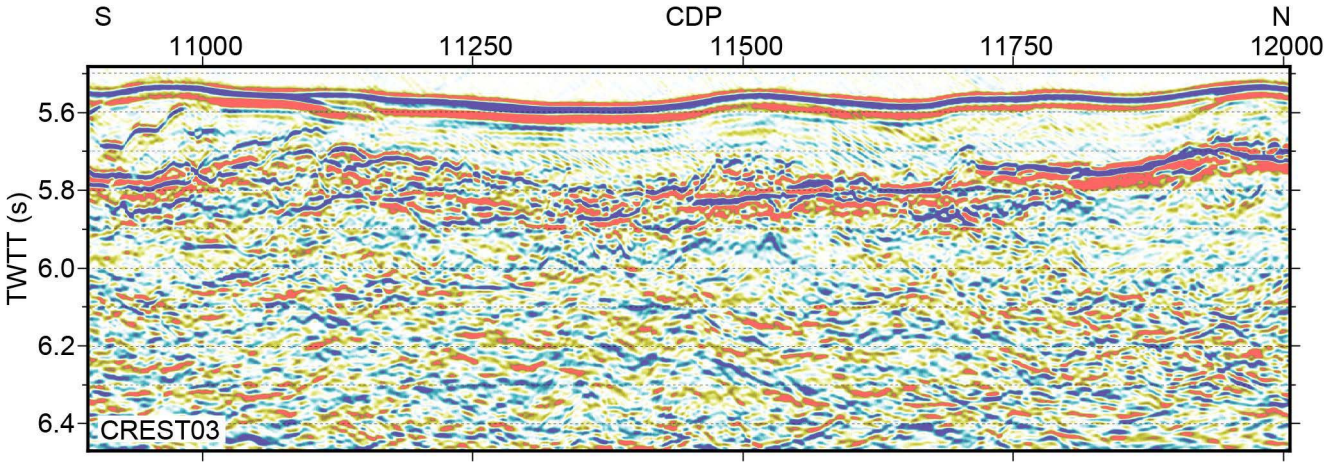

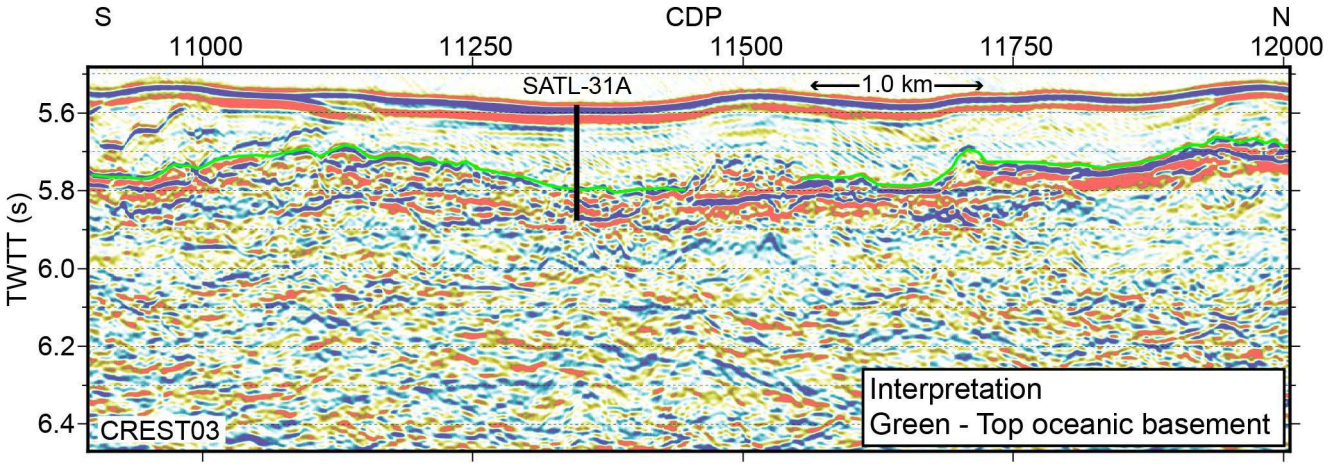

Site SATL-35A

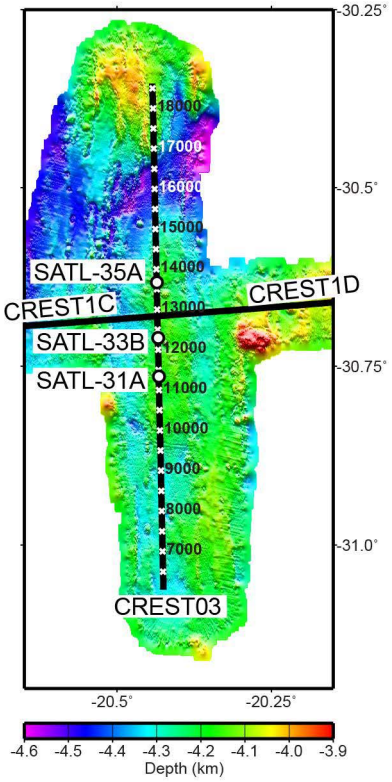

Site	SATL-35A
Priority	Alternate
Latitude	-30.63251
Longitude	-20.43586
Water Depth (m)	4157
Sediment Thickness (m)	93
Age (Ma)	30.6
Half Spreading Rate (mm/yr)	24.0
Seismic Location	CREST03 CDP 13680

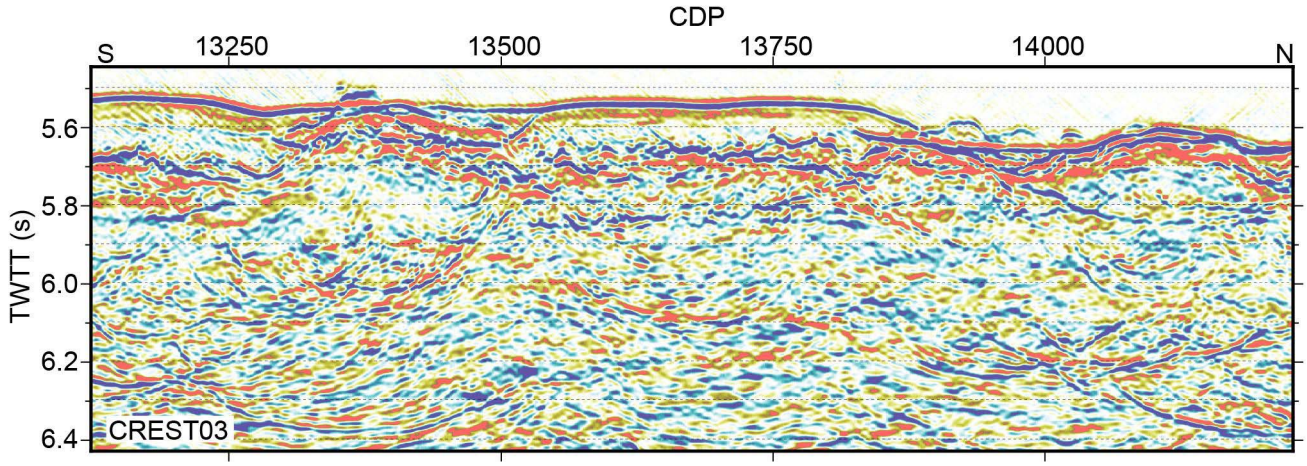

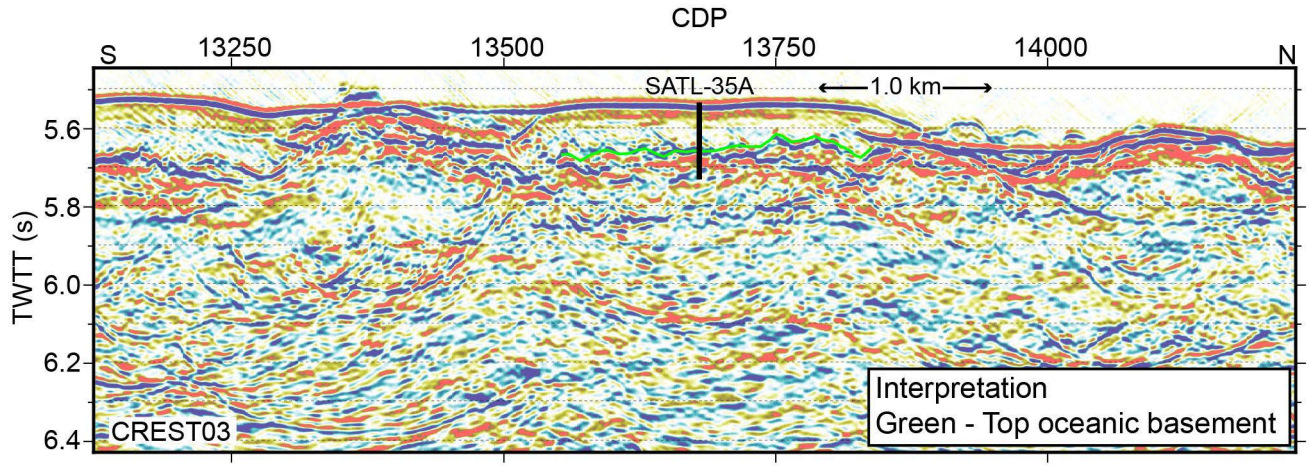

Site SATL-41A

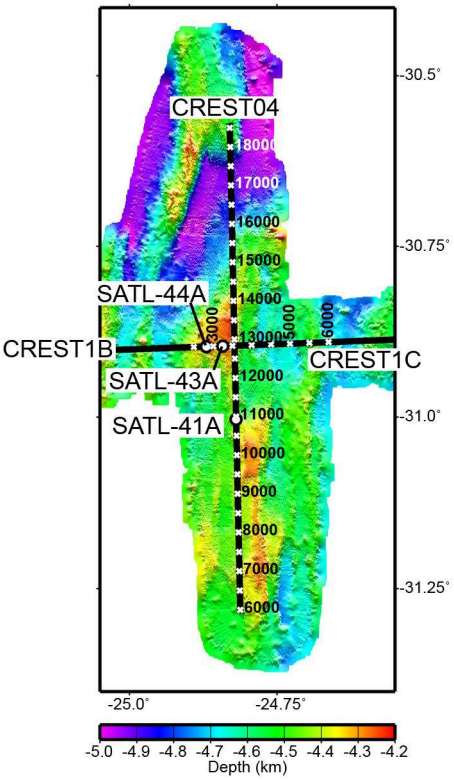

Site	SATL-41A
Priority	Alternate
Latitude	-31.00332
Longitude	-24.81913
Water Depth (m)	4408
Sediment Thickness (m)	203
Age (Ma)	49.2
Half Spreading Rate (mm/yr)	19.5
Seismic Location	CREST04 CDP 10926

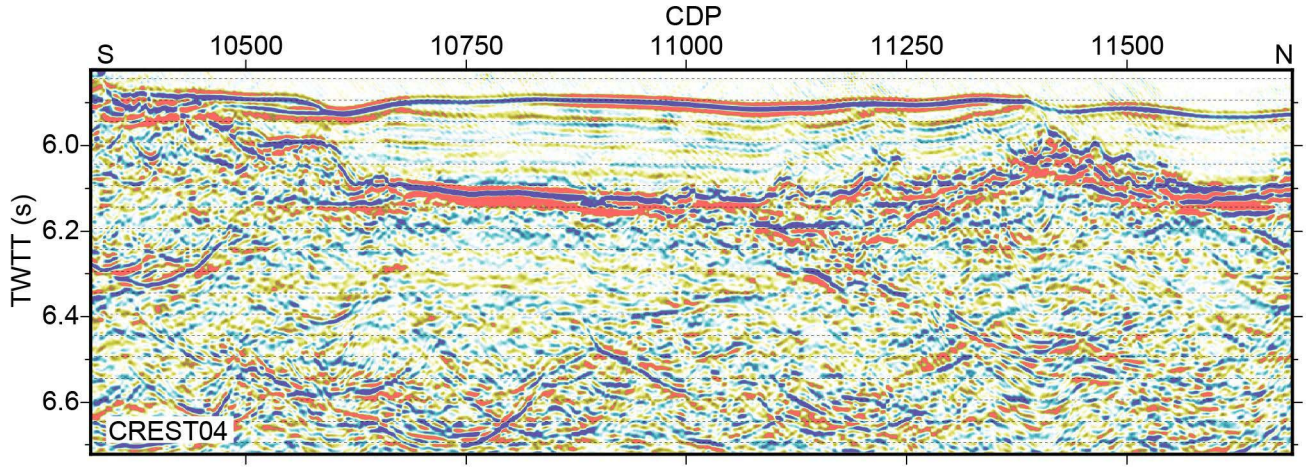

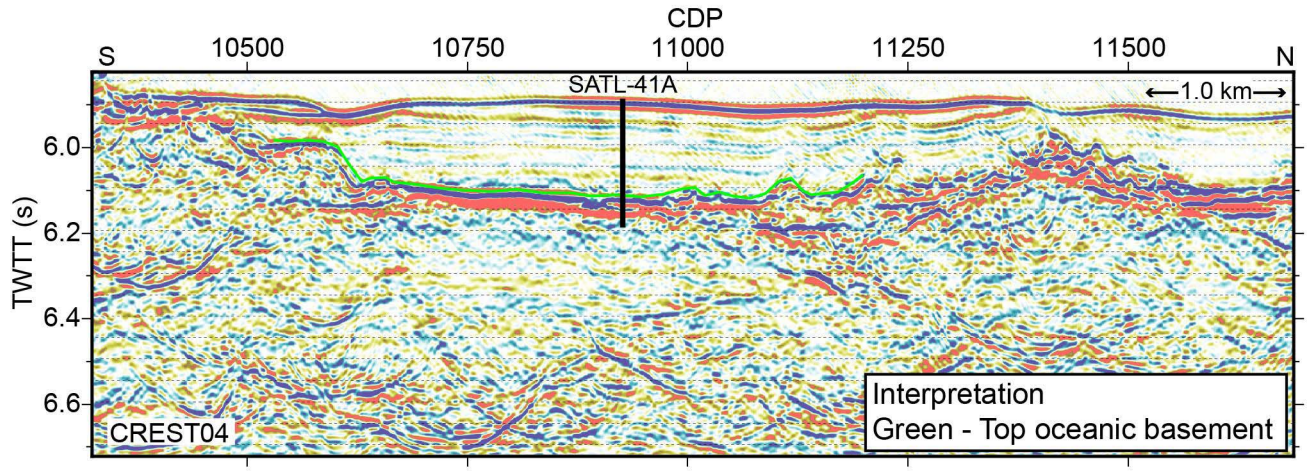

Site SATL-44A

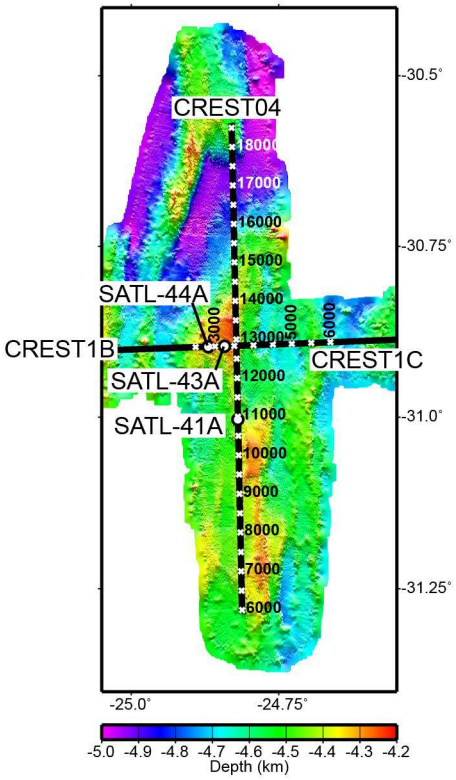

Site	SATL-44A
Priority	Alternate
Latitude	-30.89703
Longitude	-24.86951
Water Depth (m)	4283
Sediment Thickness (m)	176
Age (Ma)	49.2
Half Spreading Rate (mm/yr)	19.5
Seismic Location	CREST1BC CDP 2825

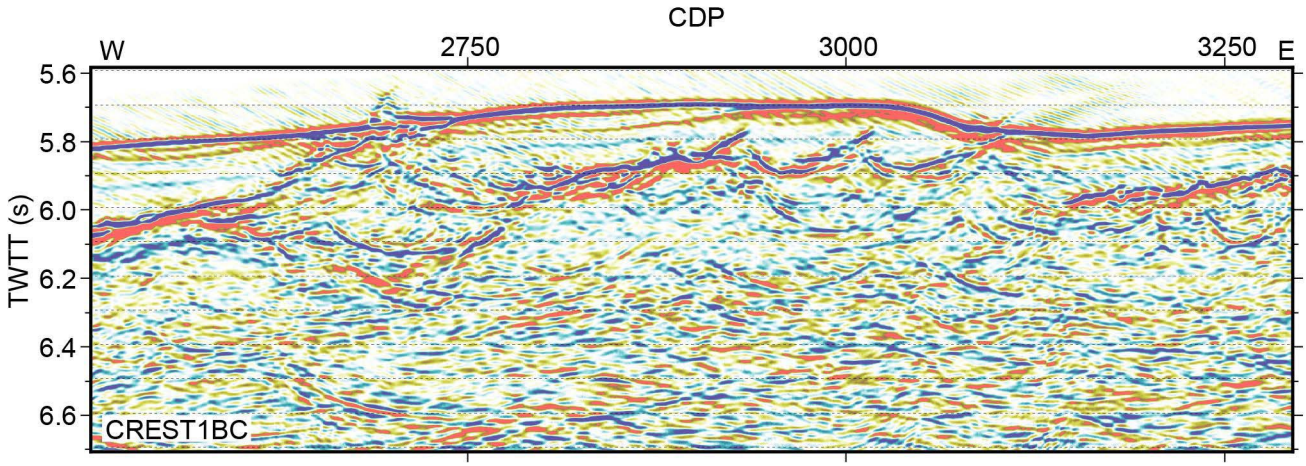

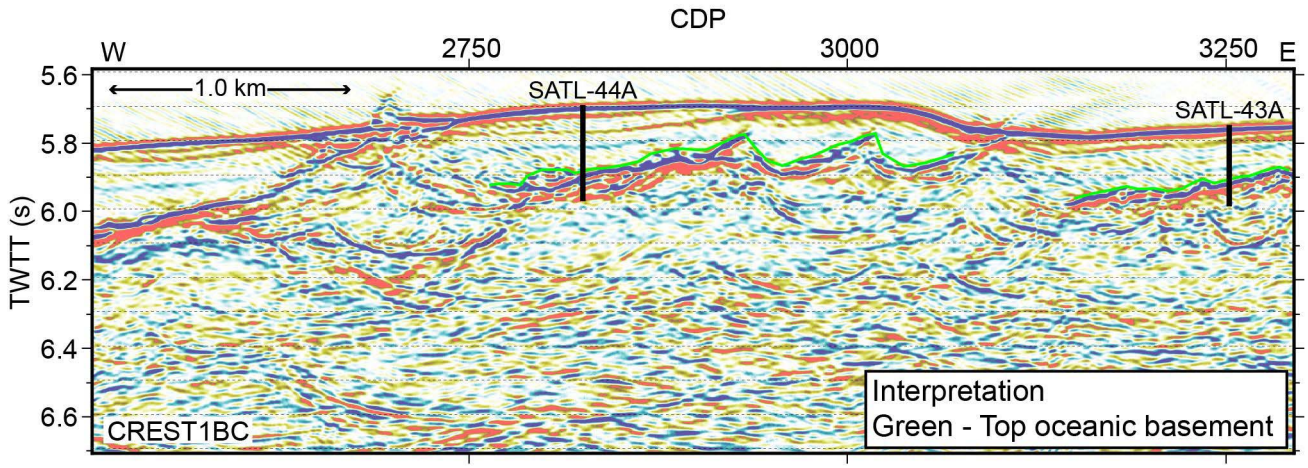

Site SATL-55A

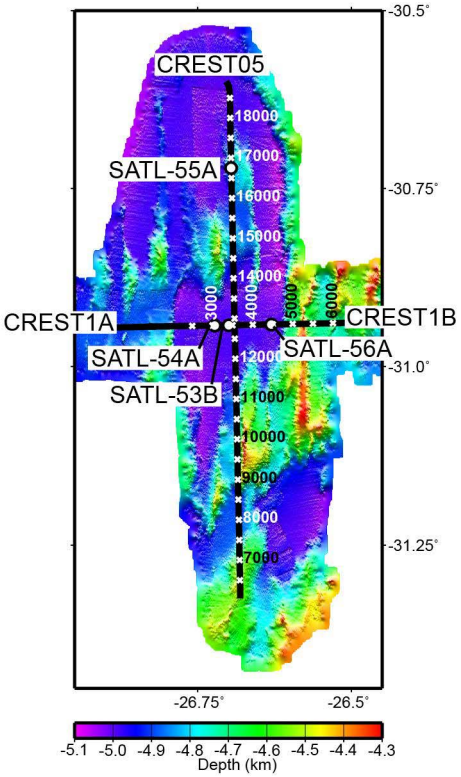

Site	SATL-55A
Priority	Secondary
Latitude	-30.72151
Longitude	-26.69525
Water Depth (m)	4857
Sediment Thickness (m)	126
Age (Ma)	61.2
Half Spreading Rate (mm/yr)	13.5
Seismic Location	CREST05 CDP 16750

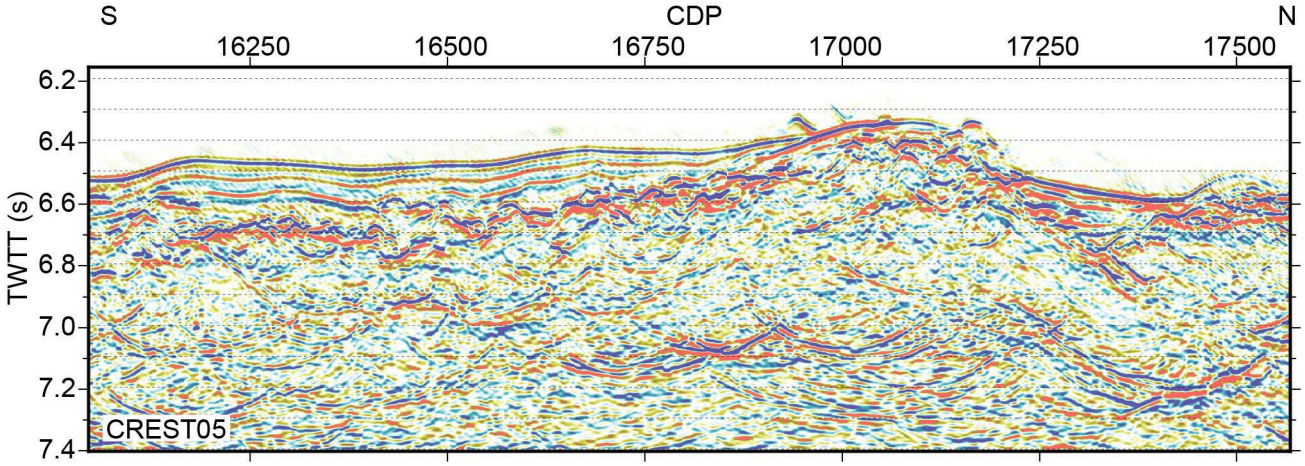

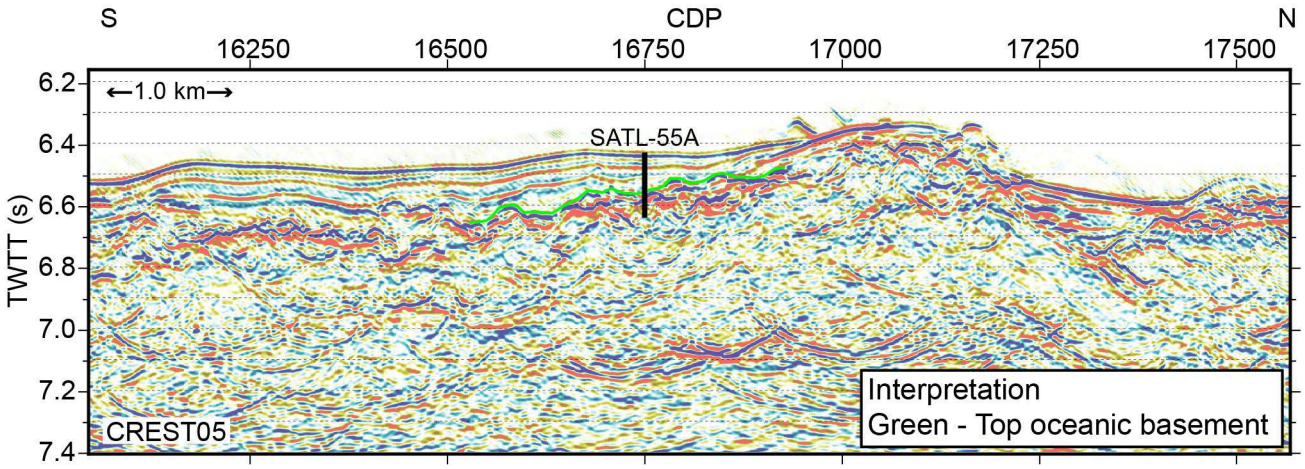

Site SATL-56A

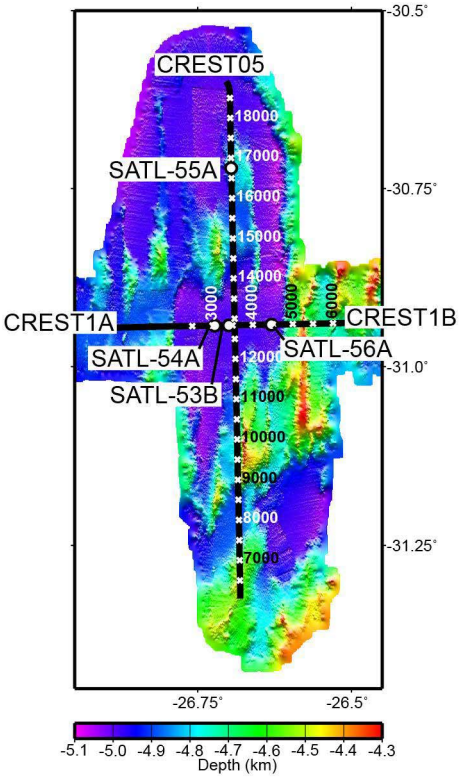

Site	SATL-56A
Priority	Secondary
Latitude	-30.94091
Longitude	-26.62983
Water Depth (m)	4998
Sediment Thickness (m)	510
Age (Ma)	61.2
Half Spreading Rate (mm/yr)	13.5
Seismic Location	CREST1AB CDP 4470